Title

Exploring the Transporters Dynamics in Blood-Brain Barrier Functionality and Innovative Treatments for Non-Alcoholic Fatty Liver Disease/Steatohepatitis

Author

Zhou, Xujia

Publication Date

2024

Peer reviewed|Thesis/dissertation

Exploring the Transporters Dynamics in Blood-Brain Barrier Functionality and Innovative Treatments for Non-Alcoholic Fatty Liver Disease/Steatohepatitis

by
Xujia Zhou

DISSERTATION
Submitted in partial satisfaction of the requirements for degree of
DOCTOR OF PHILOSOPHY

in

Pharmaceutical Sciences and Pharmacogenomics

in the

GRADUATE DIVISION
of the
UNIVERSITY OF CALIFORNIA, SAN FRANCISCO

Approved:

DocuSigned by:
Michelle Arkin
992885B79658434...

Michelle Arkin
Chair

DocuSigned by:
Nadav Ahituv

Nadav Ahituv

DocuSigned by:
Kathleen Giacomini

Kathleen Giacomini

DocuSigned by:
Ken Nakamura
83D6801FCC3C4A4...

Ken Nakamura

Committee Members

This thesis is dedicated to my family—my late grandmother, my parents, my husband, my son, and our two cherished cats. Each of you has been my biggest support, and your unconditional love and unwavering encouragement have been my guiding light throughout this journey.

Acknowledgments

There are many people to acknowledge and thank for supporting me throughout my journey at graduate school and in the completion of this dissertation. I would like to extend my deepest appreciation to each of you below.

First, to my mentors and dissertation advisors, Dr. Kathleen Giacomini and Dr. Nadav Ahituv. My journey to completing this dissertation would not have been possible without your guidance and support. Your expertise and insight have been pivotal in shaping the scientist I have become. Kathy, you pushed me beyond my limits, helping me realize that I am capable of achieving far more than I ever imagined. The trust you placed in me and the autonomy you provided allowed me to pursue research that truly fascinates me. I see you as a role model who continually sets higher standards for herself. The changes I have undergone as a scientist and as a woman since joining your lab are profound, and I am deeply grateful for this experience. Nadav, your mentorship, which has unwaveringly supported both my scientific pursuits and personal well-being, has been invaluable. You have always encouraged me to engage with projects that spark my passion, never pressuring me to conform to pursuits that felt misaligned with my interests. Your respect for my approach to PhD studies and for maintaining a healthy work-life balance has been immensely empowering. The insights I have gained from you about the nuances of science and the essence of great mentorship are treasures I will carry with me always. Together, Drs. Ahituv and Giacomini, you have provided an environment that champions curiosity, rigor, and integrity. It is really my honor to have learned from and worked alongside you. Thank you for your profound contributions to my personal and academic growth. The mentorship you have provided will undoubtedly inspire my future endeavors.

Next, to my second academic mentor Dr. Sook Wah Yee. Your guidance and support have gone far beyond the functional techniques critical to my research; you have adeptly guided me

through the intricacies of graduate school and the art of research. Likewise, I owe a tremendous thank you to Dr. Navneet Matharu for not only teaching me the skills that became the fundamental of my research, but also providing invaluable support in my personal life. And to Dr. Hai Nguyen, your guidance on my project has been indispensable. More than that, the insights and skills you've shared have been crucial in shaping me into an effective collaborator and researcher within the academic community. And to Dr. Willow Coyote-Maestas, thank you so much for this amazing collaboration and all your guidance on the ABCG2 deep mutational scanning project; I will truly miss working with you and learning from you.

To my thesis committee member, thank you for your time, expertise, and invaluable counsel. Your collective wisdom has been a cornerstone of my academic journey. To Dr. Michelle Arkin, for your insightful questions and suggestions, which prompted me to think in new directions and delve deeper into my research. To Dr. Ken Nakamura, for your careful attention to detail and your unwavering commitment to academic rigor.

A heartfelt acknowledgment goes to my colleagues from the Ahituv Lab — Serena Tamura, Dianne Laboy Cintron, Mai Nobuhara, Rachael Bradley, Kelly An, Yusuke Ito, Breanna Paredes, and Cassandra Biellak — as well as those from the Giacomini Lab — Jia Yang, Mina Azimi, Andrew Riselli, Bianca Vora, Dina Buitrago, Megan Koleske, Mark Ware and Kyle Sun. Beyond science, it is the support, and shared laughter that have truly cheered me up during those long days. Sharing this chapter of my life with all of you, learning and growing together, has been an honor and a privilege. Your friendship has been a source of comfort and joy in this demanding academic pursuit.

My sincere thanks go to my fellow PSPG classmates, who let me feel that San Francisco is my second home. A special note of gratitude to Emily Connelly, Michelle Wang, and Nilsa La Cunza

for being an exceptionally caring and understanding support system throughout my graduate school journey.

To my friends in far-flung corners of the world, Ruizhuo Chen, Boya Zhang, and Irene Kwok, whose friendships have not only with stood the trials of distance and time but have flourished. I am grateful and feel empowered to be in the company of such exceptionally successful women. Your achievements, support, and inspiration continue to amaze, uplift, and motivate me without end.

First and foremost, I extend my deepest gratitude to my family, whose unconditional love and support have been my greatest blessing. To my parents, my pillars of strength, thank you for every sacrifice, every lesson, and every bit of encouragement that has brought me to this pivotal moment in my life. Your guidance is the compass by which I navigate, and words fall short of capturing my immense appreciation. To my late grandmother, my heartfelt thanks for your unwavering support. From my earliest memories, you have been a constant presence in my life, always there for me whenever I needed you. Hope I did make you proud. To my mother, Zili, my unwavering supporter, thank you for being there for every phone call, big or small. You have been my inspiration since childhood, embodying the scientist I aspired to become. Your relentless encouragement and belief in me have shaped me in ways immeasurable. Your love, support, and encouragement are the foundations of my achievements. To my father, Jianming, thank you for being the epitome of kindness and patience. Your life has been a masterclass in resilience and grace, guiding me through my own journey with the quiet strength of your example.

Most importantly, to my husband Zizheng. Without you, I could not have accomplished all that I have. Your steadfast support has been my constant source of strength. You are my best partner

and my everything. I genuinely consider myself incredibly blessed to have you walking beside me through every chapter of our lives. To my son Leo, your presence in my life is a blessing I cherish deeply. Your smile is a powerful reminder and helps me maintain focus on what truly matters. Watching you grow and become your own person brings me an indescribable joy. I love you immensely and am grateful every day for the light you bring into our lives.

Contributions

This dissertation is structured into two main parts. Part A delves into the exploration of lifespan expression and the functional impact of polymorphisms on Blood-Brain Barrier transporters. Part B is dedicated to the development of cis-regulation therapy for Non-alcoholic Fatty Liver Disease/Steatohepatitis, comprising multiple chapters within each part. Several chapters from this dissertation are currently unpublished and are being prepared for manuscript submission. The chapters presented herein may not reflect their final published form and, in certain instances, have been moderately edited for clarity and coherence.

In part A:

Chapter 2 contains unpublished results from a manuscript that is in progress and will be submitted to a peer-reviewed journal: A Global Proteomics Analysis of Ontogeny and Aging of Protein on Blood-Brain Barrier. The author list is as follows and may not reflect the final order for the published form: Xujia Zhou, Mina Azimi, Niklas Handin, Andrew Riselli, Bianca Vora, Eden Chun, Qi Liu, ShiewMei Huang, Per Artursson, Sook Wah Yee, Kathleen M Giacomini.

Chapter 3 presents experimental results that have not yet been published, featuring contributions from Willow Coyote-Maestas, Christian Macdonald, and Jingyou Rao. Willow Coyote-Maestas was instrumental in the conceptualization and design of the ABCG2 DMS library. Christian Macdonald and Jingyou Rao performed the data analysis.

In Part B:

Chapter 2 contains unpublished experimental findings, with significant contributions from Kelly An, Yusuke Ito, Zizheng Li, Jia Yang, Liz Murray, Mai Nobuhara, Breanna Paredes, and Cassandra Biellak. Zizheng Li was responsible for administering the intravenous tail vein injections. Kelly An, Breanna Paredes, and Cassandra Biellak provided support for conducting

both the glucose tolerance and insulin tolerance tests. Furthermore, an extensive collaborative effort in dissection and sample collection was made by Yusuke Ito, PhD, Jia Yang, PhD, Liz Murray, Mai Nobuhara, Kelly An, and Breanna Paredes.

"Do not go where the path may lead, go instead where there is no path and leave a trail." -

Ralph Waldo Emerson

Exploring the Transporters Dynamics in Blood-Brain Barrier Functionality and Innovative Treatments for Non-Alcoholic Fatty Liver Disease/Steatohepatitis

Xujia Zhou

Abstract

This dissertation presents a multifaceted study exploring critical aspects of drug development, focusing on the transporters on Blood-Brain Barrier (BBB) and a novel approach for Non-Alcoholic Fatty Liver Disease/Steatohepatitis (NAFLD/NASH).

The first segment of this research offers an in-depth analysis of the BBB transporters, focusing on age-related changes in protein expression and the functional impact of polymorphisms. The Blood-Brain Barrier (BBB) serves as a selective barrier for a variety of small molecules, including chemical carcinogens, environmental toxins, and therapeutic drugs. This barrier is constructed from brain capillary endothelial cells, pericytes, and astrocytic end-feet, working in unison to protect neurons and maintain brain homeostasis throughout life. The selective nature of the BBB is attributed to the tight junctions within the capillaries, which prevent the free passage of small molecules, and also to an array of transporters that regulate the influx of essential nutrients and the exclusion of many xenobiotics. The goal of this part of the dissertation is to elucidate the effect of aging from neonates to elderly on the human BBB, with an emphasis on transporters. A secondary goal is to examine in detail the determinants of function of a key transporter in the human BBB, ATP-binding cassette transporter, ABCG2 (BCRP).

This part of the dissertation begins with an overview of the current understanding of elements that influence the operation of the BBB, particularly transporters. It starts with a review of the BBB's structural components and their joint function in sustaining barrier integrity. It then summarizes how the BBB controls the movement of nutrients and medicines into the brain through various transport methods. The discussion includes the development of the BBB, how it changes as we age, and how diseases may affect it, emphasizing the dynamics of BBB and the challenges it creates for creating brain-targeted drugs. The chapter then shifts to how genetic variants in transporters influence BBB function and drug disposition, focusing particularly on the prominently expressed ATP-binding cassette transporters ABCB1 and ABCG2. After the overview, this dissertation provides a rich set of comprehensive analyses how age and genetic variations in transporters impact the functionality of BBB to advance our understanding of the multifaceted regulatory framework that controls BBB in physiological and pathological contexts. Major gaps in our understanding of the BBB, which are addressed by this dissertation research, are highlighted.

Chapter 2 examines changes in the human BBB proteome throughout a human lifespan, noting the significant shifts in protein expression that influence barrier permeability and the transport of nutrients and drugs. It is acknowledged that the BBB matures after birth, adjusting its transport mechanisms to align with each stage of development, and later alters due to aging and neurodegenerative disorders. Yet, fully grasping these modifications in the human BBB is an ongoing challenge. This chapter introduces a comprehensive proteomic analysis of the evolution and senescence of proteins in brain microvessels (BMVs). Samples from healthy individuals across a wide age spectrum and Alzheimer’s disease patients were analyzed using LC-MS/MS. A plethora of proteins, including numerous SLC and ABC transporters, were identified. Network analysis of the BMV proteome suggested potential alterations in BBB permeability over time and pinpointed transporters crucial for nutrient supply and drug

penetration that exhibit age-dependent expression patterns. This investigation sheds light on the dynamic regulation of BBB proteins, emphasizing how transporter variations with age can affect drug permeability. These findings are crucial for refining pharmacokinetic modeling and therapeutic approaches across different stages of life.

The dissertation (Part A) then pivots to explore how genetic factors may alter the functionality of transporters, potentially causing variances in drug distribution within the brain. It focuses particularly on ABCG2, a transporter highly expressed at the BBB, noting that genetic variations leading to functional changes can result in differing drug responses. Utilizing deep mutational scanning (DMS), an innovative technique that combines next-generation sequencing (NGS) with functional outcomes of numerous variants, this study evaluated 12,724 variants of the ABCG2 gene. Our experimental setup was crafted to assess over ten thousand of missense, synonymous, and deletion variants of ABCG2 in a high-throughput manner. The abundance of ABCG2 was quantified, its surface expression was measured, and the functional effects of each variant were examined using the anti-cancer drug, mitoxantrone. The resulting detailed functional map, visualized through heatmaps and integrated with the structural data of ABCG2, helped identify crucial residues essential for ABCG2's function and poly-specificity. This study enhances our understanding of ABCG2 and lays the groundwork for future investigations into other ABC transporters. It underscores the value of DMS in dissecting the intricacies of pharmacogenetics and the mechanisms underlying drug resistance.

In summary, this part of the dissertation presents a comprehensive examination of the factors important for the functionality of BBB, shedding new light on transporters. Importantly, we unveil the BBB's dynamic protein regulation across the human lifespan, demonstrating how age-related changes affect drug permeability through a detailed proteomic analysis. Furthermore,

the dissertation explores how mutations influence transporter functionality, ABCG2 as an example for developing the platform. The innovative use of Deep Mutational Scanning (DMS) to assess thousands of ABCG2 variants provides a rich functional map, revealing key insights into the transporter's operation and offering a valuable resource for future pharmacogenetic and drug resistance research. Overall, these studies highlight the necessity of understanding the BBB's complex mechanisms to enhance drug delivery strategies and overcome barriers in treating neurological disorders including neurodegenerative diseases.

The second part of the dissertation (Part B) shifts focus to the global health issue of NAFLD and its more severe form, NASH. It investigates *Cis*-Regulation Therapy (CRT) as a novel treatment approach, utilizing nuclease-deficient gene-editing technologies to modify gene regulatory elements for therapeutic ends. Approximately 30% of people worldwide are affected by NAFLD, and about 25% of these cases may advance to NASH. NASH represents a more serious stage of NAFLD, marked by liver inflammation and damage due to fat accumulation in the liver. About 25% of those with NAFLD progress to NASH, characterized by significant liver inflammation and damage due to fat accumulation. Currently, the pharmacological treatment options for NAFLD/NASH are severely limited. Our study investigates the potential of CRT as an innovative treatment strategy. In our research, we explored the effectiveness of CRT as a promising new treatment strategy. CRT employs nuclease-deficient gene-editing technologies, such as dead Cas9 (dCas9) combined with transcriptional modulators, to alter the activity of gene regulatory elements for therapeutic purposes. The goal of this part of the dissertation research specifically focuses on the nuclear receptor-like protein 1 (NURR1, NR4A2), a transcription factor critical in regulating inflammation which is a hallmark of NASH.

This part of the dissertation initiates with an overview of existing treatment options for NAFLD/NASH, pinpointing their limitations and the urgent need for more effective interventions.

It further explores contemporary strategies in drug and therapeutic development targeting NAFLD/NASH, with a particular emphasis on animal models. After the overview, we present our findings that activating *Nurr1* through CRISPR activation (CRISPRa) offers a promising therapeutic strategy for NAFLD/NASH within FATZO mouse models. This technique has shown efficacy in improving glucose metabolism abnormalities and reducing the *CCL2-CCR2* axis, a critical inflammatory pathway, both before and after the onset of the disease. Our findings introduce a promising new therapeutic avenue for NAFLD/NASH, highlighting the capability of *Nurr1* activation to control and possibly reverse the disease's progression.

In summary, this dissertation delivers a comprehensive analysis of the variables impacting the functionality of BBB transporters and presents a promising therapeutic approach for NAFLD/NASH. Through this research, we aim to pave new pathways for the advancement of treatments for neurological and hepatic disorders.

Table of Contents

List of Figures

List of Tables

List of Abbreviations

AAV: Adeno-associated virus

ABCB1: ATP-binding cassette B1; P-gp, P-glycoprotein

ABCC: ATP binding cassette subfamily C member 4; MRP, Multidrug resistance protein

ABCG2: ATP-binding cassette super-family G member 2; BCRP, Breast cancer resistance protein

AD: Alzheimer's disease

BBB: Blood-brain barrier

BMVs: Brain microvessels

CNS: Central nervous system

CSF: Cerebrospinal fluid

DMS: Deep mutational scanning

NAFLD: Nonalcoholic fatty liver disease

NASH: Non-alcoholic steatohepatitis

Nurr1: Nuclear receptor related 1 protein; Nr4a2, Nuclear receptor 4A2

OAT: Organic Anion Transporter

OCT: Organic Cation Transporter

PBPK: Physiologically based pharmacokinetic

SLC transporter: Solute carrier transporter

SLCO: Solute carrier organic anion transporter family member; OATP, Organic anion transporting polypeptides

SNPs: single nucleotide polymorphisms

WDF: Western diet supplemented with 5% fructose water

Part A

Transporters in the Blood-Brain Barrier: Age-Related Changes in Protein Expression and Functional Impact of Polymorphisms

Chapter 1. Overview of the Blood-Brain Barrier: Structure, Transport Mechanisms, and Implications for Disease and Drug Delivery

1.1 Abstract

The Blood-Brain Barrier (BBB) is a critical regulator of the central nervous system's microenvironment, ensuring the selective entry of substances while protecting the brain from toxins and facilitating the transport of essential nutrients. This chapter focuses on the factors that influence BBB function, particularly transporters. The chapter begins with an overview of the structural components of the BBB and their collective role in maintaining barrier integrity. Subsequently, the focus shifts to transport mechanisms in the BBB, including active efflux transport, carrier-mediated transport, and transcytosis, underscoring their critical roles in the delivery of nutrients and drugs. Discussions extend to the development, aging, and effects of diseases on the BBB, highlighting its evolving nature throughout life and the consequent implications for drug development. Importantly, the obstacles presented by the BBB in the development of CNS drugs and the genetic factors that affect BBB function and disposition of drugs, are described, with a particular emphasis on two highly expressed ATP-binding cassette transporters, ABCB1 and ABCG2. The chapter ends with a brief discussion for future research needed to deepen our understanding of the BBB's physiological roles and the importance of developing targeted approaches to enhance drug delivery to the brain.

1.2 Structure of the Blood-Brain Barrier

To facilitate the optimal function of the central nervous system (CNS), a well-regulated microenvironment is essential. Serving as a selective interface, the Blood-Brain Barrier (BBB) regulates the passage of small molecules, including chemical carcinogens, environmental toxins, and therapeutic drugs [1]. The existence of the BBB was initially observed by Paul Ehrlich and subsequently validated by Edwin Goldmann [2]. It is composed of brain endothelial cells (BECs) that form the cerebral capillaries, pericytes that surround these capillaries, and the basement membrane (BM), a non-cellular layer produced by brain endothelial cells (BECs),

pericytes, and astrocytes. This structure provides not only physical support but also facilitates intercellular communication. Together with microglia and neuronal cells, these components constitute what is known as the neurovascular unit [3].

1.2.1 Brain Endothelial Cells (BECs)

As the core anatomical element of the BBB's architecture, BECs construct the cerebral vessels including the brain microvessels(BMVs) and interact with various cell types within the CNS. These cells differ significantly in both morphology and function from their peripheral counterparts [4].

Morphologically, they are connected by tight junctions and adherens junctions, creating distinct luminal and abluminal membrane domains. The tight junctions, composed of claudin, occludin, and junction adhesion molecules (JAMS), along with accessory proteins like Zonula occludens-1, -2, -3 (ZO-1, ZO-2, ZO-3), and cingulin, seal the intercellular space and regulate paracellular permeability and the diffusion of membrane proteins and lipids, thus preserving cellular polarity [5]. The formation of tight junctions is an early developmental feature of the BBB, establishing a selective barrier that only delivers essential molecules into the brain[6]. On the other hand, a reduction in tight junction proteins can lead to a loss of the BBB's integrity [7]. The adherens junctions, consisting of a cadherin-catenin complex and associated proteins, are vital for the structural cohesion of the BBB and the correct arrangement of tight junction proteins. These junctions provide mechanical support and play a role in signaling by linking to the tight junction protein ZO-1 and the cytoskeleton. [8] Beyond these specialized junctions, BECs are characterized by the absence of fenestrations (which are present in vascular endothelia of most other tissues), resisting the passive diffusion and rapid exchange of substances between the brain and the bloodstream[9].

Functionally, BECs exhibit a net negative surface charge, deterring negatively charged molecules, and express minimal levels of leukocyte adhesion molecules, limiting immune cell entry[10]. They are equipped with specific transporters for the precise regulation of substrate influx and efflux and are distinguished by a high trans-endothelial electrical resistance, which restricts the number of transcellular vesicles traversing the vessel wall [11].

1.2.2 Basement Membrane

The basement membrane, a layer of complex extracellular matrix proteins, supports epithelial and endothelial cells while segregating them from the underlying connective tissue. In the CNS, it separates the endothelial cells from neurons and glial cells. It is constructed from four primary structural proteins: collagen IV, nidogens, heparan sulfate proteoglycans (like perlecan), and laminins. Produced by BECs, pericytes, and astrocytes, the basement membrane is integral to vessel formation and the establishment and preservation of the BBB[12].

1.2.3 Pericytes

Pericytes, the mural cells found periodically along capillary walls, are embedded within the basement membrane and positioned on the outer side of endothelial cells[9]. Their proximity to endothelial cells facilitates the cross-talk between each other. For instance, endothelial cells release platelet-derived growth factor B (PDGF- B), which binds to PDGFRβ on pericytes, attracting them to the vasculature[13]. Conversely, pericytes can emit signals that influence endothelial cells by modulating tight junctions and orienting astrocytic end feet[14]. Besides their role in modulating the BBB, pericytes also participate in regulating angiogenesis, and neuroinflammation[15].

1.2.4 Astrocytes

Astrocytes, the dominant glial cells in the CNS, display a polarized and complex morphology that varies throughout the brain. Astrocytic foot processes envelop the innermost layer of the BBB, interweaving to create a nearly complete coverage. They play important roles in maintaining BBB function with dynamic signaling, which includes modulation of brain blood flow, vascular function, ion homeostasis, and regulation of neuroimmune responses[16]. Moreover, astrocytes contribute to the integrity of the BBB by secreting proteins like angiotensinogen, angiopoietin-1, and sonic hedgehog, which bind to BEC receptors and fortify tight junction stability[17].

1.3 Transport system on Blood-brain barrier

The tight junctions within the BBB significantly restrict the passive paracellular transport of water-soluble substances. Only a select few solutes are capable of crossing the BBB without transporter assistance. Gases like oxygen and carbon dioxide, along with small lipid-soluble molecules that either have lower molecular weight or simpler structures can diffuse through the BBB passively[18]. To maintain brain homeostasis, the BBB possesses a variety of transport systems designed to facilitate the entry of essential molecules into the brain which includes active efflux transport, carrier-mediated transport, and transcytosis (receptor-mediated transport, absorptive-mediated transport)[19].

1.3.1 Active efflux transport

Active efflux transport is primarily carried out by the ATP-binding cassette (ABC) family of transporters, which utilize ATP as energy to move molecules against the concentration gradient. These transporters are predominantly found on the luminal side of the endothelial plasma

membrane facing the blood at the Blood-Brain Barrier (BBB). Their main function is to prevent the build-up of drugs and xenobiotics in the brain and also acting as efflux pumps for endogenous metabolites. The key efflux transporters at the BBB include P-glycoprotein (P-gp, ABCB1), Multidrug Resistance-associated Proteins (MRPs, ABCC), and Breast Cancer Resistance Protein (BCRP, ABCG2)[20]. P-gp, which are abundantly expressed on the luminal membrane of the BBB, play a critical role in transporting substrates from the BECs back into the blood[21]. On the other hand, MRPs, which preferentially transport water-soluble conjugates, can be found on either the luminal or abluminal membranes[22].

1.3.2 Passive or secondary active transport

Passive or secondary active transport plays an important role in bypassing the restrictive nature of the BBB, which otherwise limits the entry of essential polar nutrients like glucose and amino acids—vital for metabolism and neuronal development [23]. Passive or secondary active transporters, mainly characterized by their high selectivity, predominantly facilitate the uptake of nutrients from the blood into the brain, though they are also capable of mediating efflux and operating as equilibrative transporters based on the concentration gradient[24]. These transporters are critical for normal brain development, and impairments in these transporters can lead to developmental disorders, including Glucose Transporter Type 1 Deficiency Syndrome, Riboflavin Transporter Deficiency, and Allan-Herndon-Dudley Syndrome (AHDS)[25].

A significant number of these transporters are part of the solute carrier (SLC) superfamily, which consists of multi-membrane passing proteins. Key SLC transporters involved in the delivery of macronutrients to the brain include the glucose transporter SLC2A1 (GLUT1), amino acid transporters SLC7A1 (CAT1) and SLC7A5 (LAT1), lactate transporter SLC16A1 (MCT1), fatty

acid transporter SLC27A1 (FATP1), and the docosahexaenoic acid (DHA) transporter SLC59A1 (MFSD2A). Many micronutrients, including vitamins, metals, and choline, are also delivered from the blood to the brain by SLC transporters, with examples being the riboflavin (Vitamin B2) transporter SLC52A2 (RFVT2), thiamine (Vitamin B1) transporters SLC19A3 (THTR2), and zinc transporter SLC30A10 (ZNT10)[26, 27]. Additionally, some transporters, which have been primarily characterized as xenobiotic or drug transporters, in the SLC family, such as the organic anion transporting peptides SLCO1A2 (OATP1A2) and SLCO2B1 (OATP2B1), along with the equilibrative nucleoside transporter SLC29A1 (ENT1), are also expressed at the BBB[28, 29].

1.3.3 Transcytosis

Transcytosis offers a pathway for the transport of large peptides, proteins, neuroactive peptides, regulatory proteins, hormones, and growth factors essential for brain development, which cannot cross the Blood-Brain Barrier (BBB) through the conventional passive or secondary active transport systems. Despite the BBB and tight junctions (TJs) largely obstructing the passage of substantial blood-borne molecules into the brain, specialized transcytotic mechanisms enable the selective transfer of these large entities across the BBB. There are primarily two forms of transcytosis at the BBB: receptor-mediated transcytosis (RMT) and adsorptive-mediated transcytosis (AMT). RMT involves the attachment of a ligand to a specific receptor on the plasma membrane, facilitating the bidirectional transport of proteins and peptides. Receptors engaged in this process include the transferrin receptor (TfR), insulin receptor (IR), leptin receptor (LEP-R), and lipoprotein receptors 1 and 2 (LRP1/2). The TfR and IR, in particular, have been extensively targeted for the delivery of drugs to the central nervous system (CNS)[30]. On the other hand, AMT operates independently of receptors, relying on caveolae. It starts with the attachment of molecules via electrostatic interactions with the

glycocalyx of endothelial cells, followed by endocytosis and subsequent transcytosis through BBB[31].

1.4 Development and aging of Blood brain barrier

The BBB is extremely important for maintaining homeostasis in the brain as well as for protecting neurons from neurotoxic substances present in the systemic circulation through our lifetimes.

1.4.1 Development of Blood-brain barrier

The construction of the selective barrier function of the blood-brain barrier (BBB) is not an intrinsic characteristic of endothelial cells when they initially migrate into the CNS. Rather, it is the result of a developmental process shaped by interactions with the neural environment during embryogenesis [32]. In rodents, the genesis of the BBB is marked by brain vascularization starting around embryonic day 11.5, as vessels from the perineural vascular plexus penetrate the brain by sprouting angiogenesis. Vascularization starts with growth factors released from the neural tube, which guide the vessels by engaging with receptors on the endothelial cells. As these vascular sprouts infiltrate the neural tube, they swiftly form a network within the brain's parenchyma.[33, 34] Upon their entry into the CNS, the nascent vessels promptly form functional tight junctions. Studies utilizing tracer injections reveal that these vessels are permeable to tracers only up until around E15.5, signifying an evolving barrier influenced predominantly by the Wnt signaling pathway. Concurrently, the barrier's maturation entails a downregulation of transcytosis, with the inhibition of this process by molecules such as Mfsd2a marking the establishment of a definitive barrier[35, 36].

In humans, the developmental timeline of the BBB remains unclear due to the difficulty in obtaining samples and executing standard BBB assays. Nonetheless, physiological and molecular studies suggest that the BBB matures postnatally, adapting to the evolving demands of each developmental phase to provide necessary nutrients while barring harmful substances. Ion gradients between cerebrospinal fluid (CSF) and plasma, detectable as early as the first-month post-birth, hint at the activity of cellular pumps and functional tight junctions at the BBB. Studies also highlight that certain amino acids such as serine, valine, histidine and arginine exhibit higher CSF/plasma concentration ratios in infancy compared to later childhood, mirroring the brain's heightened metabolic needs during rapid growth phases. [37-39]

As the brain develops, it benefits from both structural and cellular mechanisms for protection, akin to those in the adult brain. The information on ATP-binding cassette (ABC) transporters in the developing human brain is limited. However, emerging research indicates that transporters such as ABCG2(BCRP) are present at the BBB from as early as five weeks post-conception, with expressions of ABCG2(BCRP) and ABCB1(P-gp) escalating through the mid-gestational period.[40, 41] Additionally, P-gp and BCRP expression levels are also regulated by factors such as hypoxic stress, which are common in pregnancy with various situations including maternal smoking, heart failure, anemia, placental insufficiency, placenta accrete, placenta previa or preeclampsia[42].

In conclusion, the development of the BBB represents a complex interplay between cellular structures and molecular signals. This precise regulation is essential during the brain's development stages, ensuring the provision of necessary compounds while preventing potentially harmful agents from entering. Despite our advancing knowledge, a comprehensive understanding of the BBB's development remains largely elusive. As our understanding

continues to deepen, it could unveil new insights into the mechanisms of neurological disorders and pave the way for innovative therapeutic approaches.

1.4.2 Aging of the Blood-brain barrier

The transport mechanisms of amino acids through the blood-brain barrier (BBB) exhibit marked differences between neonates and adults, highlighting the nature of BBB functions across the lifespan. These functions evolve in response to the brain's developmental and maturing needs. It is hypothesized that the BBB's adaptability extends to aging processes, although delineating the effects of healthy aging from those induced by senescence remains challenging. This difficulty arises because even in the absence of clinical disease diagnosis, aging brains often harbor some level of pathology. Hence, "healthy aging" here is characterized by the gradual accumulation of cellular damage, including oxidative stress, epigenetic alterations, dysregulated cell signaling, and inflammatory responses[43].

Research employing dynamic contrast-enhanced magnetic resonance imaging (DCE-MRI) has uncovered disruptions within the hippocampus's blood-brain barrier (BBB) linked to healthy aging. These disturbances are associated with cognitive declines, traditionally considered a natural part of the aging process. Although direct evidence of BBB disruption in aging, such as changes in tight-junction proteins or an uptick in pinocytic vesicles, remains controversial, a reduction in the levels of soluble PDGFRβ in the cerebrospinal fluid indicates possible pericyte damage and degeneration[44]. In rodent studies, pericyte loss or diminished coverage on BECs has been shown to lead to increased BBB permeability[45]. Aging also impacts astrocytes, leading to hypertrophy and an increase in the expression of neuroinflammatory genes[46]. Changes related to aging are also apparent in the BBB's basement membrane (BM), which typically measures 40 to 100 nm in thickness. Human studies indicate a decrease in the

coverage of vessels by collagen type IV, a primary component of the BM, while noting an accumulation of collagen at some microvessels. This results in a thickened BM and a narrowed vessel diameter[47].

Despite a limited understanding, evidence suggests that aging leads to changes in the BBB transport systems, marked by a decline in glucose metabolism. This has been demonstrated in meta-analyses comparing cerebral glucose metabolism between older adults and younger individuals across various brain regions[48]. Studies using 11C-verapamil-PET have shown that the function of ABCB1 (P-gp) at the BBB starts to decline in middle age and continues to decrease into old age[49]. Additionally, P-gp activity is further diminished in vivo by factors such as inflammation, which are common in normal aging[50].

1.4.3 Blood-brain barrier breakdown in Alzheimer's disease

Alzheimer's disease (AD) presents a significant challenge in healthcare due to the lack of effective curative treatments. This complex, multifactorial neurodegenerative disorder is the most prevalent form of dementia. The two-hit vascular hypothesis suggests that AD begins with blood vessel damage, leading to dysfunction of the blood-brain barrier (BBB) and reduced brain clearance of proteins and toxic compounds[51]. This leads to neuronal damage and accumulation of amyloid-beta (Aβ) in the brain and eventually develops AD. However, the lack of a direct correlation between Aβ deposition and the symptoms of AD has prompted the exploration of alternative hypotheses, such as the role of Tau protein aggregation in the progression of AD. Neurofibrillary tangles stand as a significant pathological hallmark of Alzheimer's disease (AD), resulting from the aggregation of hyperphosphorylated tau proteins. These neurofibrillary tangles cause inflammation within neurons and also trigger the activation of glial cells. This sequence of events has been shown to disrupts the function of BBB, further

aggravating neuronal dysfunction[52]. Despite varied hypotheses regarding AD's pathogenesis, emerging evidence underscores BBB dysfunction in AD progression. DCE-MRI studies in early-stage AD patients have confirmed BBB breakdown in various regions of grey and white matter[53]. Additionally, observations in AD patient brain tissue include reductions in capillary length, diminished expression of tight junction proteins, and changes in the capillary basement membrane. Vascular endothelial growth factors (VEGFs) play a crucial role in the growth and maintenance of BMVs. In AD patients, higher expression of VEGFB in the prefrontal cortex correlates with more severe cognitive decline. Although the exact relationship between increased VEGFB levels and accelerated cognitive impairment remains unclear, it is noted that VEGFB can inhibit pathways related to cell death in neurons through interacting with its receptor VEGFR1. Consequently, VEGFR1-mediated signaling provides neuroprotective effects. Therefore, the connection between elevated VEGFB and rapid cognitive decline might actually represent a compensatory neural repair mechanism responding to the underlying AD pathology [54]. Reduced coverage and numbers of pericytes, marked by PDGFRβ, on brain capillaries have been noted in AD patient brain samples, alongside an increase in active astrocytes[55].

APOE, a protein involved in cholesterol transport, has highly correlated with amyloid accumulation in AD. Individuals carrying the APOE*ε4 isoform (has an increased genetic risk of AD) exhibit higher BBB permeability compared to non-carriers[56]. In AD patients, transport systems on the BBB are also compromised. For example, glucose uptake into the brain, primarily facilitated by SLC2A1 (GLUT1), is significantly reduced in the hippocampus well before clinical AD diagnosis and is even lower in various brain regions in early-stage AD [57]. Additionally, the activity of ABCB1 (P-gp), a crucial efflux transporter that aids in clearing Aβ across the BBB with the help of APOE and LDL receptor-related protein-1 (LRP1), is found to be reduced in the frontal and posterior cingulate cortices and hippocampus in mild AD[43].

In conclusion, the degradation of the BBB is a phenomenon associated with aging, and may play a significant role in the onset of neurodegenerative diseases, influenced by genetics and inflammation among other factors. The study of the BBB's integrity and function during aging and AD underscores the necessity for developing therapeutics targeting these vascular changes. However, there is a noticeable shortage of comprehensive studies that simultaneously explore the effects of aging and disease. Although constrained by the limited sample size of diseased subjects, this dissertation advocates for the intensification of BBB research examine the effects of aging and disease at the same time which could enhance our understanding and facilitate the development of early diagnostics for AD

1.5 Blood-brain barrier and CNS drug development

The Blood-Brain Barrier (BBB) plays a crucial role in protecting the brain by maintaining its homeostasis. However, it also poses a challenge for the delivery of medications to the CNS, limiting the treatment of brain-related conditions such as neurodegenerative diseases and brain tumor. BBB are closely surrounded by neurons (no further than 25μm away) which makes it a preferred pathway for drug delivery over other less direct routes. Consequently, this situation drives researchers to devise effective methods for modulating BBB permeability and developing targeted delivery systems to circumvent these limitations[58].

The main mechanisms through which drugs cross the BBB include transcellular passive diffusion, passive or secondary active transport, and transcytosis. The penetration of most drugs into the brain relies on transmembrane diffusion, with their ability to penetrate being significantly influenced by their characteristics such as lipid solubility, molecular weight, the fraction of unbound drug, and peripheral pharmacokinetics. Hydrophilic drugs find it more challenging to cross the BBB compared to lipophilic drugs and typically rely on influx transporters or

transcytosis[31]. Levodopa which is considered the standard treatment for Parkinson's disease, and low-dose levodopa therapy has been applied to treat various neurological disorders in children, including speech delay, and Rett syndrome[59]. Levodopa is too hydrophilic to diffuse freely across membranes but can cross the BBB as they are substrates for BBB transporters SLC7A5 (LAT1)[60]. Recently, the development of antibodies or peptide ligands targeting the transferrin or insulin receptors has emerged as a strategy for delivering drugs to the brain through receptor-mediated transcytosis (RMT). As of 2023, several antibody drug candidates targeting neurodegenerative diseases are in clinical trials, utilizing transferrin receptor binding (TFRC) for brain delivery, though none have yet received FDA approval[61].

Moreover, the presence of specific efflux transporters, like P-glycoprotein (P-gp), restricts the entry of numerous drugs that would otherwise permeate membranes. Research indicates that P-gp expression increases during fetal development, reaching maturity by the 40th week of gestation, and its functionality begins to decline from middle age onwards. Extended exposure to opioids and benzodiazepines in extremely preterm infants has been linked to reduced cognitive, motor, and language abilities[62]. Elderly patients also are more susceptible to neurotoxicity from these drugs, many of which are either substrates or inhibitors of P-gp[63].

Increasing evidence suggests that BBB permeability varies with age and disease due to changes in its components and transport proteins. Although it is well-known that both younger and older patients are more sensitive to neurotoxic effects, in fact, 50 to 90% of medications prescribed to these age groups are only based on safety and efficacy profiles derived from adult studies. Therefore, a deeper understanding of how age-related alterations in the BBB affect CNS drug delivery is vital for the development of safer and more effective treatments for both pediatric and geriatric populations.

1.6 Genetic impact on BBB function and brain drug disposition

The functionality of the Blood-Brain Barrier (BBB) is known to vary with age and is also influenced by factors such as hypoxia, inflammation, and genetics[64]. Mutations in key components of the basement membrane, specifically Collagen Type IV Alpha 1 and Alpha 2 (COL4A1 and COL4A2), are linked to brain small vessel disease-2. This condition is marked by a range of neurological impairments resulting from disrupted BBB that leads to cerebral degeneration[65]. Additionally, defects in SLC49A2 (FLVCR2), a heme transporter on the BBB essential for brain angiogenesis, are associated with Fowler syndrome. This syndrome is characterized by hydranencephaly and a unique glomerular vasculopathy in the central nervous system[66]. Genetic variations in transporters also contribute to alterations in drug distribution within the brain, potentially leading to neurotoxicity or reduced effectiveness of drugs on their intended targets. While mutations in influx transporters significantly affect the brain disposition of certain drugs, ABC transporters—particularly ABCB1 (P-gp) and ABCG2 (BCRP)—play crucial roles in brain drug delivery. Highly expressed on the BBB, these transporters have broad substrate specificity, including various anticancer drugs, antiepileptic drugs, and statins, thereby preventing their entry into the brain.

1.6.1 The ATP-binding cassette B1(ABCB1)

The initial identification of daunorubicin's active efflux from cells marked the earliest documentation of a chemotherapy resistance mechanism facilitated by a member of the ABC transporter family in 1973[67]. Subsequent research revealed that this transporter was a cell surface glycoprotein, which was eventually designated as the ATP-binding cassette B1 (ABCB1, or P-glycoprotein). ABCB1 functions as a unidirectional transmembrane efflux pump, utilizing ATP to actively transport substances out of cells against their concentration gradients. It is predominantly expressed in tissues as protective barriers, such as the epithelial cells of the

liver, kidney, small and large intestines, and the capillary endothelial cells in the brain, ovaries, and testes[68]. ABCB1 plays a significant role in the emergence of drug resistance by being overexpressed in cancer cells and efflux anticancer drugs, thereby diminishing their effectiveness.

Furthermore, ABCB1 has also been recognized for its impact on the disposition of numerous drugs, with polymorphisms linked to variations in drug pharmacokinetics (PK) and effects. Mutations in ABCB1 have been associated with increased bioavailability of digoxin[69]. Moreover, though controversial, the ABCB1 synonymous polymorphism (3435C > T) has been linked to variations in ABCB1 expression and functionality, with affected individuals exhibiting significantly elevated cerebrospinal fluid (CSF) concentrations of phenobarbital and a higher frequency of seizures[70].

1.6.2 ATP-binding cassette super-family G member 2 (ABCG2)

The ABCG2 gene, also known as the human breast cancer resistance protein (BCRP), was first identified in a breast cancer cell line exhibiting multidrug resistance in 1998. This discovery highlighted its role in conferring resistance to chemotherapeutic drugs, including mitoxantrone and topotecan. ABCG2 (BCRP) belongs to the G-subfamily of ABC transporters and operates as a 'half-transporter', comprising one nucleotide-binding domain (NBD) and one transmembrane domain (TMD) within a single polypeptide chain. Functional ABCG2 exists as a homodimer with an approximate molecular weight of 144 kDa[71]. It is prominently expressed in the placenta, intestines, liver, BECs, and kidneys. This expression pattern enables ABCG2 (BCRP) to play a crucial role in the absorption, distribution, and excretion of drugs and endogenous substances, in addition to safeguarding tissues from harmful xenobiotic substances.

Although there has been numerous single nucleotide polymorphisms (SNPs) identified in the ABCG2 gene (gnomAD v4.0.0 variants 2725), only a handful of them have been functionally characterized. ABCG2 has two common missense genetic variants with a prevalence of ≥1%: V12M (rs2231137) and Q141K (rs2231142)[72]. The Q141K variant, situated between the Walker A motif and the signature region within the ATP-binding domain, notably affects ABCG2 expression levels[73].

Research has established a robust connection between ABCG2 variants and gout, indicating that polymorphisms in ABCG2 can elevate serum urate levels (hyperuricemia). Analyses have supported the theory that ABCG2 influences gout through reduced intestinal excretion of urate. Specifically, the Q141K genotype has been associated with a diminished response to allopurinol and its metabolite, oxypurinol, which are commonly used urate-lowering treatments[74, 75]. Furthermore, statins, essential for preventing cardiovascular diseases, have been explored for their potential to slow cognitive decline in the elderly. Lipophilic statins can passively diffuse across the blood-brain barrier (BBB), but many commonly prescribed statins, including atorvastatin, pravastatin, and rosuvastatin, are substrates for ABCG2. Studies in rodents have shown that the brain disposition of statins is reliant on ABCG2's functional expression at the BBB, with inhibition of ABCG2 resulting in increased atorvastatin brain exposure by 30%[76]. Recent research has also proposed a link between ABCG2 and Alzheimer’s disease, characterized by early brain accumulation of Aβ peptides and plaques. Findings suggest that ABCG2 is upregulated in the brains of Alzheimer’s patients and that the absence of Abcg2 in mice leads to greater Aβ peptide accumulation and increased NF-KB activation[77, 78]. This indicates that BCRP may protect the brain from Aβ peptides through its efflux mechanisms.

1.7 Conclusion

The BBB stands as a pivotal guardian of the brain's homeostasis, and is designed to regulate the entry and exit of substances. Its complex structure and transport mechanisms ensure the brain's protection from harmful agents and the efficient delivery of essential nutrients. In spite of its critical role, the blood brain barrier has not garnered sufficient attention from researchers and there are major gaps in our understanding of its physiologic, pharmacologic and pathologic roles. Thus, there is a pressing need for more research on the BBB in humans. Increasing evidence indicates that the development of the BBB is a finely tuned process that adapts to the changing needs of the brain from embryogenesis through aging. Yet, human-centric studies are notably limited. To date, the most comprehensive investigation into human BBB development is a small-scale, single-cell RNA sequencing study focused on fetal samples. This research faces limitations due to small sample sizes and the gap between mRNA expression and protein activity. Significant differences between species especially in the brain make the direct application of findings from animals challenging and underscore the need for more studies in human BBB and in particular in the developing human BBB. In addition, aging is associated with many changes in the brain yet research in BBB from elderly and across the human lifespan is clearly needed to understand changes in the BBB function with age.

Although it is well-known that ATP-binding cassette transporters are crucial in mediating drug disposition and also resistance, thereby influencing disease treatment and the management of drug effectiveness and safety, the functionality of genetic variants in these transporters, especially ABCG2, has been largely unexplored. There has been no comprehensive screening of all variants of any ABC transporter, significantly impeding the development of new treatments and strategies for effective brain drug delivery.

This part of the dissertation aims to elucidate the BBB's complex roles and the determinants of its function, which are essential for the progression of therapeutic approaches targeting the central nervous system. It introduces the first extensive proteomics analysis of the BBB across the human lifespan, from neonates to the elderly, providing valuable insights into the BBB's functional evolution. Moreover, this dissertation also presents the first exhaustive screening of ABCG2 variants, highlighting a path toward improved therapeutic effectiveness and drug delivery strategies. Through this work, we aim to pave the way for advancements in treating neurological disorders and enhancing drug delivery efficacy.

1.8 Figures

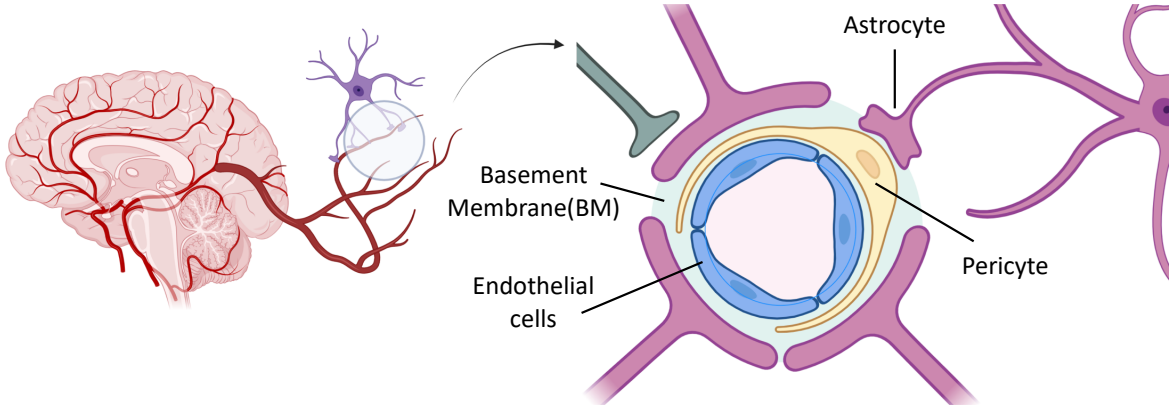

Figure 1.1. The structure of blood brain barrier

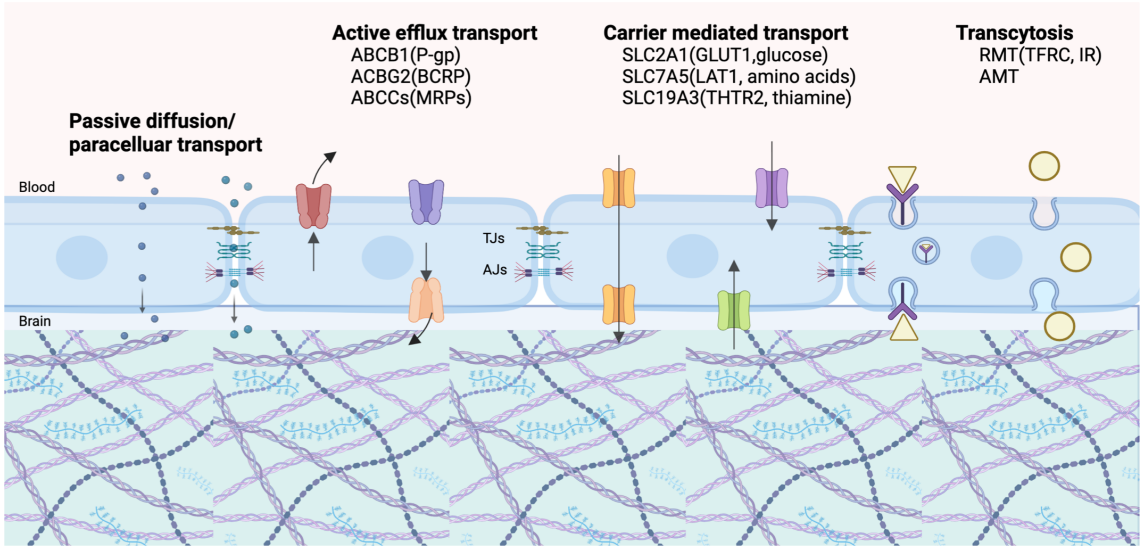

Figure 1.2. Transport mechanisms across the blood-brain barrier

1.9 References

1. Barar, J., et al., *Blood-brain barrier transport machineries and targeted therapy of brain diseases.* Bioimpacts, 2016. **6**(4): p. 225-248.
2. Liebner, S., C.J. Czupalla, and H. Wolburg, *Current concepts of blood-brain barrier development.* Int J Dev Biol, 2011. **55**(4-5): p. 467-76.
3. McConnell, H.L. and A. Mishra, *Cells of the Blood-Brain Barrier: An Overview of the Neurovascular Unit in Health and Disease.* Methods Mol Biol, 2022. **2492**: p. 3-24.
4. Reese, T.S. and M.J. Karnovsky, *Fine structural localization of a blood-brain barrier to exogenous peroxidase.* J Cell Biol, 1967. **34**(1): p. 207-17.
5. Luissint, A.C., et al., *Tight junctions at the blood brain barrier: physiological architecture and disease-associated dysregulation.* Fluids Barriers CNS, 2012. **9**(1): p. 23.
6. Abbott, N.J., et al., *Structure and function of the blood-brain barrier.* Neurobiol Dis, 2010. **37**(1): p. 13-25.
7. Furuse, M., et al., *Occludin: a novel integral membrane protein localizing at tight junctions.* J Cell Biol, 1993. **123**(6 Pt 2): p. 1777-88.
8. Stamatovic, S.M., et al., *Junctional proteins of the blood-brain barrier: New insights into function and dysfunction.* Tissue Barriers, 2016. **4**(1): p. e1154641.
9. Daneman, R. and A. Prat, *The blood-brain barrier.* Cold Spring Harb Perspect Biol, 2015. **7**(1): p. a020412.
10. Santa-Maria, A.R., et al., *Flow induces barrier and glycocalyx-related genes and negative surface charge in a lab-on-a-chip human blood-brain barrier model.* J Cereb Blood Flow Metab, 2021. **41**(9): p. 2201-2215.
11. Zhao, Y., et al., *The Role of Ferroptosis in Blood-Brain Barrier Injury.* Cell Mol Neurobiol, 2023. **43**(1): p. 223-236.

12. Thomsen, M.S., L.J. Routhe, and T. Moos, *The vascular basement membrane in the healthy and pathological brain.* Journal of Cerebral Blood Flow and Metabolism, 2017. **37**(10): p. 3300-3317.

13. Hellstrom, M., et al., *Role of PDGF-B and PDGFR-beta in recruitment of vascular smooth muscle cells and pericytes during embryonic blood vessel formation in the mouse.* Development, 1999. **126**(14): p. 3047-55.

14. Armulik, A., et al., *Pericytes regulate the blood-brain barrier.* Nature, 2010. **468**(7323): p. 557-61.

15. Hattori, Y., *The Multiple Roles of Pericytes in Vascular Formation and Microglial Functions in the Brain.* Life (Basel), 2022. **12**(11).

16. Abbott, N.J., L. Ronnback, and E. Hansson, *Astrocyte-endothelial interactions at the blood-brain barrier.* Nat Rev Neurosci, 2006. **7**(1): p. 41-53.

17. Puebla, M., P.J. Tapia, and H. Espinoza, *Key Role of Astrocytes in Postnatal Brain and Retinal Angiogenesis.* Int J Mol Sci, 2022. **23**(5).

18. Pardridge, W.M., *Drug transport across the blood-brain barrier.* J Cereb Blood Flow Metab, 2012. **32**(11): p. 1959-72.

19. Knox, E.G., et al., *The blood-brain barrier in aging and neurodegeneration.* Mol Psychiatry, 2022. **27**(6): p. 2659-2673.

20. Gil-Martins, E., et al., *Dysfunction of ABC transporters at the blood-brain barrier: Role in neurological disorders.* Pharmacol Ther, 2020. **213**: p. 107554.

21. Virgintino, D., et al., *Fetal blood-brain barrier P-glycoprotein contributes to brain protection during human development.* J Neuropathol Exp Neurol, 2008. **67**(1): p. 50-61.

22. Roberts, L.M., et al., *Subcellular localization of transporters along the rat blood-brain barrier and blood-cerebral-spinal fluid barrier by in vivo biotinylation.* Neuroscience, 2008. **155**(2): p. 423-38.

23. Nguyen, Y.T.K., et al., *The role of SLC transporters for brain health and disease.* Cell Mol Life Sci, 2021. **79**(1): p. 20.

24. Khan, N.U., et al., *Carrier-mediated transportation through BBB*, in *Brain targeted drug delivery system*. 2019, Elsevier. p. 129-158.

25. Lin, L., et al., *SLC transporters as therapeutic targets: emerging opportunities.* Nat Rev Drug Discov, 2015. **14**(8): p. 543-60.

26. Tiani, K.A., P.J. Stover, and M.S. Field, *The Role of Brain Barriers in Maintaining Brain Vitamin Levels.* Annu Rev Nutr, 2019. **39**: p. 147-173.

27. Hu, C., et al., *The solute carrier transporters and the brain: Physiological and pharmacological implications.* Asian J Pharm Sci, 2020. **15**(2): p. 131-144.

28. Morris, M.E., V. Rodriguez-Cruz, and M.A. Felmlee, *SLC and ABC Transporters: Expression, Localization, and Species Differences at the Blood-Brain and the Blood-Cerebrospinal Fluid Barriers.* AAPS J, 2017. **19**(5): p. 1317-1331.

29. Sweeney, M.D., et al., *Blood-Brain Barrier: From Physiology to Disease and Back.* Physiol Rev, 2019. **99**(1): p. 21-78.

30. Pulgar, V.M., *Transcytosis to Cross the Blood Brain Barrier, New Advancements and Challenges.* Front Neurosci, 2018. **12**: p. 1019.

31. Kadry, H., B. Noorani, and L. Cucullo, *A blood-brain barrier overview on structure, function, impairment, and biomarkers of integrity.* Fluids and Barriers of the Cns, 2020. **17**(1).

32. Langen, U.H., S. Ayloo, and C. Gu, *Development and Cell Biology of the Blood-Brain Barrier.* Annu Rev Cell Dev Biol, 2019. **35**: p. 591-613.

33. Daneman, R., et al., *Pericytes are required for blood-brain barrier integrity during embryogenesis.* Nature, 2010. **468**(7323): p. 562-6.

34. Engelhardt, B., *Development of the blood-brain barrier.* Cell Tissue Res, 2003. **314**(1): p. 119-29.

35. Ben-Zvi, A., et al., *Mfsd2a is critical for the formation and function of the blood-brain barrier.* Nature, 2014. **509**(7501): p. 507-11.

36. Daneman, R., et al., *Wnt/beta-catenin signaling is required for CNS, but not non-CNS, angiogenesis.* Proc Natl Acad Sci U S A, 2009. **106**(2): p. 641-6.

37. Akiyama, T., et al., *CSF/plasma ratios of amino acids: reference data and transports in children.* Brain Dev, 2014. **36**(1): p. 3-9.

38. Scholl-Burgi, S., et al., *Amino acid cerebrospinal fluid/plasma ratios in children: influence of age, gender, and antiepileptic medication.* Pediatrics, 2008. **121**(4): p. e920-6.

39. Jimenez, E., et al., *[Amino acids in cerebrospinal fluid and plasma: its usefulness in the study of neuropaediatric diseases].* Rev Neurol, 2012. **54**(7): p. 394-8.

40. Mollgard, K., et al., *Brain barriers and functional interfaces with sequential appearance of ABC efflux transporters during human development.* Sci Rep, 2017. **7**(1): p. 11603.

41. Crouch, E.E., et al., *Ensembles of endothelial and mural cells promote angiogenesis in prenatal human brain.* Cell, 2022. **185**(20): p. 3753-3769 e18.

42. Mughis, H., et al., *Hypoxia modulates P-glycoprotein (P-gp) and breast cancer resistance protein (BCRP) drug transporters in brain endothelial cells of the developing human blood-brain barrier.* bioRxiv, 2023: p. 2023.05.24.540054.

43. Sweeney, M.D., A.P. Sagare, and B.V. Zlokovic, *Blood-brain barrier breakdown in Alzheimer disease and other neurodegenerative disorders.* Nature Reviews Neurology, 2018. **14**(3): p. 133-150.

44. Montagne, A., et al., *Blood-brain barrier breakdown in the aging human hippocampus.* Neuron, 2015. **85**(2): p. 296-302.

45. Berthiaume, A.A., et al., *Pericyte remodeling is deficient in the aged brain and contributes to impaired capillary flow and structure.* Nat Commun, 2022. **13**(1): p. 5912.

46. Palmer, A.L. and S.S. Ousman, *Astrocytes and Aging.* Front Aging Neurosci, 2018. **10**: p. 337.

47. Uspenskaia, O., et al., *Aging is associated with increased collagen type IV accumulation in the basal lamina of human cerebral microvessels.* BMC Neurosci, 2004. **5**: p. 37.

48. Deery, H.A., et al., *Lower brain glucose metabolism in normal ageing is predominantly frontal and temporal: A systematic review and pooled effect size and activation likelihood estimates meta-analyses.* Hum Brain Mapp, 2023. **44**(3): p. 1251-1277.

49. Toornvliet, R., et al., *Effect of age on functional P-glycoprotein in the blood-brain barrier measured by use of (R)-[(11)C]verapamil and positron emission tomography.* Clin Pharmacol Ther, 2006. **79**(6): p. 540-8.

50. Schulz, J.A., A.M.S. Hartz, and B. Bauer, *ABCB1 and ABCG2 Regulation at the Blood-Brain Barrier: Potential New Targets to Improve Brain Drug Delivery.* Pharmacol Rev, 2023. **75**(5): p. 815-853.

51. Zhu, X., et al., *Alzheimer's disease: the two-hit hypothesis.* Lancet Neurol, 2004. **3**(4): p. 219-26.

52. Chen, Y., et al., *Blood-brain barrier dysfunction and Alzheimer's disease: associations, pathogenic mechanisms, and therapeutic potential.* Front Aging Neurosci, 2023. **15**: p. 1258640.

53. Verheggen, I.C.M., et al., *Increase in blood-brain barrier leakage in healthy, older adults.* Geroscience, 2020. **42**(4): p. 1183-1193.

54. Mahoney, E.R., et al., *Brain expression of the vascular endothelial growth factor gene family in cognitive aging and alzheimer's disease.* Mol Psychiatry, 2021. **26**(3): p. 888-896.

55. Sagare, A.P., et al., *Pericyte loss influences Alzheimer-like neurodegeneration in mice.* Nat Commun, 2013. **4**: p. 2932.

56. Kirchner, K., et al., *Detrimental Effects of ApoE epsilon4 on Blood-Brain Barrier Integrity and Their Potential Implications on the Pathogenesis of Alzheimer's Disease.* Cells, 2023. **12**(21).

57. Nordberg, A., et al., *The use of PET in Alzheimer disease.* Nat Rev Neurol, 2010. **6**(2): p. 78-87.

58. Wu, D., et al., *The blood-brain barrier: structure, regulation, and drug delivery.* Signal Transduction and Targeted Therapy, 2023. **8**(1).

59. Hoshino, K., et al., *Very-Low-Dose Levodopa Therapy for Pediatric Neurological Disorders: A Preliminary Questionnaire in Japan.* Frontiers in Pediatrics, 2021. **9**.

60. Rusch, C., et al., *To restrict or not to restrict? Practical considerations for optimizing dietary protein interactions on levodopa absorption in Parkinson's disease.* NPJ Parkinsons Dis, 2023. **9**(1): p. 98.

61. Choi, E.S. and E.V. Shusta, *Strategies to identify, engineer, and validate antibodies targeting blood-brain barrier receptor-mediated transcytosis systems for CNS drug delivery.* Expert Opin Drug Deliv, 2023. **20**(12): p. 1789-1800.

62. Puia-Dumitrescu, M., et al., *Assessment of 2-Year Neurodevelopmental Outcomes in Extremely Preterm Infants Receiving Opioids and Benzodiazepines.* Jama Network Open, 2021. **4**(7).

63. Jansen, P.A. and J.R. Brouwers, *Clinical pharmacology in old persons.* Scientifica (Cairo), 2012. **2012**: p. 723678.

64. Galea, I., *The blood-brain barrier in systemic infection and inflammation.* Cellular & Molecular Immunology, 2021. **18**(11): p. 2489-2501.

65. Zagaglia, S., et al., *Neurologic phenotypes associated with COL4A1/2 mutations: Expanding the spectrum of disease.* Neurology, 2018. **91**(22): p. e2078-e2088.

66. Kvarnung, M., et al., *Mutations in FLVCR2 associated with Fowler syndrome and survival beyond infancy.* Clin Genet, 2016. **89**(1): p. 99-103.

67. Dano, K., *Active outward transport of daunomycin in resistant Ehrlich ascites tumor cells.* Biochim Biophys Acta, 1973. **323**(3): p. 466-83.

68. Ahmed, J., II, et al., *P-glycoprotein: new insights into structure, physiological function, regulation and alterations in disease.* Heliyon, 2022. **8**(6): p. e09777.

69. Kurata, Y., et al., *Role of human MDR1 gene polymorphism in bioavailability and interaction of digoxin, a substrate of P-glycoprotein.* Clin Pharmacol Ther, 2002. **72**(2): p. 209-19.

70. Basic, S., et al., *The influence of C3435T polymorphism of ABCB1 gene on penetration of phenobarbital across the blood-brain barrier in patients with generalized epilepsy.* Seizure, 2008. **17**(6): p. 524-30.

71. Taylor, N.M.I., et al., *Structure of the human multidrug transporter ABCG2.* Nature, 2017. **546**(7659): p. 504-509.

72. Cleophas, M.C., et al., *ABCG2 polymorphisms in gout: insights into disease susceptibility and treatment approaches.* Pharmgenomics Pers Med, 2017. **10**: p. 129-142.

73. Furukawa, T., et al., *Major SNP (Q141K) variant of human ABC transporter ABCG2 undergoes lysosomal and proteasomal degradations.* Pharm Res, 2009. **26**(2): p. 469-79.

74. Brackman, D.J. and K.M. Giacomini, *Reverse Translational Research of ABCG2 (BCRP) in Human Disease and Drug Response.* Clin Pharmacol Ther, 2018. **103**(2): p. 233-242.

75. Vora, B., et al., *Oxypurinol pharmacokinetics and pharmacodynamics in healthy volunteers: Influence of BCRP Q141K polymorphism and patient characteristics.* Clin Transl Sci, 2021. **14**(4): p. 1431-1443.

76. Betterton, R.D., et al., *Regulation of Blood-Brain Barrier Transporters by Transforming Growth Factor-beta/Activin Receptor-Like Kinase 1 Signaling: Relevance to the Brain Disposition of 3-Hydroxy-3-Methylglutaryl Coenzyme A Reductase Inhibitors (i.e., Statins).* Drug Metab Dispos, 2022. **50**(7): p. 942-956.

77. Xiong, H., et al., *ABCG2 is upregulated in Alzheimer's brain with cerebral amyloid angiopathy and may act as a gatekeeper at the blood-brain barrier for Abeta(1-40) peptides.* J Neurosci, 2009. **29**(17): p. 5463-75.

78. Shen, S., et al., *ABCG2 reduces ROS-mediated toxicity and inflammation: a potential role in Alzheimer's disease.* J Neurochem, 2010. **114**(6): p. 1590-604.

Chapter 2. A Global Proteomics Analysis of Ontogeny and Aging on the Expression Levels of Proteins in the Human Blood-Brain Barrier

2.1 Abstract

The Blood-Brain Barrier (BBB) is a crucial selective barrier that regulates the entry of molecules like nutrients, environmental toxins, and therapeutic medications into the brain. This function relies heavily on brain endothelial cell proteins, particularly transporters and tight junction proteins. It's recognized that BBB continues to develop postnatally, adapting its transport mechanisms to suit each stage of growth, and it also changes due to aging and neurodegenerative diseases. However, comprehensively understanding the mechanism of these changes in human BBB remains challenging.

This study presents a global proteomics analysis focused on the ontogeny and aging of proteins in the brain microvessels (BMVs), predominantly composed of brain endothelial cells. BMVs from healthy individuals (n=34, neonates to elderly) and Alzheimer's disease patients (n=3) were assessed using LC-MS/MS. 6,887 proteins were identified from in the BMV proteome including 136 SLC transporters and 26 ABC transporters. Differential protein expression analysis and network analysis revealed possible BBB permeability alteration through human lifetimes and also identified age-dependent expression patterns in transporters that are important for nutrient delivery and drug penetration.

In summary, this study provides insights into the dynamic regulation of BBB proteins, highlighting the age-dependent variation of transporters and their implications for drug permeability. These results can be used to improve physiologically based pharmacokinetic modelling and therapeutic strategies across different life stages.

2.2 Introduction

The Blood-Brain Barrier (BBB) stands as an important tight barrier that selectively regulates the entry of various small molecules, including nutrients essential for brain function, chemical carcinogens, and therapeutic medications. This barrier comprises brain microvessels (BMVs) that form the capillaries, pericytes that envelop them, astrocytic end-feet surrounding these two layers, and the basement membrane (BM), a non-cellular component synthesized by BMVs, pericytes, and astrocytes, providing structural support and facilitating cell communication[1, 2]. The tight junctions between BMVs, including claudin, occludin, junction adhesion molecules, and zonula occludens proteins, are one of the key components to keep BBB functioning, significantly restrict the passive paracellular transport of water-soluble substances[3].

To maintain brain homeostasis, the BBB possesses a variety of transport systems that enable the entry of essential molecules into the brain and prevent the accumulation of potential toxins, such as active efflux transport, carrier-mediated transport, and transcytosis (receptor-mediated and absorptive-mediated transport)[4]. Active efflux transporters, mainly represented by the ATP-binding cassette (ABC) family members, P-gp (ABCB1) and BCRP (ABCG2), are highly expressed on the luminal side of endothelial plasma membranes at the BBB. Their primary role is to prevent the accumulation of xenobiotics in the brain, while also functioning as efflux pumps for endogenous metabolites[5]. On the other hand, many CNS active drugs fail in drug development BMVause lack of drug entry into the brain restricted by these transporters. Uptake transporters are crucial for circumventing the restrictive nature of the BBB, which would otherwise limit the entry of vital macronutrients (like glucose and amino acids) and micronutrients (such as vitamins and metals)[6, 7]. Many of these transporters belong to the solute carrier (SLC) superfamily, including the glucose transporter SLC2A1 (GLUT1), amino acid transporter SLC7A5 (LAT1), riboflavin transporter SLC52A2 and heme transporter

SLC49A2 (FLVCR2)[6, 8-10]. These transporters are essential for normal brain development, and impairments can lead to developmental disorders, such as Glucose Transporter Type 1 Deficiency Syndrome, Brown-Vialetto-Van Laere syndrome-2 and Fowler syndrome(https://www.omim.org/).

Despite the important role of these transporters in maintaining BBB integrity and homeostasis, research exploring their variation over a lifetime is limited. While previous proteomic studies have identified SLC transporters in the BBB, these studies often had small sample sizes and a narrow focus on adult and elderly populations[11-13]. Evidence suggests that the BBB undergoes significant developmental changes after birth, adjusting its transport mechanisms to align with each growth stage[14]. However, transcriptomic and immunohistochemical research focused on early BBB development has been constrained by small cohorts and the well-documented gap between mRNA expression and protein activity—the latter being the key modulators of biological functions and metabolic pathways[15-17]. The exact correlation between protein expression of transporters in the developing human brain and BBB function remains to be established.

Furthermore, while the abundance of transporters and BBB permeability are recognized as influencing drug exposure in the brain, most pharmacological studies have been conducted on adult patients. In fact, 50 to 90% of drugs prescribed to children or the elderly are based on the safety and efficacy data from adult studies, leading to a higher incidence of adverse drug reactions and therapeutic failures in these vulnerable populations[18, 19]. Therefore, there is a major gap in our understanding of age-dependent changes in transporter expression within the BBB. In addition, various neurological disorders, such as stroke, epilepsy, and Alzheimer's disease, can alter BBB function[20-22]. These alterations can either hinder drug penetration or permit excessive drug entry, causing potential toxicities. Although considerable focus has been

on the efflux pump ABCG2 (P-gp) and tight-junction proteins[23-25], the effect of these disorders on the expression levels of other vital transporters, especially those involved in nutrient penetration, and other proteins important for BBB permeability has not been thoroughly examined.

This study aims to provide a comprehensive analysis of protein expression changes at the BBB across three critical age stages — development, adulthood, and old age — focusing specifically on transporters, as their expression levels can significantly impact the pharmacokinetics of drugs in the brain. In addition, we present an exploratory study of the expression of transporters in BBB of a few patients with Alzheimer's disease. Addressing these knowledge gaps is crucial for ensuring proper dosing, minimizing neurotoxicity, and maximizing therapeutic efficacy.

2.3 Results

2.3.1 Workflow and overview of BMV proteome

Global proteomic analysis using LC-MS/MS was conducted on BMVs isolated from thirty-four healthy brain specimens, collected from neonate to elderly individuals, as well as four Alzheimer's disease samples (Supplemental Table 2.1). For analysis, we separated our brain samples into three age categories: development (-37 weeks to 3 years), adult (4 to 60 years), and elderly (over 60 years). In total, we identified 9005 protein groups across all samples (including disease samples). To account for missing data and also to include the possibility that some proteins may be expressed only in specific age groups, we included those proteins quantified in at least 70% of samples in one of the age groups in subsequent analyses, resulting in the final quantification of 6,887 proteins. We employed PANTHER (www.pantherdb.org/) to categorize this BMV proteome based on their protein classes. Our BMV proteome is distributed

across 13 distinct protein classes which include transporters (7.54%) and cell adhesion molecules (2.14%). Furthermore, gene ontology (GO) enrichment analysis of this BMV proteome reveals BBB-associated GO terms such as cell-substrate adhesion, cell junction assembly, and transporters across the BBB.

2.3.2 BMV proteome reveals expression patterns that are indicative of brain development stages and the aging process

Differential expression was assessed on the dataset using a statistical t-test analysis, which identified proteins with significantly altered abundance levels (Absolute Fold Change> |±1.5|, P < 0.1) between the Developmental group and Adults group as well as the Adults group and Elderly group. As demonstrated in Fig. 2.2A, there were a total of 258 proteins with significantly increased abundance during the developmental stage which includes COL4A1(P-value=0.031), and COL4A2 (P-value= 0.017). These proteins encode the alpha1 and the alpha2 chains of type IV collagen, respectively, and are the major component of the basement membrane which is responsible not only for BBB stabilization but also maintenance of its integrity[26]. Gene ontology (GO) enrichment analysis of these increased proteins revealed strong links to BBB function, such as cell-substrate adhesion, cell-matrix adhesion, and regulation of metal ion transport (Fig. 2.2B). Conversely, there were a total of 837 proteins that decreased significantly in abundance during development, including SERPINH1(a collagen-specific ER chaperone; P-value=9.18 × 10−7) and SPARC (extracellular chaperone required for spatial assembly of collagen IV; P-value= 0.00980), which are important for the development of basement membrane [27]. GO analysis revealed these proteins were strongly associated with extracellular matrix organization and also mRNA processing, a similar trend to what has been observed when comparing human neonatal brain endothelial cells from the 15–18 and 20–23 gestational weeks[16]. Our results here support that this expression change continues during early

development to adulthood, indicating BBB development is still undergoing after we are born and the metabolic process of RNA in early childhood is different from adults.

We also identified a total of 168 proteins with significantly increased abundance and 427 proteins with significantly decreased abundance during the aging process (Fig. 2.3A). These differentially expressed proteins included several well-known proteins playing important roles in the aging process, such as Apolipoprotein D (APOD) which is a secreted lipocalin important for lipid metabolism and has been known to increase in aging human brains[28]. As well as LRRC32, a protein involved in the regulation of transforming growth factor beta, whose increased expression has been reported to correlate with cognition impairment and inflammation response in the brain [29]. Gene ontology (GO) enrichment analysis of these 168 significantly increased proteins revealed strong links to cell-substrate adhesion and leukocyte migration (Fig. 2.3B). Conversely, the 427 significantly decreased proteins were strongly associated with endocytosis, cell-junction maintenance, and zinc ion transmembrane transport. These protein expression shifts indicate the permeability and function of BBB may be broken down as we get older and also may lead to a higher risk of onset of neurodegenerative diseases [30, 31].

2.3.3 Network BMV proteome reveals modules linked to barrier integrity and transport system on BBB

We subsequently performed a network analysis of the discovery BMV proteome using the weighted gene co-expression network analysis (WGCNA) algorithm, which organizes the dataset into modules of proteins with similar expression patterns across cases [32] and is more often used to discover the relationship between network, gene and sample traits in a system with higher sensitivity, capturing proteins with smaller fold change or with lower abundance. This

analysis identified 30 modules (M) of co-expressed proteins ranked and numbered according to size from largest (M1, n = 1006 proteins) to smallest (M30, n = 34 proteins) (Fig. 2.4A). The biology represented by each module was determined using network analysis provided by Cytoscape [33] (https://cytoscape.org/). To assess whether a module was related to the age shift, we correlated each module eigenprotein, or the first principal component (PC) of module protein expression, to each sample's specific age (in days). We observed that 9 modules show a significant positive correlation > 0.1 and 7 modules show a significant negative correlation < -0.1 through early developmental stage to elderly. Modules positively correlated with age include protein groups related to selective autophagy and regulation of protein deacetylation. Modules negatively correlated with age shift include protein groups related to regulation of mRNA processing and cytoplasmic translation. Since our BMV proteome includes samples from a large range of ages and many proteins do not have a linear change throughout lifetime, in order to dissect further how these modules are altered through development and in the aging process respectively, we compared the module eigenprotein across age groups (Development, Adult, and Elderly). Module linked to collagen fibril organization (M11, P=0.0042) which includes proteins such us COL1A2 (Collagen type I alpha 2 chain), COL11A1 (Collagen type XI alpha 1 chain) and LUM (Lumican) significantly decreased expression only during the developmental stage (Fig. 2.4C). This is consistent with the GO enrichment analysis we did utilizing the differential expressed proteins among the Development and Adult groups (Fig. 2.2B). We also identified a module linked to glomerular basement membrane development (M24, P= 0.000025) which includes COL4A3 (Collagen type IV alpha 3 chain), COL4A4 (Collagen type IV alpha 4 chain) and LAMB2 (Laminin subunit beta 2). These proteins displayed a notable increase as individuals transitioned into adulthood. Combined with the results from the Differential Protein Expression analysis, we identified the major collagen families between early development and adulthood is distinct, with Type 4 collagen, a major component of the vascular basement membrane responsible for BBB stabilization and maintenance, showing an age-dependent

increase (Fig. 2.3D, E). These observations suggest that BBB permeability may vary with age and that the BBB undergoes a maturation process as individuals progress through different life stages. While the selective barrier function of the BBB is derived from the tight junctions between BMVs and the vascular basement membrane surrounding the BMVs, transporters are another crucial component for restricting entry of many xenobiotics into brain, as well as for delivering essential nutrients for brain development and homeostasis. Our analysis identified significant alteration in module linked to transporters across the blood-brain barrier (M16 P=0.040) during early developmental stages, with nutrient transporters like SLC7A1(CAT1) and SLC7A5 (LAT1; amino acid transporters), and SLC19A1(RFC; folate vitamin transporter) exhibiting age-dependent changes.

2.3.4 Nutrient transporters are expressed age-dependently on BBB

The human brain goes through significant changes even after birth. While a newborn already has most of its lifelong neurons, the brain's size doubles in the first year due to an accelerated rate of myelination and the formation of synapses during early childhood ([34],[35]). Proper nutrition is crucial for normal brain and neurocognitive development. Our proteomic analysis revealed that the BBB, which controls the delivery of essential nutrients to support brain and neuron development, has different properties with regard to protein expression during early development, including that of multiple nutrient transporters. The top five highly expressed micronutrient or macronutrient transporters in our dataset are depicted in Figure 2.5A. Micronutrients such as vitamins and minerals are crucial for normal neurodevelopment (Table 2.2). For example, riboflavin is important for neurodevelopment and deficiency in riboflavin has been associated with autism spectrum disorders and developmental delay [36, 37]. In the elderly population, riboflavin supplement has been linked to better cognitive performance via reducing the oxidative stress in the brain [38, 39]. The riboflavin transporter, SLC52A2

(Km=0.33uM), exhibited a significantly decreased expression with age while another riboflavin transporter SLC52A3 (Km=0.98uM), which is in the same family but has a higher Km, exhibited an increase in expression in the aging process. These data suggest that riboflavin delivery to the brain may change depending on age [35, 40] (Fig. 2.5B). Amino acids such as l-arginine and l-serine are required for regulating synapse formation/ patterning and neurotransmitter synthesis [41]. Studies in rodents have shown that these amino acids accumulate at higher concentrations in younger brains and that the protein expression of Slc7a1 and Slc1a4, transporters responsible for the uptake of these amino acids, is significantly higher at earlier developmental stages [42, 43]. Our present study in humans further supports this early requirement of nutrients in the brain. In our dataset, we found that the l-arginine transporter, SLC7A1(CAT1) and the l-serine transporter, SLC38A5(SNAT5) were highly expressed during early childhood, with expression levels reduced in adulthood (Fig. 2.5C). Furthermore, in our dataset, SLC3A2 (CD98hc/4F2hc) and SLC7A5 (LAT1), the two most highly expressed amino acid transporters in BMVs, also exhibit a significant negative correlation with age (Table 2.2).

2.3.5 Transporters for Mendelian diseases

Given the pivotal physiological roles of SLC transporters in maintaining brain homeostasis and their critical involvement in delivering essential nutrients for brain development, it is unsurprising that a malfunction in a single SLC transporter can lead to severe diseases manifesting neurological symptoms. Mutations in 20% of known SLC transporters in humans are associated with Mendelian diseases, with 38 identified in our BMV proteome (Table 2.3). We observed that 31.6% of those SLC transporters, whose primary substrates are known to be crucial for brain development and maturation, were prominently expressed in early childhood, such as SLC16A2 (MCT8), SLC30A10 (ZNT10) and SLC49A2 (FLVCR2). Thyroid hormones play a critical role in brain development, impacting brain function throughout life. Mutations in the thyroid hormone

transporter SLC16A2 (MCT8) are linked to Allan-Herndon-Dudley syndrome (AHDS), characterized by severe intellectual impairment, dysarthria, athetoid movements, muscle hypoplasia, and spastic paraplegia [44]. We discovered that the expression of SLC16A2 in BMVs was highest in the very young and exhibited a significant negative correlation with age which indicating that the BBB adjusts the transport of thyroid hormones into the brain in response to developmental needs. Manganese (Mn) is an essential trace nutrient for brain development, serving as a co-factor to enzymes vital for neuron function[45]. However, excess Mn in the brain leads to neurotoxicity. Loss-of-function mutations in SLC30A10, a cell surface–localized manganese efflux transporter, result in hypermagnesemia with dystonia-1 [46]. We identified that the expression of SLC30A10 on BMVs was most highly expressed in the very young, and showed a strong negative correlation with age. While SLC39A8, whose mutation leads to congenital disorder of glycosylation type IIn, is responsible for manganese transport[47]. Expression of SLC39A8 on BBB maintains stable expression from early development to adulthood and exhibits a significant decrease in aging. This suggests that manganese concentration is rigorously regulated by BMV transporters. SLC49A2 (FLVCR2) transports heme and choline and is essential for brain vascular sprouting [48]. Hydranencephaly-hydrocephaly syndrome (PVHH), or Fowler syndrome, is a recessive prenatal lethal disorder characterized by severe hydrocephalus, a thin cerebral cortex, and abnormal vascular structures in the brain[49]. This syndrome is attributed to mutations in SLC49A2, which we found was highly expressed in BMVs from neonates and children, a critical period during which the brain undergoes maturation, and rapid angiogenesis is essential for providing appropriate oxygenation for brain development.

2.3.6 Drug transporters are expressed on BBB

Due to limited transport across the BBB, FDA-approved drugs for the CNS are typically restricted to lipid-soluble small molecules that can pass BBB through passive diffusion and enter the brain. Nonetheless, these drugs must also avoid efflux from transporters, such as ABCB1 and ABCG2, in order to maintain their brain concentration. However, drugs that initially cannot cross the BBB can be modified for transport via inherent BBB mechanisms, such as carrier-mediated transport and receptor-mediated transport systems. SLC7A5 and TFRC are well-known targets for endogenous BBB carrier-mediated and receptor-mediated drug transport, and both are correlated with age, showing high expression during development and a decrease in expression as we age (Fig. 2.5C, 2.6B).

Known polyspecific drug transporters on the BBB include ABCB1, ABCG2, ABCC4 (MRP4), SLCO2B1 (OATP2B1), SLCO1A2 (OATP1A2), and SLC29A1 (ENT1) [50], are all present in our BMV proteome. The top ten highly expressed drug transporters in our dataset are depicted in Figure 2.6A. Consistent with prior studies, ABCB1 and ABCG2 are the most highly expressed among ABC transporters, although no notable age-related expression differences were observed. Age-dependent expression is evident in some transporters; ABCC4 is prevalent in developmental and aging groups, while SLCO1A2 declines with age (Fig. 2.6B). SLCO2B1 and SLCO1A2 transport statins, which are among the most commonly prescribed medications worldwide and are used in children with heterozygous familial hypercholesterolemia from as early as age 8 years old [51, 52]. The effect of statins on the brain is controversial with some studies suggesting that statins protect the brain from cognitive decline while others suggesting that some people have developed reversible memory loss or confusion while taking the drugs.

Moreover, we also identified other drug transporters on the BBB that exhibit differential expression. SLC22A3 (OCT3) shows higher expression levels in adults but not in early childhood or the elderly. On the other hand, SLC22A6 (OAT1) is expressed only in early childhood (Fig. 2.6C). Methotrexate is a well-known substrate of SLC22A6 (OAT1), and studies have shown that ABCC4 plays an important role in the brain distribution of methotrexate[53, 54]. Methotrexate is a key chemotherapy for acute lymphoblastic leukemia (ALL), the most common cancer diagnosed in those under 15 years of age in the United States. However, methotrexate is associated with significant neurotoxicity during therapy, as well as long-term neurological deficits. Older age has been previously reported as a risk factor for methotrexate-induced neurotoxicity [55, 56]. Although ABCC4 [$Mean_{[D]}$ (mean of Development group) = 0.0785 fmol/μg] may not be the main contributor to keeping MTX from the brain due to its lower expression compared to ABCB1($Mean_{[D]}$= 7.67 fmol/μg) and ABCG2($Mean_{[D]}$= 4.51 fmol/μg), and the localization of SLC22A6($Mean_{[D]}$= 0.096 fmol/μg) on BBB still remains unclear, the interplay of higher expression of SLC22A6 and ABCC4 during early childhood may contribute to reduced neurotoxicity in younger ALL patients with MTX treatment. Interestingly, SLC22A8 (OAT3), which is highly expressed in the rodent BBB[57], was undetectable in our samples highlighting the species difference of BBB. MFSD10, a member of the SLC22A family, not typically known as a drug transporter but shown to transport NSAIDs in one study[58], exhibits high expression levels during early development.

2.3.7 Simulations demonstrate the impact of transporter expression and BBB permeability on CSF drug exposure

In this proof-of-concept study, we employed physiologically based pharmacokinetic (PBPK) simulations with a four-compartment, permeability-limited brain model to examine the effects of BBB passive permeability and ABCB1 expression on drug distribution[59]. The altered BBB permeability was inferred from developmental changes in basement membrane composition, as

revealed by our proteomic analysis. The simulation results, depicted in Figure 2.7, demonstrate the concentration-time profiles of the antiepileptic drug phenytoin in plasma, cerebrospinal fluid (CSF), and brain mass. Notably, our simulations show that changes in BBB permeability and ABCB1 expression lead to pronounced changes in phenytoin exposure within the spinal CSF and brain tissue compartment, with minimal impact on plasma phenytoin levels (Fig. 2.7). Given the narrow therapeutic range of phenytoin, elevated CNS concentrations can lead to neurotoxicity, manifesting as symptoms ranging from mild nystagmus to ataxia, lethargy, and in severe cases, coma and death. Conventionally, serum phenytoin levels are monitored to ensure appropriate dosing and minimize adverse effects. However, our study suggests that serum phenytoin concentrations may not accurately indicate the risk for neurotoxicity, as they do not adequately represent variations in brain drug levels attributable to differences in BBB permeability and transporter activity.

2.3.8 Proteins associated with higher risk of Alzheimer's disease are correlated with age and differentially expressed in AD patients

Genome-Wide Association Studies (GWAS) have been an important tool in identifying genes linked to the risk of Alzheimer's disease (AD), henceforth referred to as AD GWAS genes. We focused on 45 AD GWAS genes with a strong association with AD, and 22 of these genes are expressed in our BMV dataset and 12 of them exhibited age-dependent expression patterns [17](Fig. 2.8A). WW domain-containing oxidoreductase (WWOX), recognized as an AD risk factor, plays a pivotal role in the disease's neurodegenerative processes. WWOX interacts with Tau and engages with the Tau phosphorylating enzymes like ERK, JNK, and GSK-3β. This interaction is significant in curbing AD's progression. Although the role of WWOX specifically in BMVs is remain unclear, studies have shown that WWOX downregulation increase of the hypoxia-induced factor 1 alpha (HIF1α) which may potentially lead to BBB damage ([60], [61]).

Interestingly, our studies indicate a reduction in WWOX expression in the AD group compared to a healthy, elderly group[62](Fig. 2.8B). Furthermore, aging is acknowledged as a principal risk factor for AD. Pathologically, senescent cells accumulate in aging tissues and are implicated in various age-related diseases, including AD[63]. Understanding the alterations in protein expression of normal aging processes and their transition to neurodegenerative states is crucial. Research indicates that in AD development, neurons, astrocytes, and microglia may enter a state of chronic senescence and targeting senescent cells has emerged as a promising strategy to address the aging phenotype and potentially thwart the onset and progression of AD[64]. However, the aging process of BMVs is still largely unknown, particularly regarding its link to AD risk. In our BMVs dataset, six AD GWAS genes demonstrate age-specific correlations, underscoring their potential role in the aging aspects of AD. Among these genes, APOE is notable for its role in lipid metabolism and significant contribution to AD pathology[65]. Its expression, known to increase with age, is associated with key AD features like amyloid-beta aggregation and clearance[66]. Consistent with previous studies, in our proteomic dataset, APOE shows high expression in BMVs, with a positive correlation with age. Additionally, PICALM, one of the most significant loci identified in AD susceptibility GWAS, encodes the phosphatidylinositol binding clathrin assembly protein, involved in endocytosis and autophagy. Studies suggest that reduced PICALM expression exacerbates tau pathology[67]. Our data reveal a negative correlation of PICALM expression with aging (Fig. 2.8B). Vascular endothelial growth factor B (VEGFB) is a crucial protein for blood-brain barrier repair and has been known to increase its expression when BBB is damaged. Studies have shown a negative correlation between brain VEGFB expression and cognition scores in AD patients[68]. We observed that VEGFB was initially absent in the BBB of the developmental group but significantly increased with age, with even higher levels in AD patients which is consistent with BBB disruption in AD patients (Fig. 2.8C). These findings illuminate the dynamic expression patterns of these genes

in relation to aging and AD, opening new pathways to understand the molecular drivers behind AD progression.

2.4 Methods

2.4.1 Human Brain Tissue Samples

Thirty-four healthy donors and four Alzheimer's Disease patients' post-mortem frozen brain cortical tissue samples and were obtained from the National Institutes of Health NeuroBioBank at the University of Maryland, Baltimore, MD. Tissues were stored at −80°C until the day of microvessel isolation. The demographic information of donors is reported in Supplemental Table 2.1. The pediatric population was separated into different age groups according to the International Council for Harmonisation guidelines: newborns (PNA 0–28 days, GA>37 weeks), infants (1–24 months old), children (2–12 years old), and adolescents (12–16 years old). Donors over 16 years old were defined as adults and over 60 years old were defined as geriatric population. However, due to the small sample size of each group, newborn and infant groups were combined and children, adolescents, and adult groups were combined to increase the power of the study after confirming no proteins were differentially expressed between these groups respectively.

2.4.2 Isolation of Human Brain Microvessels

The process of isolating brain microvessels (BMVs) from human brain cortical tissue was conducted with some modifications based on a previously described protocol[69]. The procedure started with using less than 1 gram of tissue which was thawed and homogenized in protease inhibitors (cOmplete protease inhibitor cocktail, Sigma-Aldrich, St. Louis, MO) contained HBSS solution with 20 up- and-down strokes in a Potter-Elvehjem glass

homogenizer. The resulting homogenate was centrifuged at 1200 g for 10 min at 4C, and the BMV enriched pellet was resuspended in a 17.5% dextran-70/HBSS solution and centrifuged and centrifuged at 4300 g for 15 min at 4C in a swinging bucket rotor. The myelin-rich layer on the top and the supernatant were aspirated and the pellet was resuspended in HBSS with 1% Bovine Serum Albumin (BSA). This solution was filtered with a 40 µm nylon mesh strainer and the BMVs captured on the strainer were washed with 35 ml of 1% BSA/ HBSS buffer. The BMVs were then collected off the filter with 1% BSA/HBSS buffer and centrifuged at 3000 g for 5 min at 4C. The supernatant was removed and the resulting BMV pellet was immediately frozen at -80°C for further analysis. All the steps were carried out at 4°C or on ice.

2.4.3 Global Proteomics Using Liquid Chromatography Tandem Mass Spectrometry

The process of LC/MS is based on a previously described protocol[69]. BMV samples were lysed in a 100 mM Tris-HCl buffer (pH 7.8) containing 50 mM dithiothreitol and 2% sodium dodecyl sulfate, followed by a 5-minute incubation at 95°C. Subsequently, the samples underwent sonication using a Branson-rod-typesonicator and were then centrifuged at 14,000 g for 10 minutes. To determine protein concentration, a tryptophan fluorescence assay was employed. For multi-enzyme digestion, 100 µg of protein was utilized in the filter-aided sample preparation (MED-FASP) protocol, where sequential digestion with LysC and trypsin occurred. Following digestion, the resulting peptides were concentrated via a GeneVac EX-2plus system. Subsequently, peptide separation was achieved using an Ultimate 3000 RSLCnano system, employing an easy spray C18 reversed-phase column (50 cm, ID 75 µm) with a gradient of water/acetonitrile containing 0.1% formic acid over a 145-minute period. The eluted peptides were analyzed with a Top15 method, involving full MS followed by ddMS2 scans, using an Orbitrap Q Exactive HF mass spectrometer (ThermoFisher, Waltham, MA). Data analysis was conducted using MaxQuant version 1.6.10.43, with the complete human proteome extracted

from UniProt (September 2020). A false discovery rate of 0.01 was set, and match-between-runs was enabled for enhanced accuracy. Protein abundance quantification was performed using the total protein approach (TPA) for proteins with three or more razor+unique peptides. The mass spectrometry proteomics data have been deposited in the ProteomeXchange Consortium through the PRIDE partner repository.

2.4.4 Differential expression analysis

Unpairwise differentially expressed proteins were identified using Student's t-test, followed by Benjamini-Hochberg (BH) FDR correction (Significant as absolute fold change> 1.5, P-value < 0.1). Differential expression was presented in volcano plots, which were generated with the "EnhancedVolcano" version 1.14.0 package in R[70].

2.4.5 Weighted gene correlation network analysis Discovery brain proteome

Weighted protein coexpression network of the discovery BMV dataset was derived from the protein abundance values using the blockwiseModules WGCNA function ([32]WGCNA 1.72.5 R package) with the following settings: soft threshold power beta = 6, deepSplit=2, minimum module size = 30, merge cut height = 0.25, TOMDenominator = "min", a signed network with partitioning about medioids (PAM) respecting the dendrogram. This approach calculates pairwise biweight mid-correlations (bicor, a robust correlation metric) between each protein pair and transforms this correlation matrix into a signed adjacency matrix. After blockwiseModules network construction, 30 modules consisting of 34 or more proteins were detected. Module eigenproteins, which are defined as the first principal component (PC) of each module protein expression, were correlated with age(days) using bicor analysis.

2.4.6 Gene Ontology Enrichment Analysis

The enriched GO terms (biological process, cellular component, and molecular function) of the differential expressed proteins during the developmental stage and aging process were identified and visualized based on the clusterProfiler version 4.4.4 package in R software using the default value[71].

2.4.7 PBPK modeling

Systemic and central nervous system (CNS) drug concentrations were simulated using both whole-body and four-compartment permeability-limited brain models within the Simcyp PBPK Simulator (version 21.1, Certara, Princeton, NJ, USA). The pharmacological and physiological parameters for the model were adapted from a previously published PBPK model for phenytoin [59]. Simulations were conducted over 10 trials, each consisting of 10 virtual healthy volunteers, using the same demographic and dosing information as the referenced phenytoin model. Default settings for BBB P-glycoprotein (P-gp) abundance (3.25 pmol/mg of brain capillary protein) and permeability (46.44 L/h) were applied to generate baseline curves. To mirror the proteomic data observed in our study, adjustments were made to these parameters, and the results of these modifications are presented with the respective parameter values in Figure 2.7.

2.5 Discussion

The goal of this study was to determine the developmental and aging effects on BBB, with a focus on the role and dynamics of transporters. Our key findings are: (a) Alteration in basement membrane components occurs during the early developmental stage; (b) Selected nutrient transporters that are important for brain development are enriched during early development; (c) Some drug transporters that are expressed on the plasma membrane of BBB exhibit age-dependent expression patterns; (d) Exploratory studies suggest that some proteins associated

with AD exhibit altered expression levels in BMVs from patients with AD. Each of these findings is discussed below followed by the limitations of the study.

2.5.1 Alteration in Basement membrane component occurs during early developmental stage

Unlike the cellular components of the BBB, the basement membrane has only been recently recognized for its importance in maintaining BBB permeability[1]. Aging-related changes were evident in the BBB's basement membrane. Our BBB proteome study, for the first time, comprehensively identified the collagen families composing the basement membrane across various age groups (from neonates to the elderly). It revealed that the predominant collagen families in the basement membrane differ between the early developmental stage and adulthood. In early childhood, the Collagen VI family (COL6A1 and COL6A3) is the most highly expressed, whereas in adulthood, the Collagen IV family (COL4A1 and COL4A2) is predominant. These 2 collagens are distinct in terms of their morphology. Collagen VI is an unusual collagen comprising both collagenous and non-collagenous domains that assemble into beaded filaments whereas Collagen IV forms a protomer fiber made of three α chains. While Collagen IV is well-known to form the backbone of the basement membrane[72]. The Collagen VI family is highly expressed in various human tumors and influences cell proliferation and angiogenesis[73]. This role aligns with the ongoing postnatal vascularization in humans. Future research is needed to understand how different collagen families may affect BBB permeability.

2.5.2 Transporters important for brain development are mainly enriched during early development

Our study represents a pioneering effort to map the development and aging trajectory of nutrient transporters on the human BBB. We found that the l-arginine transporter SLC7A1 (CAT1) and

the l-serine transporter SLC38A5 (SNAT5) show high expression levels during early childhood (Fig. 2.5C) which aligns well with clinical findings that these amino acids present higher CSF/plasma concentration ratios in infancy than in later childhood[74]. Furthermore, we identified nutrient transporters like the riboflavin transporter SLC52A2, the thyroid hormone transporter SLC16A2, and the heme/choline transporter SLC49A2 are all enriched in the early developmental stage. These transporters are associated with Mendelian diseases that exhibit severe brain developmental phenotypes. This underscores the brain's heightened metabolic needs during rapid growth phases and highlights the critical importance of precisely regulating the expression of these transporters on the BBB for normal brain function.

2.5.3 Drug Transporters on BBB exhibit age-dependent patterns

Many known drug transporters on the BBB, including ABCB1, ABCG2, ABCC4, SLCO2B1, SLCO1A2, SLC19A3, and SLC29A1, are expressed in our BMV proteome[50]. In alignment with prior research, ABCB1 and ABCG2 were the most prevalent ABC transporters identified. While no significant age-related differences were noted in these transporters, our data revealed a wide range in ABCB1 expression levels among individuals, from 1.45 fmol/μg to 13.78 fmol/μg. This 9.5-fold difference could potentially lead to significant variations in brain drug concentrations among individuals. Age-dependent variations in the expression were observed in other transporters such as SLCO1A2, ABCC4, and SLC22A6. Despite the controversial results from clinical studies on the benefit of statins in autism or Alzheimer’s disease, their ability to affect brain cholesterol levels cannot be ignored[75-77]. Results from our study have pointed out the possibility that statins may cross BBB through SLCO1A2 which has lower expression in the elderly population. Expression changes in BBB drug transporters may also contribute to neurotoxicity. Studies showed that older children tend to be more sensitive to methotrexate - induced neurotoxicity(reference). SLC22A6 facilitates methotrexate transport, while ABCC4 plays a role in its efflux, both highly expressed during developmental stages. Future research

should aim to determine the localization of these transporters and explore how SLC22A6 and ABCC4 interaction during early childhood could lead to improved therapeutic strategies to mitigate neurotoxicity in methotrexate-treated patients. Our proteome analysis also identified the species differences between humans and rodents which has been discussed in Yang et al[78]. This finding underscores the critical need for human-based BBB studies, given that most CNS drug development failures stem from a lack of efficacy, highlighting the essential gap that needs bridging between preclinical models and human studies.

2.5.4 Proteins highly associated with AD have significant age-related changes in expression levels

Alzheimer's disease (AD) poses a formidable challenge in healthcare due to the absence of effective treatments to cure the disease. Of all risk factors for AD, aging plays the most substantial role. Despite the limitation of having only three samples from patients with AD, and acknowledging that sporadic AD is believed to exhibit high heterogeneity, our exploratory research has potentially illuminated the impact of aging on protein expression levels in AD patients. This insight contributes to our understanding of the disease's progression and may inform future studies. In our study, we discovered that 8.6% (595) of proteins in our BBB samples either increase or decrease with aging. Notably, proteins involved in inflammation (leukocyte migration), show a marked increase with age, while zinc transport proteins exhibit a significant decline. Zinc deficiency has been linked to an increased risk of Alzheimer's disease, possibly due to heightened inflammation. Our findings reveal a reduction in the expression of zinc transporters SLC30A1, SLC30A5, and SLC30A10 among the elderly. Additionally, we observed that APOE, known for its significant role in lipid metabolism and contribution to AD pathology, is highly expressed in BMVs, comparable to the BMV marker SLC2A1 (GLUT1), and its expression increases with age. Overexpression of APOE in pericytes can lead to their

degeneration, which severely impacts BMV functionality and results in cognitive decline[79]. However, the implications of elevated APOE expression in BMVs remain controversial, with studies indicating it may induce inflammation and subsequently impair BBB integrity[80]. Our study for the first time, revealed that VEGFB was absent in early child hood and was significantly elevated with age, showing even higher levels in AD patients. This finding is consistent with BBB disruption in AD, since VEGFB is essential for BBB repair, and may have increased in response to BBB damage. Among the 22 AD GWAS genes expressed in our dataset, over half showed a correlation with age, either positive or negative. These results highlight the dynamic nature of gene expression related to aging and AD, offering potential new insights into the molecular mechanisms driving AD progression.

The major limitation of this study is the analyzed set of samples was from a small number of donors, especially for the samples from AD patients (N=3), which should be considered when using the generated data. Extending this study to cover a large number of samples from both health population with different age and also disease populations should confirm these conclusions. Another limitation is the potential contamination of other brain cell types in our brain microvessel (BMV) isolation technique. Indeed, we did observe some astrocyte proteins in our dataset, likely stemming from astrocytic endfeet projections that make contact with BMVs. This type of potential contamination has been reported before when trying to study the blood-brain barrier (Table 2.4, [12, 13]). Nonetheless, we did have clear enrichment of BMVs in our samples when comparing key BBB genes (ie. GLUT1, LAT1, SYP (neuronal), GFAP(astrocyte)) between the BMVs and whole brain via qPCR (Supplemental Figure 2.1). Previous studies have been done to assess transporter proteins at the BBB, although limited to adult brains [11-13]. Our results were consistent with all other studies in terms of demonstrating that SLC2A1, which is a marker of BBB, is one of the highest expressed SLCs. However, our BMVs showed much higher expression of SLC7A5(our study 3.05 fmol/µg vs Uchida et al 2011 0.431 fmol/µg). One

possible explanation for this differential finding could be due to our BMV isolation technique compared to Uchida et al. A final limitation of our study is related to the source of the brain samples, which were obtained from the University of Maryland NeuroBioBank. Some time after death may pass before tissues are frozen (https://www.medschool.umaryland.edu/btbank/brain-donation/the-tissue-donation-process/) .

In conclusion, our study, for the first time, inclusively identified proteins in BMVs which display age-dependent patterns. These findings not only shed light on the physiological transformations that occur in the human brain across development and aging but also hint at the possibility that drug distribution into the brain may vary with age. Changes in BBB permeability and also in the expression of transporters in the BBB play a crucial role in the pharmacokinetics of CNS drugs. Our study presents the ontogeny and aging of proteins on BBB and suggests that both the membrane transporters and the basement membrane of the BBB might undergo alterations during development and aging. Through a proof-of-concept study utilizing the publicly available phenytoin PBPK model, we illustrate how drug exposure in the brain could be influenced by differences in transporter expression and BBB permeability. Future research should aim to refine these findings and generate more precise parameters based on our BMV proteome with more clinical data. This information can then be integrated into modeling and simulation efforts to enhance predictions regarding drug disposition, clearance, and optimal dosing in pediatric and geriatric patients. This work is vital for improving the design of clinical studies for drugs intended as medical countermeasures for children and the elderly, populations for whom research poses ethical and logistical challenges. We hope our findings will provide valuable insights for guiding dosage adjustments in pediatric and geriatric patients.

2.6 Figures

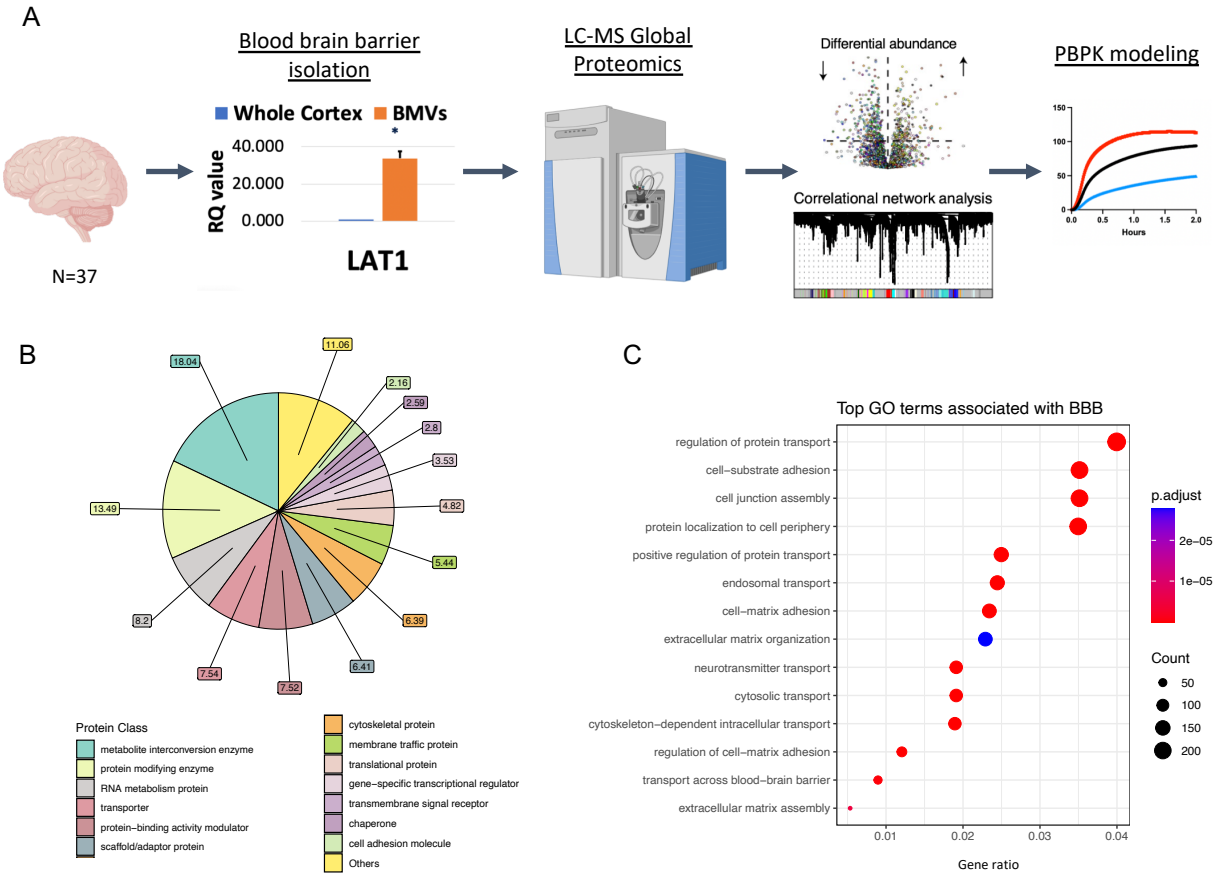

Figure 2.1. Brief experimental workflow and overview of BMV proteome
(A) Brief experimental workflow. Brain microvessels were isolated from frozen insular cortical bran tissue, which were then digested and analyzed using LC–MS/MS proteomic methods. Differential protein analysis and weighted correlation network analysis(WGCNA) were performed to identified proteins different between age groups and possible altered Blood brain barrier parameters were incorporated into physiologically based pharmacokinetic (PBPK) modeling simulation. (B) The PANTHER protein class of the proteins in BMV proteome. (C) Top BBB related GO terms associated with our BMV proteome are shown. X-axis is the gene enrichment ratio (Gene ratio) and the bubble size indicates the numbers of proteins associated a biological

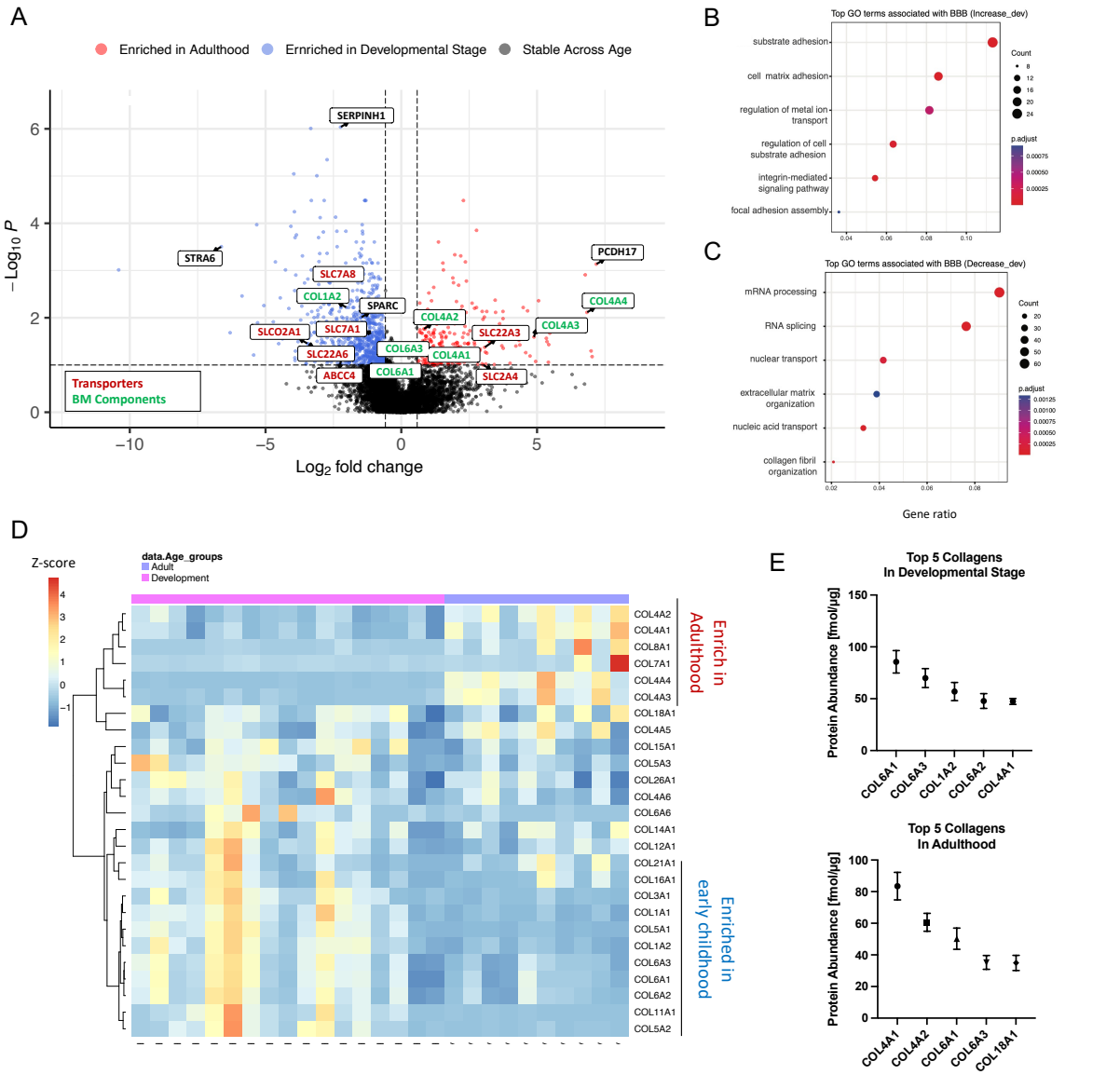

Figure 2.2. Differential expression of discovery BMV proteome through early childhood (A) Volcano plot displaying the log2 fold change (x axis) against the t test derived log10 statistical P value (y axis) for all proteins differentially expressed between Development group and Adult group of the BMV proteome. Proteins with significantly decreased levels in Adults ($P < 0.1$) are shown on the left side, while the proteins with significantly increased levels through developement are shown on the right side. Transporters are labeled in red and proteins as basement membrane (BM) components are labeled in green. (B,C) Top BBB related GO terms associated with proteins significantly increased or decreased with age are shown. X-axis is the gene enrichment ratio (Gene ratio) and the bubble size indicates the numbers of proteins associated a biological process GO term, with color maps the FDR value (p.adjust) of the enrichment analysis. (D) Protein expression of Collagens which are expressed in our proteomic dataset and exhibit positive(red) or negative(blue) correlation with age. (E)Top 5 most abundant collagens in Developmental group and Adult group are shown in bar graph.

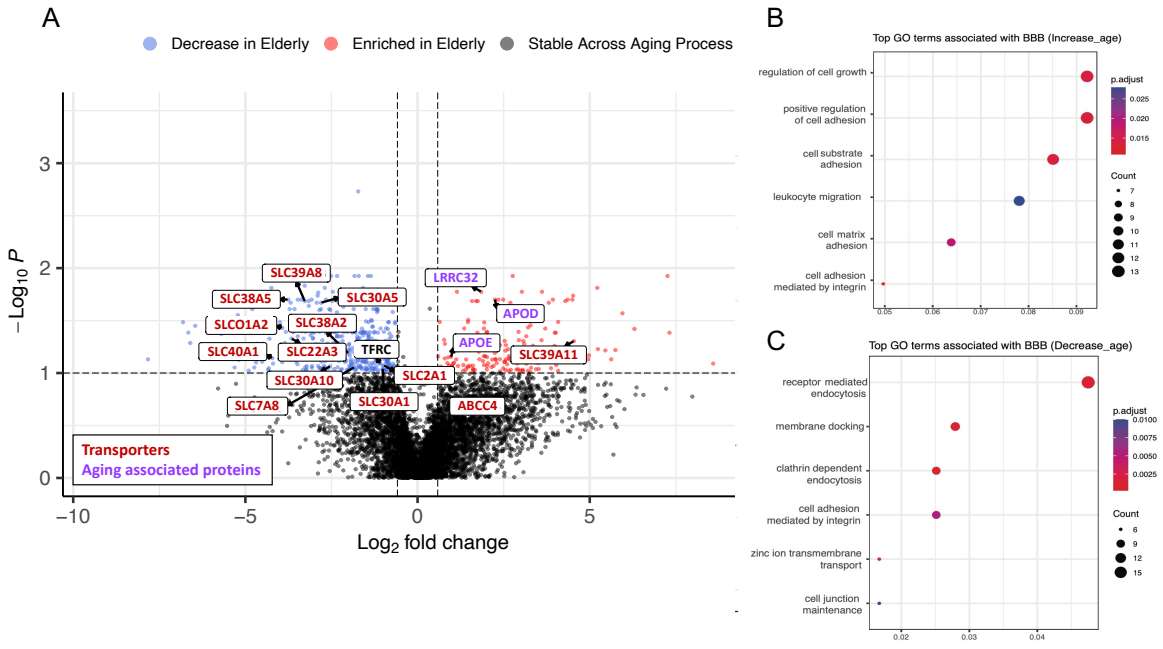

Figure 2.3. Differential expression of discovery BMV proteome during aging process
(A) Volcano plot displaying the log2 fold change (x axis) against the t test–derived −log10 statistical P value (y axis) for all proteins differentially expressed between Adult group and Elderly group of the BEC proteome. Proteins with significantly decreased levels in elderly population ($P < 0.1$) are shown on the left side, while the proteins with significantly increased levels with aging are shown on the right side. Transporters are labeled in red and proteins important for aging are labeled in green. (B, C) Top BBB related GO terms associated with proteins significantly increased or decreased with age are shown. X-axis is the gene enrichment ratio (Generatio) and the bubble size indicates the numbers of proteins associated a biological process GO term, with color maps the FDR value (p.adjust) of the enrichment analysis.

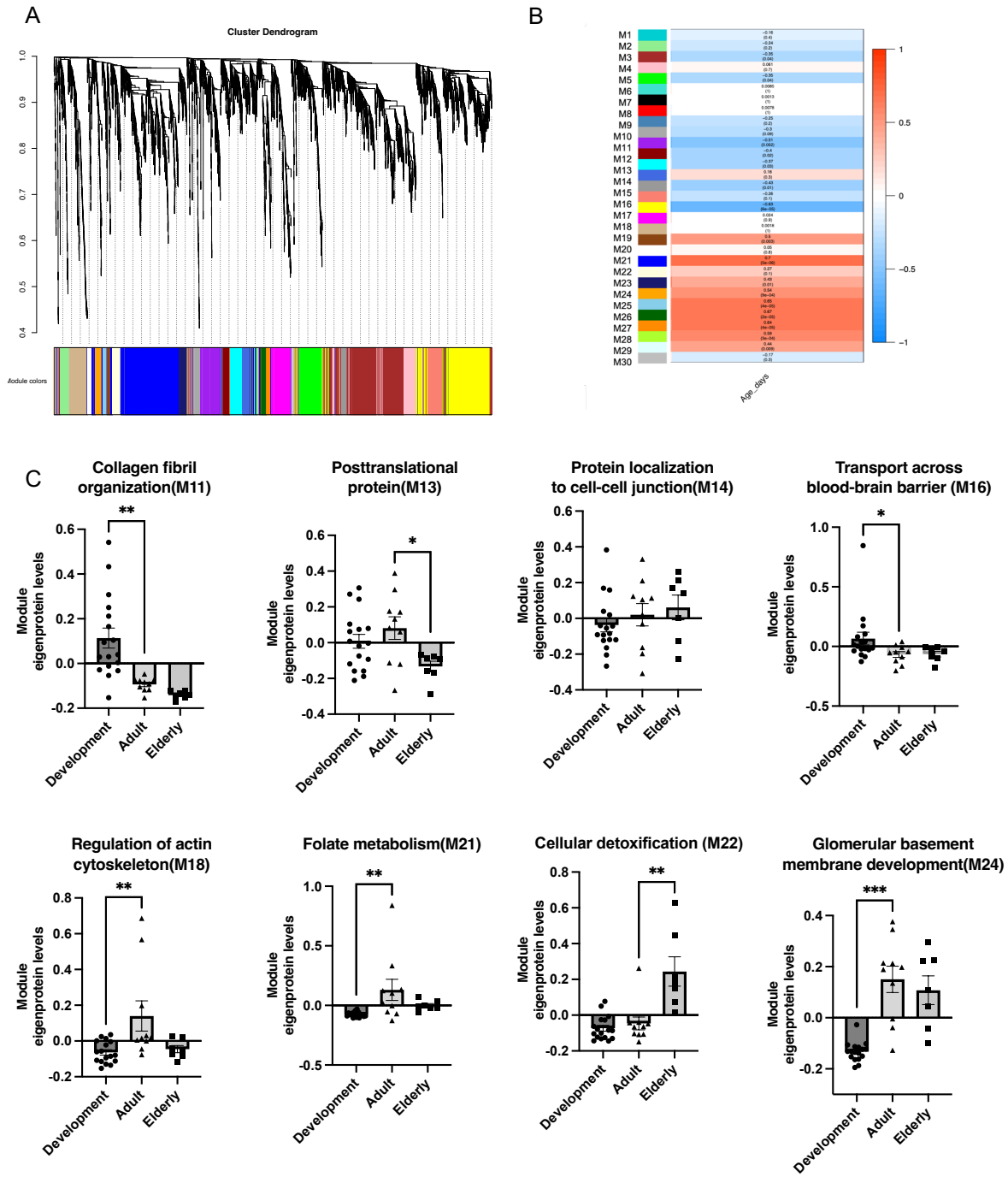

Figure 2.4. BMVs proteins co-expression network

(A**)** WGCNA hierarchical clustering dendrograms of identified thirty distinct modules of highly co-expressed genes; all modules are marked with different colors. (B) The correlation between modules and age. Heatmaps shows the correlation between eigengene and age and each cell contains the corresponding correlation followed by p-value. (C) Module eigenprotein levels by age groups (Development, Adult, Elderly) for the 8 blood brain barrier related modules. Modules are grouped by different age groups. Differences in module eigenprotein by age groups were assessed by Kruskal–Wallis tests. Dunn's post hoc test were used for multiple comparisons of expression levels between age groups. The error bars represents SEM and each points represent one sample. *P < 0.05, **P < 0.01, ***P < 0.001

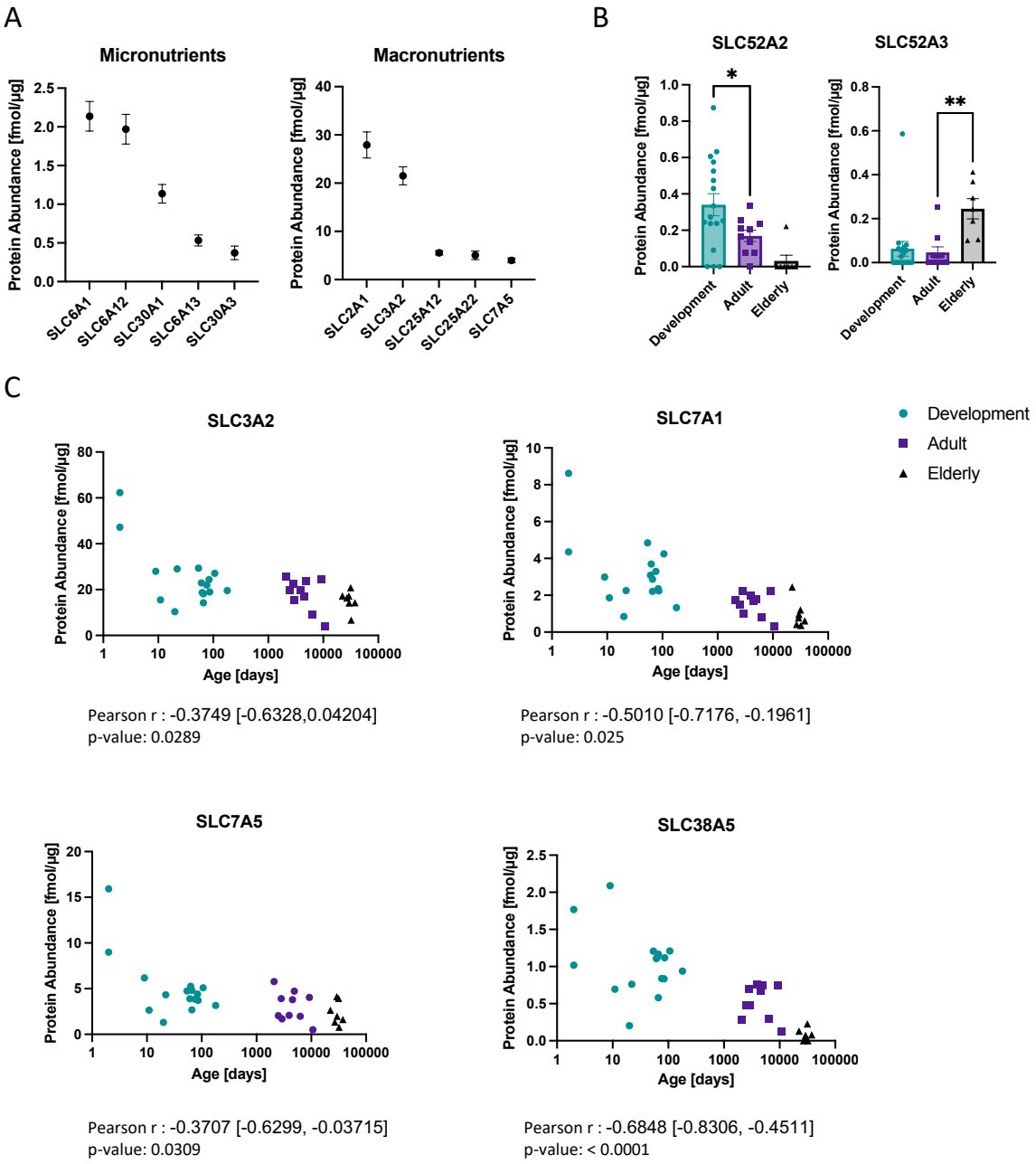

Figure 2.5. Macronutrient and micronutrient transporters on BBB
(A)Top 5 most abundant micronutrients transporters and macronutrients and in our BECs proteomic dataset are shown in bar graph (B) Protein abundance levels of riboflavin transporters SLC52A2 and SLC52A3 in different age groups. Expression difference between age groups were assessed by Kruskal–Wallis tests. Dunn's post hoc test were used for multiple comparisons of expression levels between age groups. The error bars represents SEM and each points represent one sample. *P < 0.05, **P < 0.01, ***P < 0.001 (C) Ontogeny of protein abundance of amino acid transporters SLC3A2, SLC7A1, SLC7A5, SLC38A5 are described as simple linear regression model. Individual Pearson correlation coefficient (Pearson r) and p-values are presented below each scatter plots.

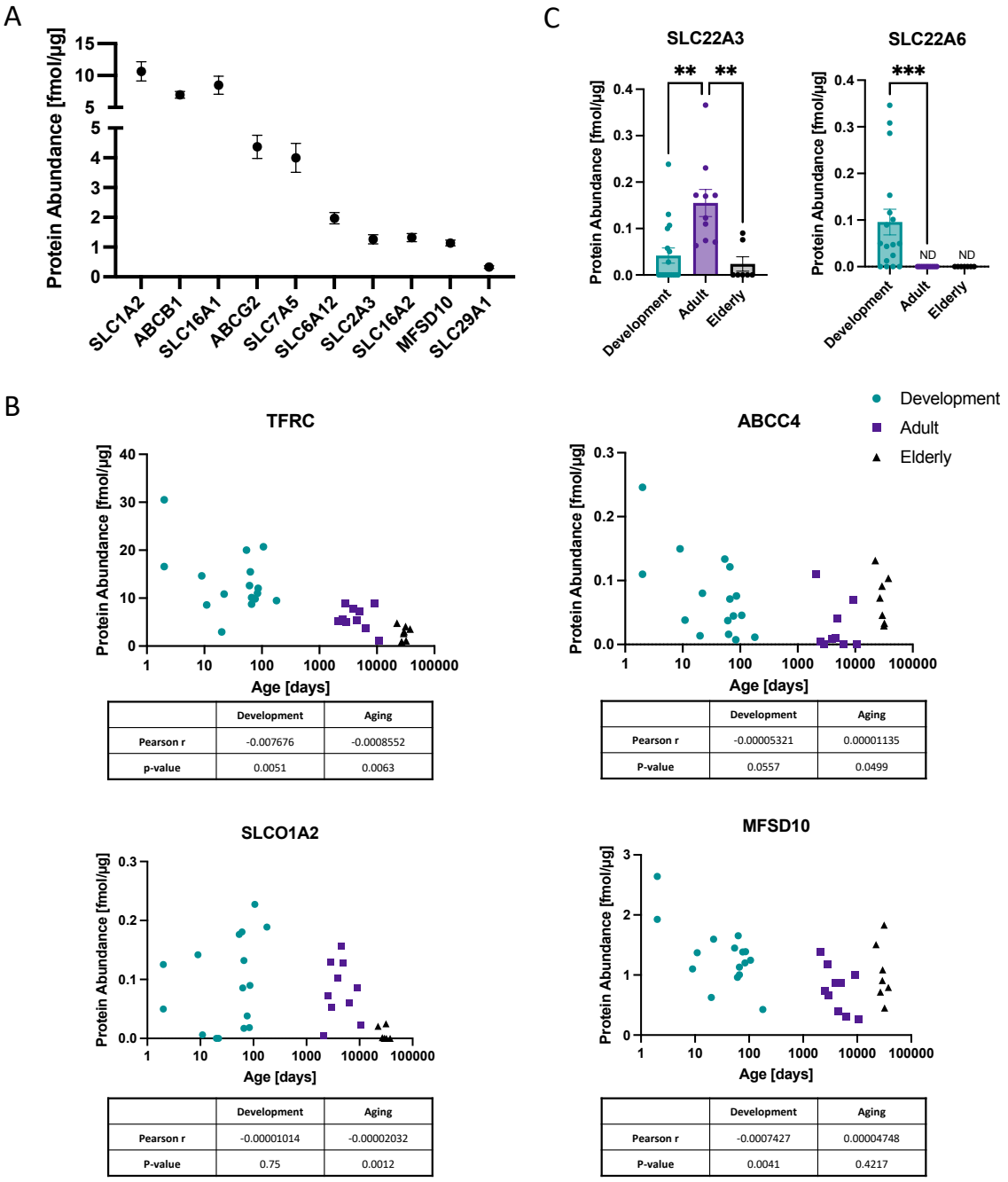

Figure 2.6. Drug transporters on BBB

(A)Top 10 most abundant drug transporters in our BEC proteomic dataset are shown in bar graph. (B) Ontogeny of protein abundance of amino acid transporters TFRC, ABCC4, SLCO1A2, MFSD10 are described as simple linear regression model. Individual Pearson correlation coefficient (Pearson r) and p-values for developmental stage and aging process are presented below each scatter plots respectively. (C) Protein abundance levels of SLC22A3 and SLC22A6 in different age groups. Expression difference between age groups were assessed by Kruskal–Wallis tests. Dunn's post hoc test were used for multiple comparisons of expression levels between age groups. The error bars represent SEM and each points represent one sample. *P < 0.05, **P < 0.01, ***P < 0.001, ND= Not Detected

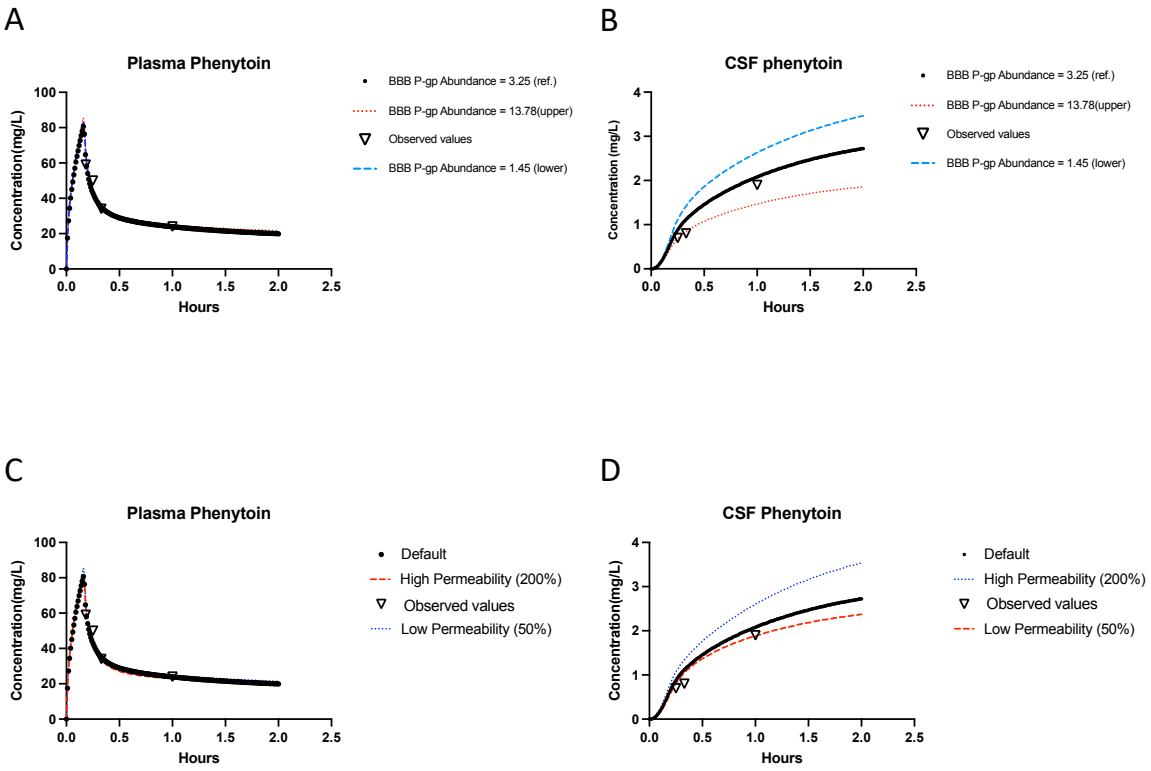

Figure 2.7. Simulated concentration- time profiles of the P-gp substrate phenytoin with either altered P-gp expression or different levels of BBB permeability.
(A,B) Reduced P-gp expression on BBB with administration of Phenytoin results in increased exposure in CSF, with a 2.24 fold (default 3.25 vs. 1.45) reduction increasing the AUC by 26.7%. Conversely, increased P-gp expression with a 4.24 fold (default 3.25 vs. 13.78) leads to a 29.5% reduction in CSF phenytoin AUC, respectively. (C,D) Lower BBB permeability results in decreased phenytoin exposure in CSF, with a two-fold reduction increasing the AUC 10.2%. Conversely, higher BBB permeability leads to 26.1% increase in phenytoin AUC.

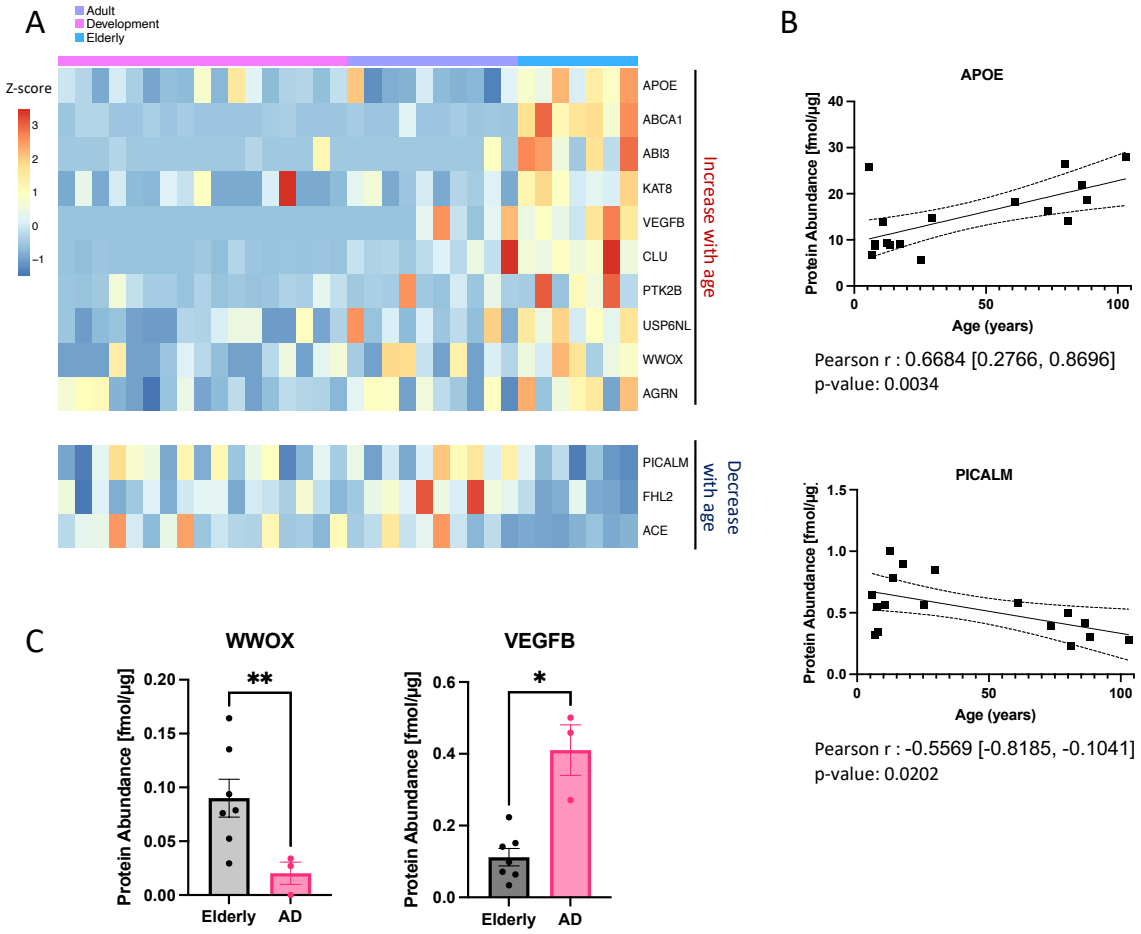

Figure 2.8. AD GWAS genes exhibit age-dependent and disease-dependent expression patterns

(A) Protein expression of AD GWAS genes which are expressed in our proteomic dataset and exhibit positive(red) or negative(blue) correlation with age. (B) Protein abundance of APOE and PICALM through aging are described as simple linear regression model. Individual curve are presented in (solid lines). Dashed lines represent the 95% confidence bands. Individual Pearson correlation coefficient (Pearson r) and p-values are presented below each scatter plots. (C) Protein abundance levels of WWOX and in healthy elderly population or in patients with AD. Expression difference between disease condition were assessed by student T test. *P < 0.05, **P < 0.01, ***P < 0.001

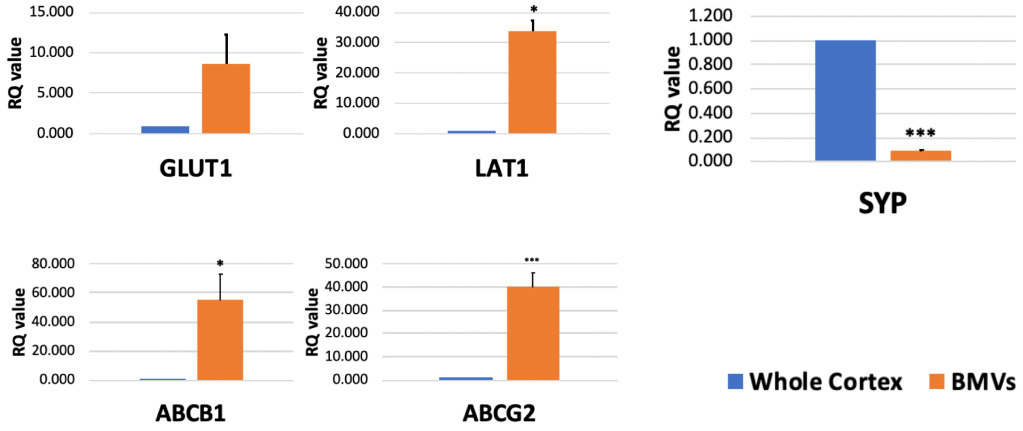

Supplemental Figure 2.1. BMV markers are enriched in isolated brain microvessel samples

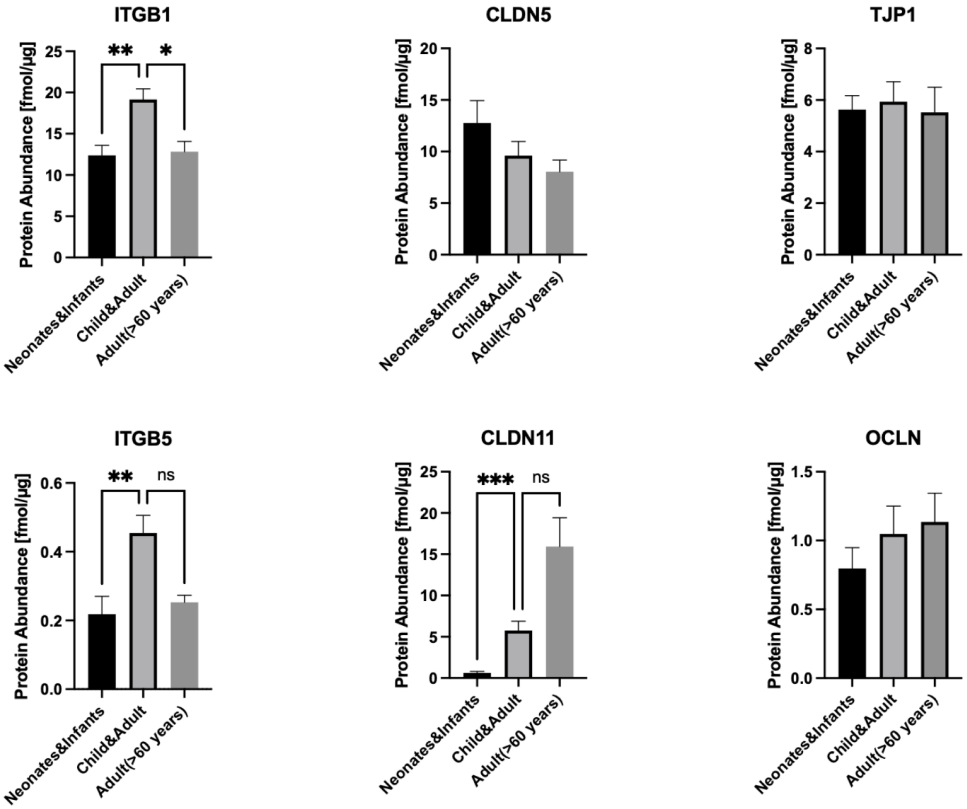

Supplemental Figure 2.2. Protein expression of major tight junction proteins and integrins on BBB

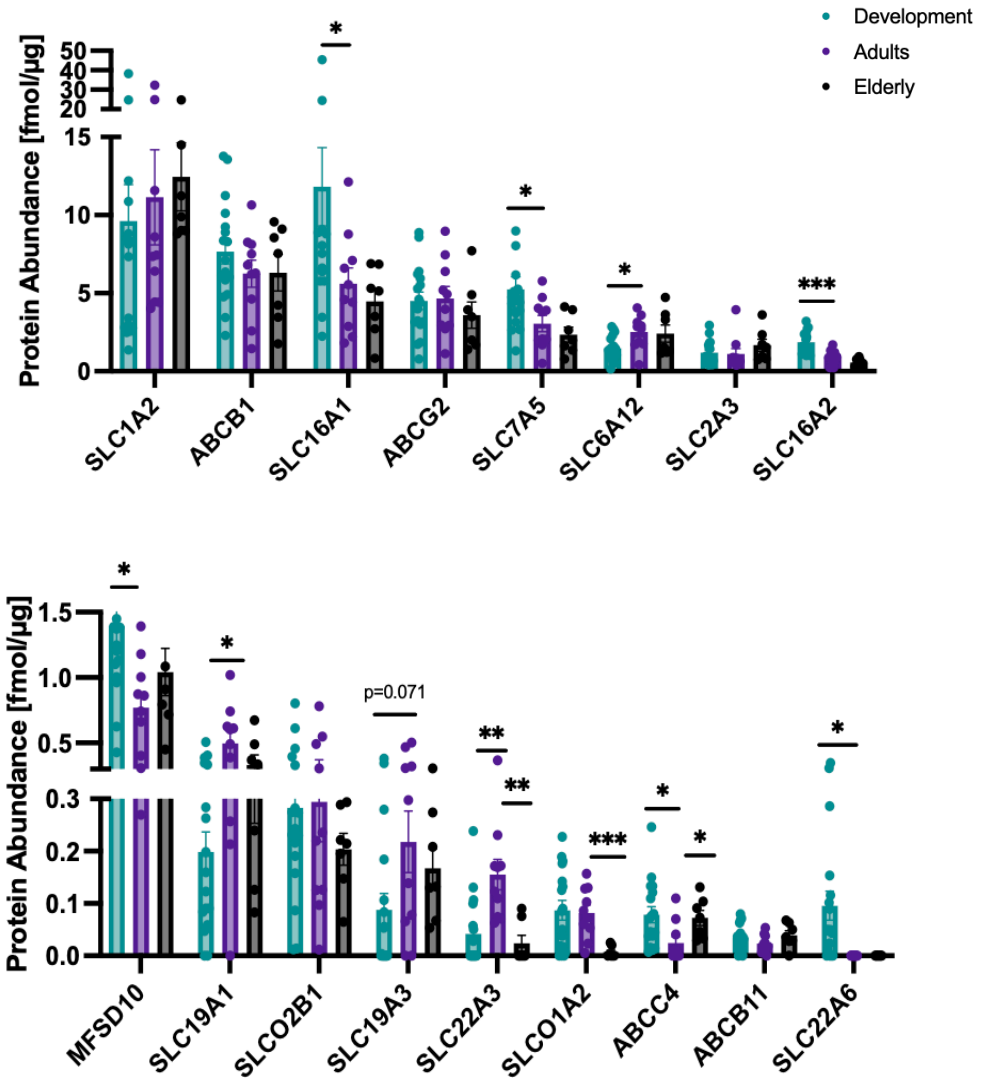

Supplemental Figure 2.3. Protein expression of drug transporter expression on BBB

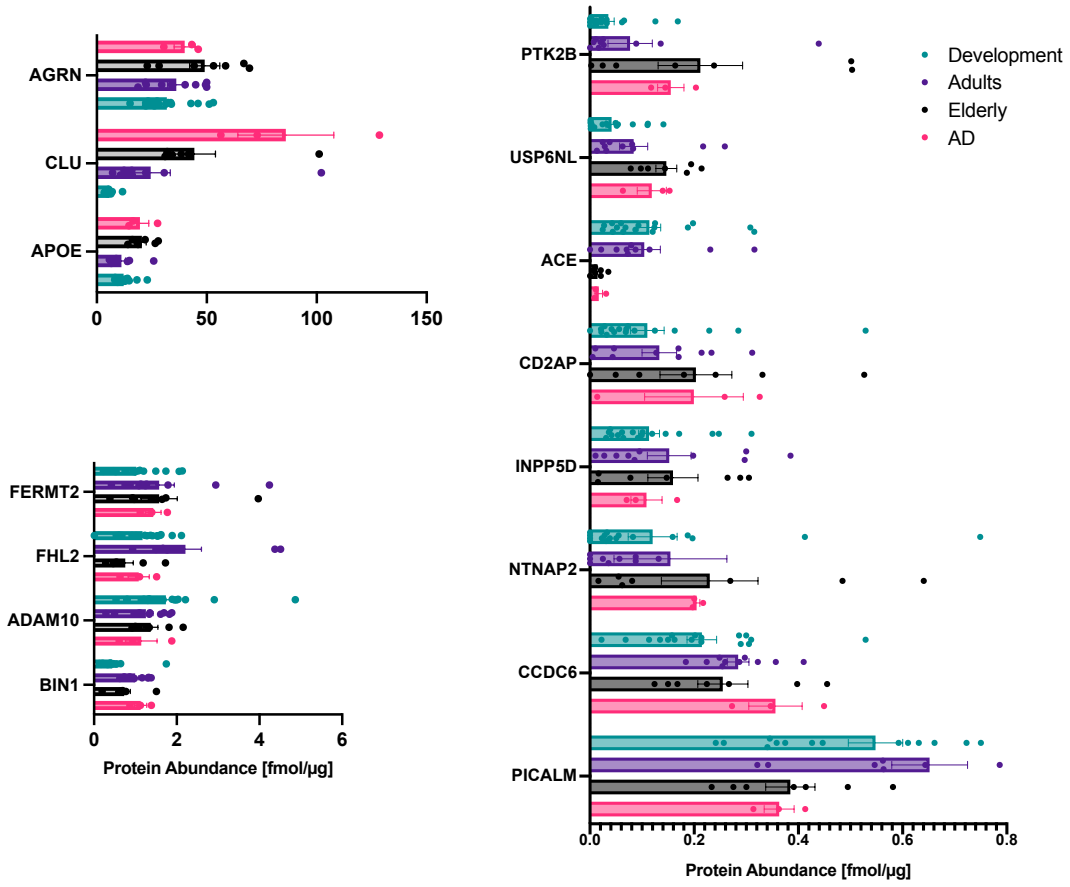

Supplemental Figure 2.4. Protein expression of AD GWAS genes between age groups and with AD

2.7 Tables

Table 2.1. Micronutrients transporters on BBB

			Protein Abundance [pmol/mg]				
Substrate Category	**Gene (Protein)**	**Predominant substrate(s)**	**Infants**	**Adults**	**Elderly**	**Developmental Changes (p-value*)**	**Aging Changes (p-value*)**
Vitamins	SLC19A1(RFC)	Folates	0.199	0.495	0.331	↑(0.012)	
	SLC19A3(THTR2)	Thiamine	0.088	0.218	0.167		
	SLC52A2(RFVT2)	Riboflavin	0.34	0.169	0.032	↓(0.02)	↓(0.008)
	SLC52A3(RFVT3)	Riboflavin	0.063	0.046	0.245		↑(0.004)
Metals	SLC30A1(ZNT1)	Zinc	1.255	1.279	0.642		↓(0.007)
	SLC30A10(ZNT10)	Manganese, Zinc	0.167	0.078	0.017	↓(0.012)	
	SLC30A5(ZNT5)	Zinc	0.085	0.045	0	↓(0.007)	↓(<0.001)
	SLC30A7(ZNT7)	Zinc	0.308	0.126	0.114	↓(0.002)	
	SLC39A10(ZIP10)	Zinc	0.116	0.129	0.019		↓(<0.001)
	SLC39A6(ZIP6)	Zinc	0.028	0.013	0.002		↓(0.031)
	SLC39A8(ZIP8)	Zinc, Cadmium, Manganese	0.053	0.094	0.006		↓(<0.001)
	SLC40A1(FPN1)	Ferrous iron	0.104	0.078	0		↓(0.004)
	TFRC (TFR1)	Iron	13.382	5.915	2.87	↓(<0.001)	↓(0.005)
Neuro-transmmiter	SLC6A12(BGT1)	betaine, GABA	1.473	2.506	2.409	↓(0.018)	
	SLC6A1(GAT1)	GABA	1.854	2.972	1.63	↓(0.021)	↓(0.026)

Table 2.2. Macronutrients transporters on BBB

			Protein Abundance [pmol/mg]				
Substrate Category	**Gene (Protein)**	**Predominant substrate(s)**	**Infants**	**Adults**	**Elderly**	**Developmental Changes (p-value*)**	**Aging Changes (p-value*)**
Amino Acids	SLC3A2(CD98hc/4F2hc)	-	26.093	18.151	15.261	↓(0.048)	0.313
	SLC7A1(CAT1)	CAAs (L-Arg)	3.318	1.527	0.970	↓(0.0014)	0.123
	SLC7A5(LAT1)	LNAAs	5.235	3.054	2.346	↓(0.032)	0.333
	SLC7A8(LAT2)	LNAAs	0.462	0.126	0.028	↓(0.000011)	↓(0.0066)
	SLC38A2(SNAT2)	L-Gln	0.090	0.082	0.019	0.749	↓(0.0032)
	SLC38A3(SNAT3)	L-Gln	1.220	0.566	0.555	↓(0.0015)	0.943
	SLC38A5(SNAT5)	L-Gln	1.027	0.527	0.082	↓(0.00062)	↓(0.00012)
	SLC25A13(AGC2/Aralar 2)	L-Asp, L-Glu	1.393	0.745	0.983	↓(0.00036)	0.355
	SLC43A2(LAT4)	BCAAs	0.030	0.040	0.006	0.481	↓(0.011)
Glucose	SLC2A1(GLUT1))	Glucose	25.855	38.187	18.229	0.075	↓(0.0059)
	SLC2A4(GLUT4)	Glucose	0.012	0.125	0.104	↑(0.017)	0.643
Nucleotide sugars	SLC35A4(MGC2541)	PAPS	0.357	1.137	1.604	↑(0.0054)	0.315
	SLC35B1(UGTREL1)	UDPGA	0.041	0.019	0.000	↓(0.017)	↓(0.010)
	SLC35B2(PAPST1)	PAPS	0.086	0.047	0.059	↓(0.011)	0.704
Choline	FLVCR2	Choline, heme	0.030	0.013	0.005	↓(0.035)	0.095
	SLC44A1	Choline	0.483	0.945	1.228	↑(0.0065)	0.144
	SLC44A2	Choline	2.072	2.133	2.002	0.810	0.380

Table 2.3. SLC transporters on BBB associated mendelian disease

			Protein Abundance [pmol/mg]				
Gene (Protein)	Predominant substrate(s)	Mendelian disease(s)	Infants	Adults	Elderly	Developmental Changes (p-value*)	Aging Changes (p-value*)
SLCO2A1	Prostraglandin	Hypertrophic osteoarthropathy	0.340	0.040	0.046	↓(0.0030)	0.849
SLC52A3(RFVT3)	Riboflavin	Brown-Vialetto-Van Laere syndrome	0.063	0.046	0.245	0.698	↑(0.0039)
SLC52A2(RFVT2)	Riboflavin	Brown-Vialetto-Van Laere syndrome	0.340	0.169	0.032	↓(0.020)	↓(0.0077)
SLC49A2(FLVCR2)	Choline, heme	Proliferative vasculopathy and hydranencephaly-hydrocephaly syndrome	0.030	0.013	0.005	↓(0.035)	0.095
SLC40A1(FPN1)	Ferrous iron	Hemochromatosis type 4	0.104	0.078	0.000	0.396	↓(0.0040)
SLC37A4(G6PT)	Glucose-6-phophate	Glycogen-storage disease type Ib or Ic	0.093	0.030	0.092	↓(0.024)	0.052
SLC33A1(ACATN1)	Acetyl-CoA	Spastic Paraplegia 42, Huppke-Brendel Syndrome	0.009	0.010	0.021	0.887	0.080
SLC30A10(ZnT10)	Zinc	Hypermanganesemia with dystonia-1	0.167	0.078	0.017	↓(0.012)	↓(0.0063)
SLC2A1(GLUT1)	Glucose	GLUT1 Deficiency Syndrome 1/ Syndrome 2	25.855	38.187	18.229	0.075	↓(0.0059)
SLC25A4(ANT1)	ADP, ATP	progressive external ophthalmoplegia (PEO); mitochondrial DNA depletion syndrome (MTDPS)	5.837	10.034	5.230	↑(0.020)	↓(0.021)
SLC25A3(PHC)	Phosphate	Mitochondrial phosphate carrier deficiency	26.163	26.835	17.954	0.812	↓(0.0060)
SLC25A20(CAC)	Arnitine, acylcarnitine	Carnitine- acylcarnitine translocase deficiency	0.596	0.405	0.487	↓(0.025)	0.368
SLC25A15(ORC1)	Ornithine, citrulline	Hyperornithinemia-hyperammonemia-homocitrullinuria syndrome	0.055	0.044	0.004	0.706	0.179
SLC25A13(AGC2)	Aspartate, glutamate	Adult-onset type II Citrullinemia (CTLN2); Neonatal intrahepatic cholestasis caused by citrin deficiency (NICCD)	1.393	0.745	0.983	↓(0.00036)	0.355
SLC1A4(ASCT1)	L-Ala, L-Ser	Spastictetraplegia, thincorpus callosum, and progressive microcephaly (SPATCCM)	1.305	0.393	0.692	↓(0.042)	0.065
SLC19A3(THTR2)	Thiamine	Thiamine metabolism dysfunction syndrome 2	0.088	0.218	0.167	0.071	0.480
SLC16A2(MCT8)	Thyroid hormones	Allan-Herndon-Dudley syndrome (AHDS)	1.870	0.911	0.565	↓(0.00024)	0.066
SLC16A1(MCT1)	Lactate, pyruvate	Erythrocyte lactate transporter defect; hyperinsulinemic hypoglycemia; monocarboxylate transporter-1 deficiency (MCT1D)	11.824	5.608	4.465	↓(0.032)	0.399
SLC13A5(Nac2)	Citrate, succinate	Developmental and epileptic encephalopathy 25 with amelogenesis imperfecta	0.006	0.017	0.000	0.148	↓(0.017)
RFT1	Man(5)GlcNAc (2)-PP-Dol (oligosaccharide)	Congenital disorders of glycosylation (CDG)	0.170	0.052	0.157	↓(0.00080)	0.051

Supplemental Table 2.1. Overview of sample size and age range of samples

Age group		Number of samples	Age range
Development	Fetus/Neonate	7	-37 weeks gestation – 28 days
	Infant	10	1 – 6 months
Adult	Child	5	4 – 12 years
	Adolescent/Adult	5	12 – 30 years
Elderly	Adult >60yrs	7	61 – 103 years
	Alzheimer's disease	4	
	Total	38	

Supplemental Table 2.2. Compare to previous studies (Markers for other cell types)

Markers	Cell type	The present study [fmol/µg]	Al-Majdoub et al,2019 [fmol/µg]	Shawhana et al., 2011 [fmol/µg]	Uchida et al., 2011 [fmol/µg]
GFAP	Astrocytes	205.22 ± 213.77	19.2 ± 18.4	503.2 ± 174.09	NQ
NG2(CSPG4)	Pericytes	1.21 ± 0.55	0.16 ± 0.06	1.07 ± 0.41	NQ
SYP	Neurons	11.21 ± 12.57	3.01 ± 2.45	1.45 ± 0.37	NQ

2.8 References

1. Thomsen, M.S., L.J. Routhe, and T. Moos, *The vascular basement membrane in the healthy and pathological brain.* Journal of Cerebral Blood Flow and Metabolism, 2017. **37**(10): p. 3300-3317.
2. Kadry, H., B. Noorani, and L. Cucullo, *A blood-brain barrier overview on structure, function, impairment, and biomarkers of integrity.* Fluids and Barriers of the Cns, 2020. **17**(1).
3. Luissint, A.C., et al., *Tight junctions at the blood brain barrier: physiological architecture and disease-associated dysregulation.* Fluids Barriers CNS, 2012. **9**(1): p. 23.
4. Knox, E.G., et al., *The blood-brain barrier in aging and neurodegeneration.* Mol Psychiatry, 2022. **27**(6): p. 2659-2673.
5. Morris, M.E., V. Rodriguez-Cruz, and M.A. Felmlee, *SLC and ABC Transporters: Expression, Localization, and Species Differences at the Blood-Brain and the Blood-Cerebrospinal Fluid Barriers.* AAPS J, 2017. **19**(5): p. 1317-1331.
6. Tiani, K.A., P.J. Stover, and M.S. Field, *The Role of Brain Barriers in Maintaining Brain Vitamin Levels.* Annu Rev Nutr, 2019. **39**: p. 147-173.
7. Nguyen, Y.T.K., et al., *The role of SLC transporters for brain health and disease.* Cell Mol Life Sci, 2021. **79**(1): p. 20.
8. Cater, R.J., et al., *Structural and molecular basis of choline uptake into the brain by FLVCR2.* bioRxiv, 2023.
9. Geier, E.G., et al., *Structure-based ligand discovery for the Large-neutral Amino Acid Transporter 1, LAT-1.* Proc Natl Acad Sci U S A, 2013. **110**(14): p. 5480-5.
10. Pardridge, W.M., R.J. Boado, and C.R. Farrell, *Brain-type glucose transporter (GLUT-1) is selectively localized to the blood-brain barrier. Studies with quantitative western blotting and in situ hybridization.* J Biol Chem, 1990. **265**(29): p. 18035-40.

11. Uchida, Y., et al., *Quantitative targeted absolute proteomics of human blood-brain barrier transporters and receptors.* Journal of Neurochemistry, 2011. **117**(2): p. 333-345.
12. Shawahna, R., et al., *Transcriptomic and Quantitative Proteomic Analysis of Transporters and Drug Metabolizing Enzymes in Freshly Isolated Human Brain Microvessels.* Molecular Pharmaceutics, 2011. **8**(4): p. 1332-1341.
13. Al-Majdoub, Z.M., et al., *Proteomic Quantification of Human Blood-Brain Barrier SLC and ABC Transporters in Healthy Individuals and Dementia Patients.* Molecular Pharmaceutics, 2019. **16**(3): p. 1220-1233.
14. Saunders, N.R., et al., *Physiology and molecular biology of barrier mechanisms in the fetal and neonatal brain.* J Physiol, 2018. **596**(23): p. 5723-5756.
15. Mollgard, K., et al., *Brain barriers and functional interfaces with sequential appearance of ABC efflux transporters during human development.* Sci Rep, 2017. **7**(1): p. 11603.
16. Crouch, E.E., et al., *Ensembles of endothelial and mural cells promote angiogenesis in prenatal human brain.* Cell, 2022. **185**(20): p. 3753-3769 e18.
17. Yang, A.C., et al., *A human brain vascular atlas reveals diverse mediators of Alzheimer's risk.* Nature, 2022. **603**(7903): p. 885-892.
18. Swain, T.R., *Clinical trials for children: some concerns.* Indian J Pharmacol, 2014. **46**(2): p. 145-6.
19. Ek, C.J., et al., *Barriers in the developing brain and Neurotoxicology.* Neurotoxicology, 2012. **33**(3): p. 586-604.
20. Stephenson, J., et al., *Inflammation in CNS neurodegenerative diseases.* Immunology, 2018. **154**(2): p. 204-219.
21. Sweeney, M.D., A.P. Sagare, and B.V. Zlokovic, *Blood-brain barrier breakdown in Alzheimer disease and other neurodegenerative disorders.* Nature Reviews Neurology, 2018. **14**(3): p. 133-150.

22. Prakash, R. and S.T. Carmichael, *Blood-brain barrier breakdown and neovascularization processes after stroke and traumatic brain injury.* Curr Opin Neurol, 2015. **28**(6): p. 556-64.

23. Kortekaas, R., et al., *Blood-brain barrier dysfunction in parkinsonian midbrain in vivo.* Ann Neurol, 2005. **57**(2): p. 176-9.

24. Chiu, C., et al., *P-glycoprotein expression and amyloid accumulation in human aging and Alzheimer's disease: preliminary observations.* Neurobiol Aging, 2015. **36**(9): p. 2475-82.

25. Erdo, F. and P. Krajcsi, *Age-Related Functional and Expressional Changes in Efflux Pathways at the Blood-Brain Barrier.* Front Aging Neurosci, 2019. **11**: p. 196.

26. Thomsen, M.S., L.J. Routhe, and T. Moos, *The vascular basement membrane in the healthy and pathological brain.* J Cereb Blood Flow Metab, 2017. **37**(10): p. 3300-3317.

27. Bradshaw, A.D., *The role of SPARC in extracellular matrix assembly.* J Cell Commun Signal, 2009. **3**(3-4): p. 239-46.

28. Muffat, J. and D.W. Walker, *Apolipoprotein D: an overview of its role in aging and age-related diseases.* Cell Cycle, 2010. **9**(2): p. 269-73.

29. Schachtschneider, K.M., et al., *Altered Hippocampal Epigenetic Regulation Underlying Reduced Cognitive Development in Response to Early Life Environmental Insults.* Genes (Basel), 2020. **11**(2).

30. Watt, N.T., I.J. Whitehouse, and N.M. Hooper, *The role of zinc in Alzheimer's disease.* Int J Alzheimers Dis, 2010. **2011**: p. 971021.

31. Alsaqati, M., R.S. Thomas, and E.J. Kidd, *Proteins Involved in Endocytosis Are Upregulated by Ageing in the Normal Human Brain: Implications for the Development of Alzheimer's Disease.* J Gerontol A Biol Sci Med Sci, 2018. **73**(3): p. 289-298.

32. Langfelder, P. and S. Horvath, *WGCNA: an R package for weighted correlation network analysis.* BMC Bioinformatics, 2008. **9**: p. 559.

33. Shannon, P., et al., *Cytoscape: a software environment for integrated models of biomolecular interaction networks.* Genome Res, 2003. **13**(11): p. 2498-504.

34. Knickmeyer, R.C., et al., *A structural MRI study of human brain development from birth to 2 years.* J Neurosci, 2008. **28**(47): p. 12176-82.

35. Cohen Kadosh, K., et al., *Nutritional Support of Neurodevelopment and Cognitive Function in Infants and Young Children-An Update and Novel Insights.* Nutrients, 2021. **13**(1).

36. Shamberger, R.J., *Autism rates associated with nutrition and the WIC program.* J Am Coll Nutr, 2011. **30**(5): p. 348-53.

37. Piecuch, A.K., P.H. Skarzynski, and H. Skarzynski, *A Case Report of Riboflavin Treatment and Cochlear Implants in a 4-Year-Old Girl with Progressive Hearing Loss and Delayed Speech Development: Brown-Vialetto-Van Laere Syndrome.* Am J Case Rep, 2023. **24**: p. e940439.

38. Zhou, L., *Association of vitamin B2 intake with cognitive performance in older adults: a cross-sectional study.* J Transl Med, 2023. **21**(1): p. 870.

39. Tao, L., et al., *Dietary Intake of Riboflavin and Unsaturated Fatty Acid Can Improve the Multi-Domain Cognitive Function in Middle-Aged and Elderly Populations: A 2-Year Prospective Cohort Study.* Front Aging Neurosci, 2019. **11**: p. 226.

40. Yao, Y., et al., *Identification and comparative functional characterization of a new human riboflavin transporter hRFT3 expressed in the brain.* J Nutr, 2010. **140**(7): p. 1220-6.

41. He, W. and G. Wu, *Metabolism of Amino Acids in the Brain and Their Roles in Regulating Food Intake.* Adv Exp Med Biol, 2020. **1265**: p. 167-185.

42. Radzishevsky, I., et al., *Impairment of serine transport across the blood-brain barrier by deletion of Slc38a5 causes developmental delay and motor dysfunction.* Proc Natl Acad Sci U S A, 2023. **120**(42): p. e2302780120.

43. Tachikawa, M., et al., *Developmental changes of l-arginine transport at the blood-brain barrier in rats.* Microvasc Res, 2018. **117**: p. 16-21.

44. Unsal, Y. and G. Hayran, *Impact of Early Intervention with Triiodothyroacetic Acid on Peripheral and Neurodevelopmental Findings in a Boy with MCT8 Deficiency.* J Clin Res Pediatr Endocrinol, 2023.

45. Balachandran, R.C., et al., *Brain manganese and the balance between essential roles and neurotoxicity.* J Biol Chem, 2020. **295**(19): p. 6312-6329.

46. Lechpammer, M., et al., *Pathology of inherited manganese transporter deficiency.* Ann Neurol, 2014. **75**(4): p. 608-12.

47. Boycott, K.M., et al., *Autosomal-Recessive Intellectual Disability with Cerebellar Atrophy Syndrome Caused by Mutation of the Manganese and Zinc Transporter Gene SLC39A8.* Am J Hum Genet, 2015. **97**(6): p. 886-93.

48. Santander, N., et al., *Lack of Flvcr2 impairs brain angiogenesis without affecting the blood-brain barrier.* J Clin Invest, 2020. **130**(8): p. 4055-4068.

49. Bessieres-Grattagliano, B., et al., *Refining the clinicopathological pattern of cerebral proliferative glomeruloid vasculopathy (Fowler syndrome): report of 16 fetal cases.* Eur J Med Genet, 2009. **52**(6): p. 386-92.

50. Galetin, A., et al., *Membrane transporters in drug development and as determinants of precision medicine.* Nat Rev Drug Discov, 2024.

51. Ho, R.H., et al., *Drug and bile acid transporters in rosuvastatin hepatic uptake: function, expression, and pharmacogenetics.* Gastroenterology, 2006. **130**(6): p. 1793-806.

52. Kavey, R.W., et al., *Effectiveness and Safety of Statin Therapy in Children: A Real-World Clinical Practice Experience.* CJC Open, 2020. **2**(6): p. 473-482.

53. Iwaki, M., et al., *Inhibition of Methotrexate Uptake via Organic Anion Transporters OAT1 and OAT3 by Glucuronides of Nonsteroidal Anti-inflammatory Drugs.* Biol Pharm Bull, 2017. **40**(6): p. 926-931.

54. Sane, R., et al., *The effect of ABCG2 and ABCC4 on the pharmacokinetics of methotrexate in the brain.* Drug Metab Dispos, 2014. **42**(4): p. 537-40.

55. Bhojwani, D., et al., *Methotrexate-induced neurotoxicity and leukoencephalopathy in childhood acute lymphoblastic leukemia.* J Clin Oncol, 2014. **32**(9): p. 949-59.

56. Taylor, O.A., et al., *Disparities in Neurotoxicity Risk and Outcomes among Pediatric Acute Lymphoblastic Leukemia Patients.* Clin Cancer Res, 2018. **24**(20): p. 5012-5017.

57. Mori, S., et al., *Rat organic anion transporter 3 (rOAT3) is responsible for brain-to-blood efflux of homovanillic acid at the abluminal membrane of brain capillary endothelial cells.* J Cereb Blood Flow Metab, 2003. **23**(4): p. 432-40.

58. Mima, S., et al., *Identification of the TPO1 gene in yeast, and its human orthologue TETRAN, which cause resistance to NSAIDs.* FEBS Lett, 2007. **581**(7): p. 1457-63.

59. Gaohua, L., et al., *Development of a permeability-limited model of the human brain and cerebrospinal fluid (CSF) to integrate known physiological and biological knowledge: Estimating time varying CSF drug concentrations and their variability using in vitro data.* Drug Metab Pharmacokinet, 2016. **31**(3): p. 224-33.

60. Abu-Remaileh, M. and R.I. Aqeilan, *Tumor suppressor WWOX regulates glucose metabolism via HIF1alpha modulation.* Cell Death Differ, 2014. **21**(11): p. 1805-14.

61. Shen, Y., et al., *Inhibition of HIF-1alpha Reduced Blood Brain Barrier Damage by Regulating MMP-2 and VEGF During Acute Cerebral Ischemia.* Front Cell Neurosci, 2018. **12**: p. 288.

62. Hsu, C.Y., et al., *WWOX and Its Binding Proteins in Neurodegeneration.* Cells, 2021. **10**(7).

63. Banks, W.A., et al., *Healthy aging and the blood-brain barrier.* Nat Aging, 2021. **1**(3): p. 243-254.

64. Lee, S., et al., *A guide to senolytic intervention in neurodegenerative disease.* Mech Ageing Dev, 2021. **200**: p. 111585.

65. Bertram, L. and R.E. Tanzi, *Genome-wide association studies in Alzheimer's disease.* Hum Mol Genet, 2009. **18**(R2): p. R137-45.

66. Zhao, H., et al., *Destabilizing heterochromatin by APOE mediates senescence.* Nat Aging, 2022. **2**(4): p. 303-316.

67. Ando, K., et al., *Picalm reduction exacerbates tau pathology in a murine tauopathy model.* Acta Neuropathol, 2020. **139**(4): p. 773-789.

68. Mahoney, E.R., et al., *Brain expression of the vascular endothelial growth factor gene family in cognitive aging and alzheimer's disease.* Mol Psychiatry, 2021. **26**(3): p. 888-896.

69. Chen, E.C., et al., *High Throughput Screening of a Prescription Drug Library for Inhibitors of Organic Cation Transporter 3, OCT3.* Pharm Res, 2022. **39**(7): p. 1599-1613.

70. Blighe K, R.S., Lewis M, *EnhancedVolcano: Publication-ready volcano plots with enhanced colouring and labeling. .* 2023.

71. Yu, G., et al., *clusterProfiler: an R package for comparing biological themes among gene clusters.* OMICS, 2012. **16**(5): p. 284-7.

72. Ricard-Blum, S., *The collagen family.* Cold Spring Harb Perspect Biol, 2011. **3**(1): p. a004978.

73. Cescon, M., et al., *Collagen VI sustains cell stemness and chemotherapy resistance in glioblastoma.* Cell Mol Life Sci, 2023. **80**(8): p. 233.

74. Scholl-Burgi, S., et al., *Amino acid cerebrospinal fluid/plasma ratios in children: influence of age, gender, and antiepileptic medication.* Pediatrics, 2008. **121**(4): p. e920-6.

75. Avan, R., et al., *Update on Statin Treatment in Patients with Neuropsychiatric Disorders.* Life (Basel), 2021. **11**(12).

76. Torrandell-Haro, G., et al., *Statin therapy and risk of Alzheimer's and age-related neurodegenerative diseases.* Alzheimers Dement (N Y), 2020. **6**(1): p. e12108.

77. Hussain, H.M., M. Zakria, and A.R. Arshad, *Statins, incident Alzheimer disease, change in cognitive function, and neuropathology.* Neurology, 2008. **71**(24): p. 2019; author reply 2019-20.

78. Yang, A.C., et al., *Physiological blood-brain transport is impaired with age by a shift in transcytosis.* Nature, 2020. **583**(7816): p. 425-430.

79. Blanchard, J.W., et al., *Reconstruction of the human blood-brain barrier in vitro reveals a pathogenic mechanism of APOE4 in pericytes.* Nat Med, 2020. **26**(6): p. 952-963.

80. Rieker, C., et al., *Apolipoprotein E4 Expression Causes Gain of Toxic Function in Isogenic Human Induced Pluripotent Stem Cell-Derived Endothelial Cells.* Arterioscler Thromb Vasc Biol, 2019. **39**(9): p. e195-e207.

Chapter 3. A Deep Mutational Scanning of the ATP-binding Cassette Superfamily G Member 2 (ABCG2)

3.1 Abstract

ATP-binding cassette superfamily G member 2 (ABCG2), also known as Breast cancer resistance protein (BCRP), is a key pharmacogene that plays a crucial role in drug absorption, drug disposition and in the development of anti-cancer drug resistance. While structural studies have provided insights, the full comprehension of ABCG2's mechanisms of transport, poly-specificity, expression, and localization remains elusive. Tumors can become resistant to certain chemotherapy drugs, such as topotecan and mitoxantrone, by increasing the expression of ABCG2. Researchers are actively trying to develop inhibitors that specifically target ABCG2 to overcome this defense mechanism in cancer cells. However, creating these inhibitors for clinical use is challenging due to concerns about their precision, safety, and how well they can be absorbed by the body. Therefore, a detailed understanding of the mechanism of ABCG2 transport dynamics is essential to create effective drugs to block its action.

Deep mutational scanning (DMS) is an innovative method that applies next-generation sequencing (NGS) to associate a vast array of variants with their functional outcomes. This study leverages the DMS approach to evaluate 12,724 variants of the ABCG2. Our experimental platform was designed to assay all possible single missense, as well as one synonymous for each positions and some deletion variants of ABCG2. Through this platform, we quantified the abundance of ABCG2, assessed its surface expression, and examined the functional implications of each variant using the anti-cancer drug mitoxantrone, which is a well-known ABCG2 substrate. This comprehensive analysis has generated a detailed functional map, visualized through heatmaps and integrated with the publicly experimental structure of ABCG2. By comparing our findings with existing structural information, we identified critical residues imperative for ABCG2 function. This study not only advances our understanding of ABCG2 but also sets a foundational framework for future research on other ABC transporters,

emphasizing the significance of DMS in unraveling the complexities of pharmacogenes and drug resistance mechanism.

3.2 Introduction

Mutations in pharmacogenes, such as enzymes involved in drug metabolism and transporters essential for drug distribution and disposition, can influence how the body handles drugs, leading to variations in drug effects and pharmacokinetics. A significant number of these transporters belong to the ATP-binding cassette (ABC) and Solute Carrier (SLC) superfamilies. The clinical evidence of ABCG2(BCRP) as an important target for drug-drug interactions (DDIs) has led the International Transporter Consortium to identify ABCG2 as a critical transporter to assess during the drug development process [1]. Following this, the US Food and Drug Administration (FDA) and the European Medicines Agency (EMA) have published guidances with specific criteria are advised to conduct clinical pharmacogenetic examinations for new medications that are affected by transporters with known polymorphisms [2]. Further, polymorphisms in the transporter are cited by the Clinical Pharmacogenetics Implementation consortium to play a critical role in response to rosuvastatin [3], and the International Transporter Consortium has highlighted ABCG2 as a polymorphic transporter that contributes to interindividual variation in several drugs [4]

ABCG2 is an ABC transporter found in many tissues and barriers within the body, including the placenta, brain, prostate, gastrointestinal tract, testes, ovaries, liver, kidneys, stem cells, adrenal gland, uterus, bile ducts, gallbladder, central nervous system, and the vascular endothelium. It acts as a shield for tissues against xenobiotics and harmful metabolites. ABCG2 distinguishes itself from other major human multidrug transporters through its unique structural and functional attributes. With over 200 substrates identified, ABCG2 interacts with a vast array of compounds

that exhibit a wide variety of chemical structures and biological functions [5]. While there is considerable overlap in the substrate spectra between ABCG2, ABCB1, and ABCC1, ABCG2 maintains a distinct profile, emphasizing its important role in pharmacokinetics.

The significance of ABCG2 in reducing drug penetration across the human blood-brain barrier (BBB) is a focus of recent studies ([6], [7], [8]). Studies using ABCG2 knockout models have illustrated the transporter's effectiveness in restricting the entry of various substances into the brain such as anti-cancer and antiepileptic drugs. For instance, the brain uptake of methotrexate, an antifolate chemotherapeutic agent used in treating primary CNS lymphoma, is significantly restricted, with only about 5% of the drug in plasma actually reaching the brain tissue [9]. In vivo, studies have indicated ABCG2's role in methotrexate efflux across the BBB, with a marked decrease in drug extrusion observed in ABCG2-deficient models compared to the wild-type control [10]. Similarly, the clinical effectiveness of mitoxantrone, an anthracenedione antineoplastic drug with *in vitro* efficacy against cancer brain cells, is compromised due to its limited CNS distribution. Studies have shown that mitoxantrone transport across the BBB is primarily ABCG2-dependent and revealed that the cerebral uptake of mitoxantrone increased threefold when ABCG2 inhibition was introduced in P-gp-deficient mice, underscoring ABCG2 as a critical factor in the CNS distribution of mitoxantrone [11]. Additionally, clinical observations of low penetration of these two drugs in the brains of patients with recurrent high-grade glioma, suggest a link between ABCG2 function and resistance to cancer therapies ([12], [13]). In addition, in vivo studies demonstrate that Abcg2 participates in the restriction of the brain distribution of many drugs including the anti-epileptic drugs, phenobarbital, clobazam, zonisamide, gabapentin, tiagabine, and levetiracetam [14].

Genetic variations in the ABCG2 gene can disrupt its function, leading to differences in drug distribution and effects. Despite the identification of more than hundreds of single nucleotide

polymorphisms (SNPs) within the ABCG2 gene, only a few have been thoroughly studied for their functional impact. Two common missense variants in ABCG2—V12M (rs2231137) and Q141K (rs2231142), which occur at a frequency of more than 1%, have been intensively studied. The impact of V12M on ABCG2's function remains controversial, mirroring clinical observations regarding its influence on the effectiveness of antiepileptic drugs (AEDs) [15] ([16],[17]). On the other hand, Q141K has been shown to decrease ABCG2 protein levels by increasing proteasomal degradation *in vitro* studies. ([18], [19]). This polymorphism is associated with higher systemic concentrations of certain drugs, such as sulfasalazine, rosuvastatin, and atorvastatin [1] as well as response to the anti-gout medication, allopurinol, in large genomewide association studies [20]. Further, meta-analysis has revealed that this variant has increased systemic exposure to rosuvastatin compared to those without this variant [21]. Additionally, clinical observations have noted an elevated risk of adverse reactions to gefitinib in patients who possess Q141K [22].

Additionally, mutations in the ABCG2, other than overexpression, have been known to be another possible mechanism of cancer drug resistance. Specifically, mutations in position 482 of ABCG2, initially identified in drug-resistant cancer cell lines, have been shown to modify the substrate specificity of ABCG2. Cells expressing mutated ABCG2 in position 482 demonstrated an increased ability to efflux doxorubicin and mitoxantrone while displaying diminished resistance to SN-38, a topoisomerase-inhibiting anticancer agent [23]. This suggests that mutations can significantly alter the substrate spectrum of ABCG2, leading to drug resistance.

Despite its important role in drug resistance and distribution, the full extent of how various mutations might impact ABCG2 function in drug transport remains largely unknown. This study aims to determine the effects of all potential single-point mutations and deletions on the ABCG2 protein expression levels, localization, and sensitivity to drugs.

Advancing technologies have greatly increased the scale at which traditional functional studies are possible. Deep mutational scanning (DMS) is an emerging approach used to functionally characterize thousands of protein variants in parallel [24]. Identification and development of a relevant assay for generating high-quality large-scale functional data can be challenging. Here, we present an experimental platform compatible with DMS of 12,724 variants in the pharmacogene ABCG2, including all possible single missense variants, synonymous variants and deletion mutations. We measured ABCG2 abundance, assessed surface expression, and tested functional capabilities using anti-cancer drug, mitoxantrone. Next-generation sequencing followed by computational analysis allowed us to assign scores to each variant for each assay, resulting in a detailed map of their functional effects. These findings were visualized on heatmaps and integrated into the ABCG2 experimental structure. We mapped essential residues for surface abundance using structures of ABCG2 and compared results with existing models to enhance our understanding of transporter function, building upon prior research.

3.3 Methods

3.3.1 Library generation

The ABCG2 library was generated using the DIMPLE methodology (Deep Insertion, Deletion, and Missense Mutation Libraries for Exploring Protein Variation in Evolution, Disease, and Biology), as outlined by Macdonald et al., 2023 [25]. This technique, which is adapted from SPINE, was used to design the oligonucleotides to induce mutations, insertions, and deletions [26] in the gene of interest. The code enabled the mutation of each amino acid position into any of the 19 other amino acids, alteration to a synonymous codon, and introduction of deletions. Is available at https://github.com/coywil26/DIMPLE.

3.3.2 Library generation and cloning

The methods for generating and cloning the library were previously detailed by Macdonald et al., 2023 [25]. Oligonucleotides for ABCG2 were synthesized by Agilent Technologies (SurePrint Oligonucleotide), yielding 10 pmol of lyophilized DNA. This DNA was subsequently reconstituted in 1X TE buffer. The vector harboring ABCG2 was produced by Twist Bioscience, utilizing a High Copy Number Kanamycin resistance vector backbone. The lyophilized plasmid DNA was then dissolved to a concentration of 10 ng/µL in 1X TE buffer.

Sublibraries targeting specific segments of ABCG2 were amplified through PCR, using primer-specific approaches and PrimeStar GXL DNA polymerase(Takara Bio). Thirteen distinct regions underwent amplification in 50 µL reaction volumes, utilizing 1 µL of the comprehensive OLS library as the template and undergoing 30 PCR cycles. Subsequent purification of the PCR products was performed using the Zymo Clean and Concentrate kits from Zymo Research, with the purified DNA being eluted in 10 µL of TE buffer. For each of the thirteen regions, plasmid DNA was further amplified to incorporate golden gate compatible Type IIS restriction sites, aligning with those in the sublibrary oligonucleotides. This step was executed following the manufacturer's protocol for PrimeStar GXL polymerase in 50 µL reactions, starting with 1 µL of the template vector and proceeding through 30 PCR cycles. PCR products were then subjected to electrophoresis on agarose gel and the DNA of interest was extracted using the Zymoclean Gel DNA Recovery Kit.

The PCR product of the target gene backbone and the corresponding oligonucleotide sublibrary were combined using a BsaI-mediated Golden Gate cloning approach. Post-reaction cleanup was performed using Zymo Clean and Concentrate kits, with the final products eluted in 10 µL of nuclease-free water. The prepared samples were then transformed into MegaX DH10B

electrocompetent cells (Thermo Fisher) as per the provided guidelines. Following transformation, MegaX DH10B cells were recovered for one hour at 37°C. To evaluate the efficiency of the transformation, a fraction of the transformed cells was spread on plates with varying densities. In all cases, the number of resulting colonies was at least 100 times greater than the size of the initial library. The bulk of the cells was then incubated in 30 mL of LB medium supplemented with 50 µg/mL kanamycin, shaking at 37°C until an optical density (OD) of 0.6 - 0.7 was achieved. The library DNA was subsequently extracted using a miniprep protocol from Zymo Research. The concentration of each sublibrary was determined using a Qubit fluorometer. Sublibraries corresponding to specific genes were then pooled in equimolar ratios. These pooled libraries then were inserted into a landing pad vector equipped with a BxB1-compatible attB site for recombination, utilizing BsmBI-mediated Golden Gate cloning. To ensure the preservation of library diversity, we monitored the transformation efficiency, aiming for it to be at least 100 times greater than the actual size of the library. The design of the landing pad vector was such that it included BsmBI restriction sites with overhangs compatible for integrating the library, ensuring an N-terminal Kozak sequence alignment and a C-terminal GSGS-mNeonGreen Fragment P2A-Puromycin cassette for effective positive selection. The Golden Gate cloning protocol employed involved alternating temperatures of 42°C for 5 minutes and 16°C for 5 minutes over 29 cycles, concluding with a final step at 60°C for 5 minutes, and then the mixture was stored at 4°C. This specific backbone for the landing pad was constructed using Q5 site-directed mutagenesis, adhering to the recommendations provided by Macdonald et al., 2023. Post-reaction, the samples were purified using Zymo Clean and Concentrate kits, eluted in 10 µL of nuclease-free water, and introduced into MegaX DH10B electrocompetent cells (Thermo Fisher) as per the instructions provided by the manufacturer. Following transformation, the MegaX DH10B cells were allowed to recover for one hour at 37°C. To determine the efficiency of the transformation, a select group of transformed cells was plated at various densities. In every instance, the number of colonies formed was at least 100 times the

library's volume. The rest of the cells were distributed across two large square plates (245mm x 245mm) filled with 200 mL of LB medium supplemented with Ampicillin.

Libraries were cloned into a landing pad vector containing a BxB1-compatible attB recombination site using BsmBI mediated golden gate cloning. We kept track of transformation efficiency to maintain library diversity that was at least 100x the size of a given library. We designed the landing pad vector which we recombined the library into to contain BsmBI cutsites with compatible overhangs for the library to have an in-frame with a N-terminal mNeonGreen-GSGS. This landing pad backbone was generated using Q5 site-directed mutagenesis, cleaned using Zymo Clean and Concentrate kits, and transformed into MegaX DH10B electrocompetent cells (Thermo Fisher) according to the manufacturer's instructions. MegaX DH10B cells were recovered for one hour at 37°C. A small subset of the transformed cells were plated at varying cell density to assess transformation efficiency. All transformations had at least 100x the number of transformed colonies compared to the library size. The remaining of the cells were plated into two large square plates (245mm x 245mm) containing 200 mL LB Amp.

3.3.3 Cell line generation and cell culture

The cell lines developed for this study were detailed in earlier works ([27], [28], [29]). In the process of creating these cell lines, 1500 ng of the previously mentioned library landing pad constructs were co-transfected with 1500 ng of a BxB1 expression vector (pCAG-NLS-BxB1) using 10.5 µL of Lipofectamine LTX across ten wells in a 6-well plate. The culture medium for all cells consisted of 1X DMEM supplemented with 10% FBS, 1% sodium pyruvate, and 1% penicillin/streptomycin (D10). The HEK293T-derived cell line includes a tetracycline-inducible cassette preceding a BxB1 recombination site and a split, rapamycin-analog inducible, dimerizable Casp-9 system. Two days post-transfection, the cells were treated with doxycycline

(2 µg/µL, Sigma-Aldrich) in D10 media to induce the expression of integrated genes or the iCasp-9 selection mechanism. Following the doxycycline induction, AP1903 (10nM, MedChemExpress) was administered two days later to initiate Casp9 dimerization. Only cells that have not undergone successful recombination will undergo apoptosis induced by iCasp-9 upon AP1903 treatment, as successful recombination disrupts the iCasp-9 sequence. After selection with AP1903-Casp9, the cells were detached, pooled, and distributed into two T75 flasks. The cells were cultured to near confluence before being frozen in aliquots using a cryoprotectant solution (2X HyClone, HyCryo, Cryopreservation Reagent).

Sequencing library preparation and genomic DNA extraction and data analysis

Genomic DNA was isolated from cells sorted by four distinct levels of whole-cell GFP or surface PE intensities, as well as from cells exposed to mitoxantrone at various time points, using either the Quick-DNATM Microprep Plus Kit or Quick-DNATM Miniprep Plus Kit depending on cell numbers (Zymo Research). The genomic DNA obtained was then amplified with primers (Landing_pad_backbone_for and P2A_cell_line_rev).

For sequencing preparation, the Nextera XT DNA Library Kit by Illumina was used with a starting material of 1 ng of DNA. Indexing was performed using the IDT for Illumina Nextera DNA Unique Dual Indexes Set D (96 Indexes), and SPRISelect beads (Beckman Coulter) were utilized at a 0.9x ratio for purification and size selection. The prepared libraries, each uniquely indexed, were quantified using Qubit HS and the Agilent 2200 TapeStation. One sample from cells without any treatment were sequencing using miseq to confirm the library coverage and all other samples were combined and sequenced on the NovaSeq 6000 in a paired-end configuration. After demultiplexing fastq files were generated for each sample. The analysis pipeline involved the removal of adapter sequences and contaminants with BBDuk, error correction of paired reads with BBMerge, and mapping to the reference sequence using BBMap

employing 15-mers, all tools from BBTools. Variant calling on the mapped SAM files was performed using the AnalyzeSaturationMutagenesis tool in GATK v4 (Van der Auwera and O'Connor, 2020 [30]), producing a CSV file detailing each variant's genotype and read counts. These results were refined using a Python script to exclude sequences outside the designed variants and prepare data for further data analysis [31]. Scores for each variant were then calculated and normalized against wild-type sequences. The final scores and read counts were analyzed and visualized using R. The analysis confirmed excellent coverage and minimal bias in our libraries and cell lines, as shown in Figure 3.2.

3.3.4 Cytotoxicity assay

Cytotoxicity of mitoxantrone in ABCG2 cells (cells transfected with ABCG2 library) was adapted from previous study ([32]). To determine inhibition potency of mitoxantrone to kill 50% of the cells (IC50), cells were seeded on a 96-well plate (poly-d-lysine coated) at density 4000 cells/well. After 16-24 hours, the cells were incubated with different concentrations of these three drugs, starting from 100 μM to 1.7 nM, for 72 hours. Doxycycline (2 μg/mL) was incubated in the media with each drug to induce the expression levels of ABCG2. After 72 hours, media was removed and 50 μL of media was added to each well. Then 50 μL of Promega® CellTiter-Glo® luminescent reagent was added to each well. After 10-15 min incubation, transfer 80 μL to a 96 well plate (white, opaque). The luminescent cell viability was read on the Promega plate reader. The assay is based on quantification of the ATP present in each well, which relates to the number of viable cells in each well. The luminescent signal from cells treated with DMSO alone was considered the maximal signal (i.e. 100% cell growth). The percent cell growth of each ABCG2 reference and mutants and at each concentration of either mitoxantrone was calculated. IC50 were determined using GraphPad (Prism v9.0). For the deep mutational scanning, we adapted the protocol from Yee et al., 2023 [29] which the ABCG2 cells were first

seeded into four T75 flasks. One flask only has doxycycline (2 μg/mL) and the other three flask contained doxycycline (2 μg/mL) and mitoxantrone. After 48 hours, cells in both T75 flasks were split and transferred into a new T75 flasks and treated with doxycycline (2 μg/mL) with or without these three drugs, respectively. After another 48 hours, the above process was repeated. Every 48 hours, when the cells were split, part of the cells were collected for genomic DNA extraction. The cells in the T75 flask are exposed to each drug for a total of 144 hours.

3.3.5 Fluorescence-activated cell sorting for abundance assay

In the Variant Abundance by Massively Parallel Sequencing (VAMP-seq) approach, we introduce a segment of a split-fluorescent protein (mNG2-11) to the N-terminus of ABCG2 (creating mNG2-11-ABCG2) and co-express it with the remaining segment of the fluorescent protein (mNG2-1-10). The correct folding of mNG2-11-ABCG2 allows it to effectively pair with mNG2-1-10, producing fluorescence. This fluorescence acts as a marker for proper protein folding and stability, compatible with FACS analysis. Following a 24-hour period of transiently transfecting cells with mNG2-1-10, as detailed earlier, cells were sorted using a BD FACSAria II cell sorter. The fluorescence of mNeonGreen and mCherry was activated using a 488 nm laser and a 561 nm laser, respectively. Cells were first gated on forward scattering area and side scattering area to find whole cells, forward scattering width, and height to separate single cells. Then sorting was performed based on mNeonGreen fluorescence levels, independent of mCherry fluorescence. Cells expressing mCherry were classified into four subpopulations according to their mNeonGreen fluorescence intensity. Due to the asymmetrical distribution of fluorescence, the sorting gates were divided into equal bins. Each sorted cell group was then processed for genomic DNA extraction and library preparation for sequencing, following the previously outlined methodology.

3.3.6 Surface expression cell sorting

Cells were cultured in D10 + doxycycline (2 µg/ml) starting from 2 days prior to the experiment. Cells were detached with 1 ml Accutase (Sigma-Aldrich), spun down and washed three times with FACS buffer (2% FBS, 0.1% NaN3, 1X PBS). Then cells were incubated for 1 hr rocking at 4°C with an anti-human-ABCG2-PE antibody (CD338, Thermo Fisher), washed twice with FACS buffers, filtered with cell strainer 5 ml tubes (Falcon), covered with aluminum foil, and kept on ice for transfer to the flow cytometry core.

Cells were sorted on a BD FACSAria II cell sorter. PE fluorescence was excited using a 565 nm laser. Cells were gated first to separate single cells, and label for surface-expressed cells. The surface expression label gate boundaries were determined based on unlabeled cells from the same population because controls tend to have non-representative distributions. Cells were sorted into four populations based on surface expression. Subsequently, each cell population underwent the extraction of genomic DNA and the preparation of a library for sequencing, as described in the previous method section.

3.4 Results

3.4.1 A multiparametric deep mutational scan of ABCG2

ABCG2 plays a critical role in protecting cells from xenobiotics and also keeps the proper concentration of several endogenous compounds. These functions depend upon its proper folding, dimerization, surface localization, and ATP binding.

To investigate the impact of ABCG2 mutations on these processes, we employed SPINE, a targeted deep mutagenesis technique. This approach involved altering or removing amino acids

2-656 in the human ABCG2 protein (Q9UNQ0) to different residues, as detailed in Section 3.3.1 of the Methods. In our mutagenesis library, ABCG2 is tagged at its N-terminus with a segment of the split fluorescent protein, mNeonGreen_11, linked via a double Gly-Ser sequence. This 16-amino acid segment from mNeonGreen is non-fluorescent until it is co-expressed with another fragment, mNeonGreen_1-10, which then reconstitutes the fluorescent protein through self-assembly(28851864). The mNeonGreen_1-10/11 configuration is advantageous because the mNeonGreen_11 segment's small size is unlikely to interfere with ABCG2's folding, stability, or functionality. Moreover, this strategy increases fluorescence intensity upon reassembly and greatly diminishes background fluorescence from non-assembled fragments, a notable improvement over conventional split fluorescent protein systems like GFP_1-10/11. Using this deep mutational scanning (DMS) library, we established a stable, single-copy HEK293 cell line through BxBI-mediated recombination [27], ensuring a precise correlation between genotype and phenotype. Sequencing of this cell line revealed the creation of 12,724 mutations in ABCG2, indicating excellent mutation coverage.

Given that mutations can influence any of the previously outlined processes (folding, dimerization, surface localization, and ATP binding), it's essential to employ a multiparametric approach to phenotype analysis for a thorough mechanistic insight into ABCG2 variations. Our research aims to distinguish the effects of mutations on several aspects: expression within the entire cell ('whole cell expression'), protein localization to the cell surface ('surface expression'), and the capacity to transport mitoxantrone ('function'). Given the extensive variety of variants in our library (12,724 in total), the methodologies to evaluate surface expression and functionality need to be capable of processing large numbers of samples efficiently. The cytotoxicity assay is utilized to filter variants based on ABCG2's substrate efflux capability, while FACS is applied to categorize variants by their expression phenotypes (Fig. 3.1). Subsequently, sequencing is employed to link each phenotype with its corresponding genotype.

3.4.2 Validation study indicates that ABCG2 function in landing-pad cell lines

We conducted validation studies on the functionality of human ABCG2 and its variants, Q141K and R482G, in HEK293T landing pad cells using cytotoxicity assay with mitoxantrone which are the same drugs we used for the DMS. For this purpose, HEK293T cells stably incorporating hABCG2 and the aforementioned variants were subjected to varying concentrations of these drugs, up to a maximum of 250 nM.

To evaluate cell viability, we exposed the cells to a gradient of drug concentrations, ranging from 0 to 250 nM, over a 72-hour period (Fig. 3.6). Consistent with previous findings and our own screening data, the cells harboring the ABCG2 Q141K variant showed heightened sensitivity to mitoxantrone, reflecting a loss-of-function phenotype. Similarly, in agreement with previous studies [23], cells expressing the R482G variant of ABCG2 demonstrated enhanced resistance to the cytotoxic effects of mitoxantrone.

3.4.3 Mapped regions involved in loss-of-function of ABCG2

Typically, ABC transporters consist of two transmembrane domains (TMDs), each with at least 12 α-helices spanning the membrane and two nucleotide-binding domains (NBDs) oriented towards the cytosol [33]. The TMDs including the substrate binding site, form the pathway through which substrates are translocated, while the NBDs are crucial for ATP binding and hydrolysis. In contrast, ABCG2 comprises only one NBD and one TMD, with the TMD containing six α-helices (TM1–6). This configuration classifies ABCG2 as a "half-transporter," which requires dimerization to become fully functional.

For ATP to bind properly, the dimerization of two nucleotide-binding domains (NBDs) is essential since a single NBD lacks the complete structural framework to surround an ATP molecule. This process involves two ATP molecules acting as a molecular adhesive, bridging

two NBDs together (Walker A, Q-loop, Walker B, and H-loop from NBD1; C-signature and D-loop from NBD2, labeled blue in Fig. 3.5A) [34]. Our analysis reveals that mutations in these critical regions significantly compromise the function ABCG2 (Fig. 3.5B). Specifically, among the 494 missense mutations or deletions examined in our deep mutational scanning (DMS) library, 93.7% demonstrated heightened sensitivity to mitoxantrone, indicating a loss-of-function phenotype.

The ATP binding-induced conformational shift—from two open NBDs to a closed NBD dimer—facilitates the energy transfer necessary for substrate translocation through the TMD. The substrate-binding cavity within the TMD is formed by the interaction of TM helices TM2 and TM5a from opposite ABCG2 monomers, with positions 435, 436, 439, and 546 identified as crucial for the efflux of estrone-3-sulfate [35]. Correspondingly, mutations at these positions largely result in a loss of function for mitoxantrone (89.9%). Interestingly, the M549A mutation, previously reported as neutral [36], here is classified as loss of function for mitoxantrone. Additionally, a significant majority of mutations at this site (17 out of 19 for mitoxantrone) led to a loss of function, including M549K, M549P, and M549Y. (Red box in Fig. 3.4)

ABCG2 distinguishes itself from other ABC transporters by possessing a longer extracellular loop (EL3) between transmembrane helices 5 and 6. This loop is characterized by three essential cysteine residues that facilitate the formation of disulfide bonds in two ways: intramolecularly between C592 and C608, and intermolecularly between C603 on one ABCG2 monomer and C603′ on the adjacent monomer. Research by Henriksen et al. suggests that the intramolecular disulfide bond plays a significant role in ABCG2's expression and functionality, whereas the intermolecular bond appears less crucial. Interestingly only 7 mutations at position 592 result in a reduced ability to efflux mitoxantrone. These mutations also correlate with notably lower surface expression scores, suggesting that their reduced functionality may be

caused by decreased plasma membrane presence. In contrast, mutations at position 603 do not impair ABCG2 function; intriguingly, some variants, like C603A and C603T, even enhance the efflux of mitoxantrone. Additionally, within EL3, a crucial N-glycosylation site at N596, likely modified by N-acetylglucosamine, plays an essential role in ABCG2 functionality [37]. Our results show that the majority of modifications at this site significantly compromise ABCG2's functionality (90% mutations). (Green box in Fig. 3.4)

3.4.4 Functional phenotype assays identify the molecular determinants that potentially define ABCG2 gain of function

The SNPs R482G and R482T, initially identified in drug-resistant cancer cell lines, have been found to increase the efflux ability of mitoxantrone. Aligning with prior research, ABCG2 variants R482G and R482T exhibited enhanced mitoxantrone efflux[23]. Interestingly, out of 19 mutations at this position, 14 lead to an increased ability to efflux mitoxantrone. However, two variants, R482K and R482Y, result in loss-of-function mutations.

Positioned in transmembrane helix 3 (TM3), R482 does not directly interact with the drugs but influences substrate transport and ATP hydrolysis through its interaction with TM2, which includes the critical residue F439 that directly engages with substrates in the binding cavity. It has been observed that R482's side chain interacts variably with other residues across different ABCG2 states, affecting the transporter's conformation and, consequently, its function. During turnover, the TMDs assume inward-facing orientations with varying degrees of opening towards the cytoplasmic side. Depending on the conformation, R482's side chain either points towards the cytoplasm, forming a hydrogen bond with S443 of TM2, or rotates towards the membrane's external side to contact residues near F439 in TM2 and TM4[35]. Our screening revealed that variants at position 443, lead to a distinct function profiles, 26% of the variants were found to

enhance the efflux of mitoxantrone, and at the same ratio another 26% of the variants were lead to loss of function in mitoxantrone efflux. Additionally, mutations at several other critical positions within the same or different transmembrane helices, such as S395D, F431H, Q437E, S440D and S440E, were identified as influential in mediating mitoxantrone transport by ABCG2. Furthermore, the region between helices 284-287 is also crucial for increasing mitoxantrone transport, indicating the complex interplay of multiple residues and regions in ABCG2's substrate handling (Yellow box in Fig. 3.4).

3.5 Discussion

We introduced a comprehensive screening platform designed for the high-throughput evaluation of the functional consequences of 12.724 variants in ABCG2, a critical pharmacogene with mutations that affect oral drug bioavailability, CNS drug delivery, and a key protein in anti-cancer drug resistance. This initiative represents the first study to apply deep mutational scanning (DMS) to comprehensively understand an ABC transporter.

To investigate the effects of ABCG2 mutations on its function, we were able to create mutations in each human ABCG2 residue with alternate amino acids or deletion. This approach enabled the generation of a robust, single-copy DMS library within HEK293 cells, ensuring a precise correlation between genetic variants and phenotypic outcomes. Recognizing that mutations might impair ABCG2 function through various mechanisms, such as affecting its folding, dimerization, trafficking, and ATP binding, we implemented a comprehensive multiparametric assessment of phenotypes which includes evaluation of protein expression ("whole cell expression") and cellular localization ("surface expression") using FACS, and assessment of the transport efficiency of different substrates ("function") using cytotoxicity assays. Following

sequencing to associate each phenotype with its specific genotype, we were able to identify essential regions and residues important to ABCG2 function.

ABCG2 features a single NBD and TMD, requiring it to dimerize for full functionality. This dimerization is crucial for ATP binding, as it brings together complementary structural elements from two NBDs, enabling the protein to bind ATP molecules effectively. Previous studies have already shown that mutations within these critical areas, including Walker A, Q-loop, Walker B, and H-loop C-signature and D-loop, significantly impact ABCG2's function. Our research for the first time, thoroughly demonstrates that mutations in this specific region are predominantly detrimental. Within our DMS library, which includes 494 missense mutations or deletions within these specific regions important for ATP binding, 93.7% of mutations demonstrated heightened sensitivity to mitoxantrone. This pattern strongly suggests a loss-of-function phenotype across these mutations, highlighting their significant impact on the ABCG2's ability to perform its normal biological functions.

Previous structural studies of ABCG2 have elucidated that TM2 and TM5a play an essential role in forming the substrate-binding cavity. Our research reveals that approximately 90% of mutations in the key positions within this cavity result in loss of function, affecting the efflux of mitoxantrone. Notably, we discovered that the M549A variant, previously deemed neutral, acts as a loss of function mutation for mitoxantrone. Moreover, a significant proportion of mutations at this location result in diminished function, including mutations such as M549K, M549P, and M549Y. Additionally, ABCG2 features an extended extracellular loop with three cysteine residues, crucial for forming disulfide bonds. Our DMS study uncovered that mutations at position 603, previously considered non-essential for ABCG2's functionality, surprisingly demonstrate significant gain of function effects. Specifically, variants such as C603A and C603T were found to improve the efflux capacity for mitoxantrone, highlighting an unexpected aspect of

ABCG2's operational dynamics. These observations emphasize the critical need for comprehensive DMS studies encompassing all potential mutations to dissect the mechanisms of ABC transporters thoroughly. Further validation studies need to be done to confirm these findings.

Our DMS study on ABCG2 has also shed light on the gain of function mutation for mitoxantrone, providing potential new insights into its mechanism of action. As expected, we observed that ABCG2 with R482G or R482T showed an enhanced ability to expel mitoxantrone. Notably, we found that this pattern was consistent across mutations at position 482 (14 out of 17 mutations). The study further elucidates the structural basis of this gain of function; R482, which is TM3, indirectly influences drug interaction through its interaction with TM2 which is forming the substrate binding cavity. Notably, mutations at position 443 in TM2, known to interact with R482—specifically S443A, S443D, S443E, and S443P—were identified as enhancing the transport of mitoxantrone. Beyond this, mutations in other positions, both within the same TM (e.g., F431H, Q437E, S440D, S440E) and in others (e.g. S395D), were found to be instrumental in increasing ABCG2's mediated mitoxantrone efflux. Additionally, the region between helices 284-287, where its function is unknown, was also pinpointed as crucial for gain of function for mitoxantrone efflux in our study. These findings suggest the need for further investigations to elucidate whether these residues interact with R482 indirectly or if a separate, potentially allosteric mechanism that amplifies ABCG2's efficacy in mitoxantrone transport exists.

Our DMS study on ABCG2 has significantly advanced our understanding of its transport mechanisms, indicating a potential novel action mechanism for ABCG2's gain of function. However, the study also underscores a limitation in fully grasping the substrate-specific transport capabilities of ABCG2. In line with previous reports, our findings reveal that R482G

and R482T contribute to a gain-of-function in transport mitoxantrone. Other than this, these mutations are also shown to alter ABCG2's substrate specificity. Cells with the ABCG2-R482G variant demonstrated increased transport of substances like rhodamine-123 and doxorubicin, which are not efficiently effluxed by the wild-type ABCG2. Additionally, these mutations are also known to reduce resistance to topotecan, a topoisomerase inhibitor used in cancer therapy. The specific manner in which these variants influence substrate transport highlights the necessity for further research. Deep mutational scanning across a broader spectrum of ABCG2 substrates, coupled with detailed studies on the specificities of ABCG2 variants, is crucial for a more comprehensive understanding.

In summary, here we present a robust deep mutational scanning framework for ABCG2, which is capable of functionally evaluating 12.724 ABCG2 variants. By dissecting which mutations are crucial for the transport effectiveness of mitoxantrone, we were able to pinpoint important areas and amino acids vital for ABCG2 function. Our findings are instrumental in enhancing our understanding of ABCG2's substrate transport mechanisms, thereby facilitating the development of more effective small-molecule modulators or inhibitors. These advancements aim to improve CNS drug delivery and overcome cancer drug resistance. To our knowledge, this is the first time an ABC transporter has been subjected to such an extensive DMS study, providing valuable insights that could extend to other clinically significant ABC transporters.

3.6 Figures

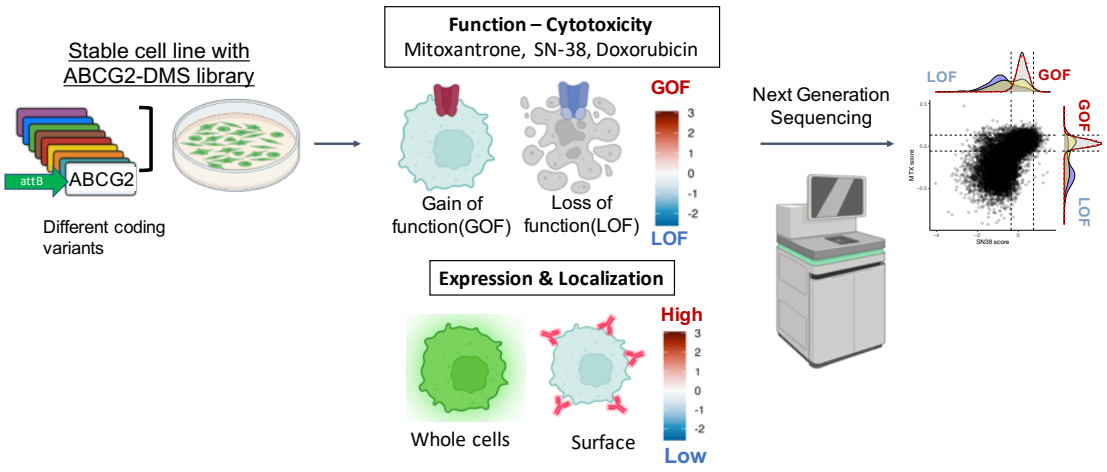

Figure 3.1. Workflow for multiparametric deep mutational scan of ABCG2

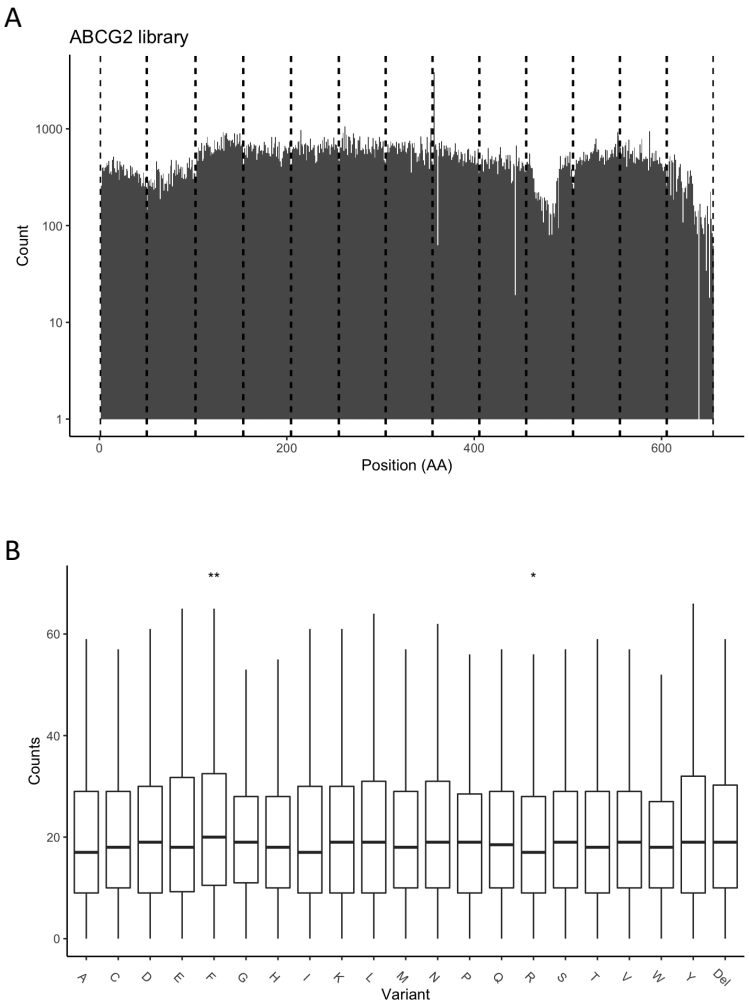

Figure 3. 2. Variants distribution in ABCG2 DMS library
(A) Barplot of counts of mutation numbers per position for ABCG2. The boundaries of each mutagenic sublibrary are indicated with dashed lines. (B) Boxplots of variants at each position across all of ABCG2. The vertical length of the box is the interquartile range (IQR), upper bound is the 75th percentile with the lower bound is the 25th percentile. Significance is tested using two-sided T-tests controlled for multiple comparisons comparing incorporation means between variants across all positions. Significance levels: **P<0.01; *P<0.05, all others not significant.

A

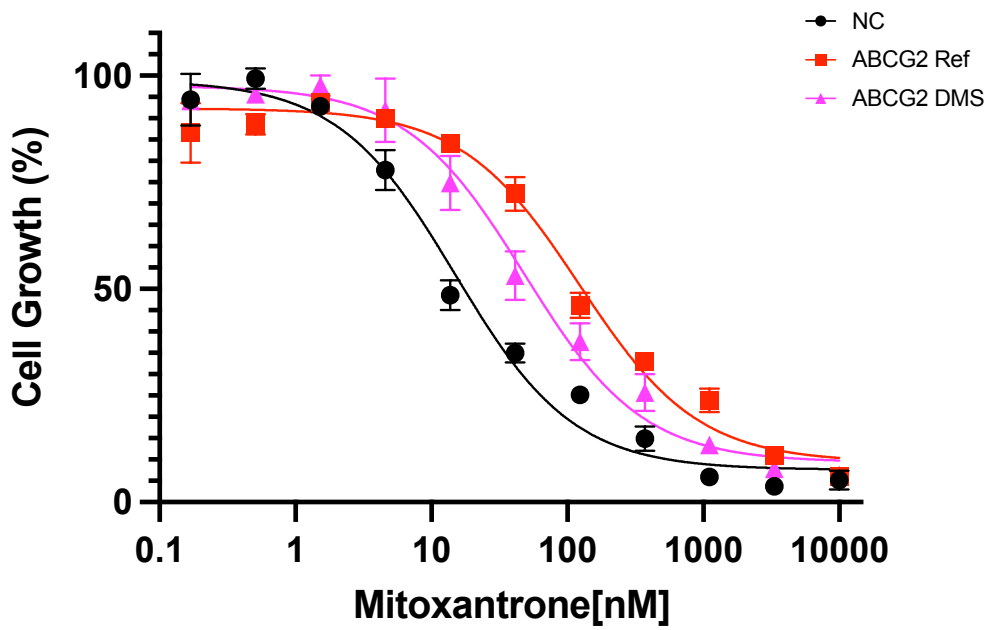

Figure 3.3. Effect of ABCG2 DMS library on cytotoxicity of mitoxantrone in stable cell lines.
HEK293T-landing pad cells and HEK293T-landing pad cells expressing reference ABCG2 and ABCG2 DMS library were exposed mitoxantrone at concentrations ranging from 0-500 nM.

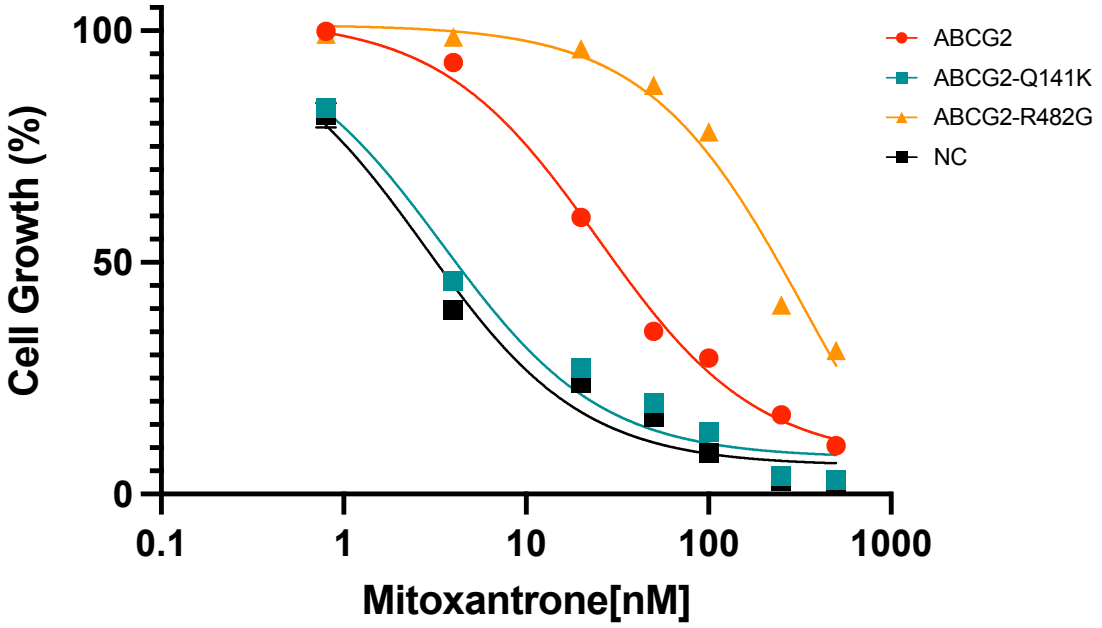

Figure 3.4 Effect of ABCG2 variants on cytotoxicity of mitoxantrone in stable cell lines. HEK293T-landing pad cells and HEK293T-landing pad cells expressing reference ABCG2 or missense variants of ABCG2 were exposed mitoxantrone at concentrations ranging from 0-250 nM. The IC50 values for the wild-type ABCG2 (red), ABCG2-Q141K variant (green), ABCG2-R482G variant (orange), and the negative control (NC, black) were 25.02 nM, 3.5 nM, 344.9 nM, and 2.80 nM, respectively.

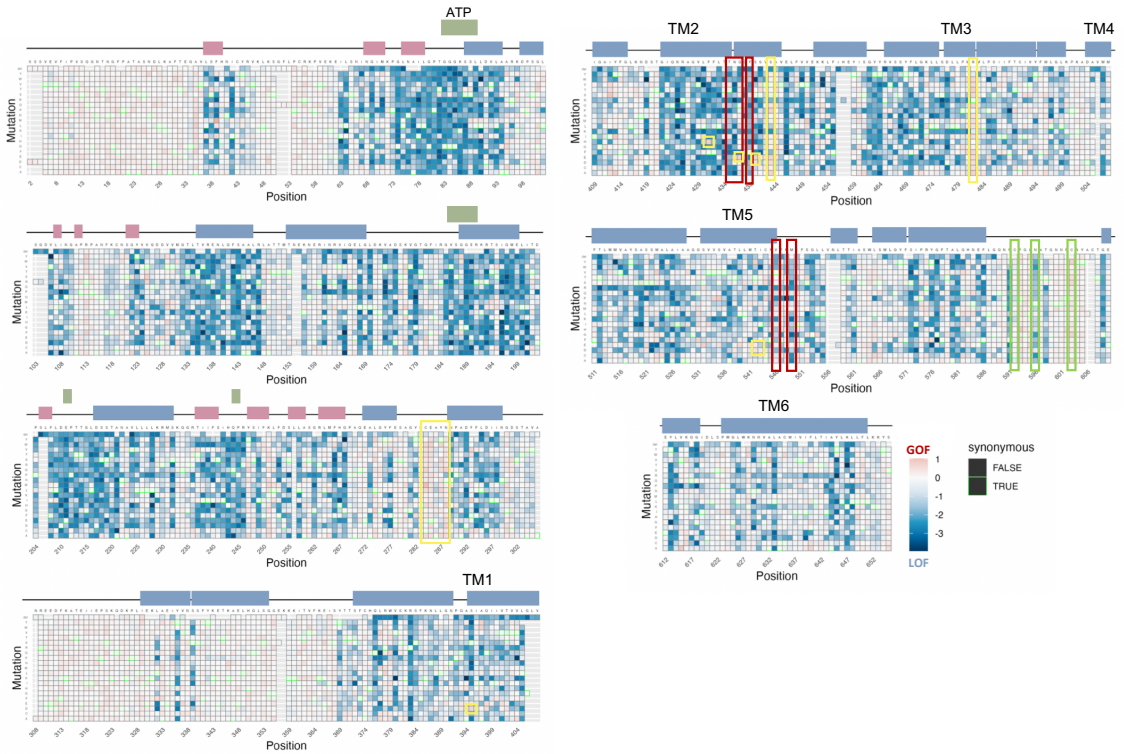

Figure 3.5 Heatmap of mitoxantrone induced cytotoxicity deep mutational scan in ABCG2.
Cytotoxicity screen fitness effects depicted as a heatmap, with (x-axis) residue position versus (y-axis) shows the type of mutation. In this assay, *loss* of transport activity (relative to wildtype) reduces the efflux of a cytotoxic substrate, thus decreases cell density (negative score, more blue) while *gain* of transport *increases* substrate efflux, which *increases* survived cell numbers (positive score, more red). Above, wildtype sequence and cartoon representation of secondary structure elements of ABCG2 with blue squares as helices and pink squares as sheet. Residues or specific variants critical for substrate binding are highlighted with red squares, those essential for disulfide bond formation and glycosylation are marked with green squares, and those significant for the gain of function are indicated with yellow squares. Missing data in gray and synonymous mutation is squared green.

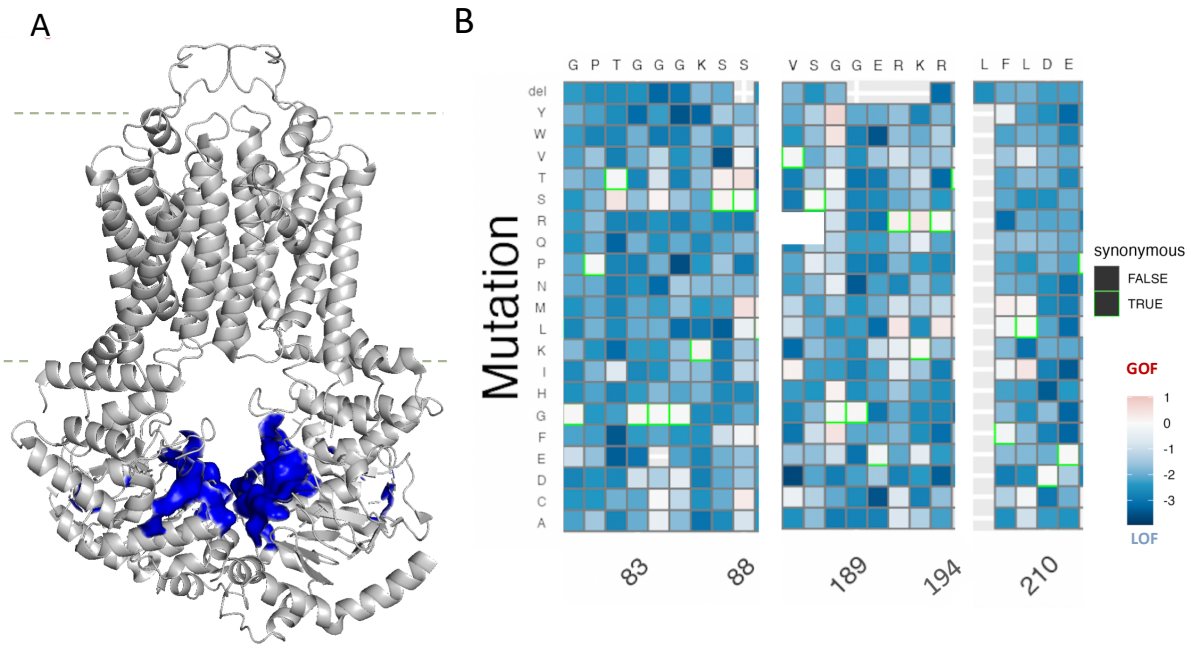

Figure 3.6 Mutations in the ATP-binding site significantly impair the functionality of ABCG2

(A) Cartoon of dimerized ABCG2 (PDB: 6VXF). Lipid bilayer boundaries are indicated by dashed lines and regions crucial for ATP binding(A-loop, Walker A, Q-loop, C-signature, and H-loop from NBD1; signature motif , P-loop, Walker B, D-loop and H-loop) is colored in blue. (B) Heatmap of fitness score in regions that important for ATP binding from mitoxantrone mediated cytotoxicity studies.

3.7 References

1. Giacomini, K.M., et al., *International Transporter Consortium commentary on clinically important transporter polymorphisms.* Clin Pharmacol Ther, 2013. **94**(1): p. 23-6.
2. Lee, C.A., et al., *Breast cancer resistance protein (ABCG2) in clinical pharmacokinetics and drug interactions: practical recommendations for clinical victim and perpetrator drug-drug interaction study design.* Drug Metab Dispos, 2015. **43**(4): p. 490-509.
3. Cooper-DeHoff, R.M., et al., *The Clinical Pharmacogenetics Implementation Consortium Guideline for SLCO1B1, ABCG2, and CYP2C9 genotypes and Statin-Associated Musculoskeletal Symptoms.* Clin Pharmacol Ther, 2022. **111**(5): p. 1007-1021.
4. Yee, S.W., et al., *Influence of Transporter Polymorphisms on Drug Disposition and Response: A Perspective From the International Transporter Consortium.* Clin Pharmacol Ther, 2018. **104**(5): p. 803-817.
5. Brackman, D.J. and K.M. Giacomini, *Reverse Translational Research of ABCG2 (BCRP) in Human Disease and Drug Response.* Clin Pharmacol Ther, 2018. **103**(2): p. 233-242.
6. Thomas, J.R., et al., *Abcg2a is the functional homolog of human ABCG2 expressed at the zebrafish blood-brain barrier.* bioRxiv, 2024.
7. Schulz, J.A., A.M.S. Hartz, and B. Bauer, *ABCB1 and ABCG2 Regulation at the Blood-Brain Barrier: Potential New Targets to Improve Brain Drug Delivery.* Pharmacol Rev, 2023. **75**(5): p. 815-853.
8. Iorio, A.L., et al., *Blood-Brain Barrier and Breast Cancer Resistance Protein: A Limit to the Therapy of CNS Tumors and Neurodegenerative Diseases.* Anticancer Agents Med Chem, 2016. **16**(7): p. 810-5.
9. Zhu, J.J., et al., *High-dose methotrexate for elderly patients with primary CNS lymphoma.* Neuro Oncol, 2009. **11**(2): p. 211-5.

10. Li, L., S. Agarwal, and W.F. Elmquist, *Brain efflux index to investigate the influence of active efflux on brain distribution of pemetrexed and methotrexate.* Drug Metab Dispos, 2013. **41**(3): p. 659-67.

11. Cisternino, S., et al., *Expression, up-regulation, and transport activity of the multidrug-resistance protein Abcg2 at the mouse blood-brain barrier.* Cancer Res, 2004. **64**(9): p. 3296-301.

12. Blakeley, J.O., et al., *Effect of blood brain barrier permeability in recurrent high grade gliomas on the intratumoral pharmacokinetics of methotrexate: a microdialysis study.* J Neurooncol, 2009. **91**(1): p. 51-8.

13. Jin, Y., et al., *ABCG2 is related with the grade of glioma and resistance to mitoxantone, a chemotherapeutic drug for glioma.* J Cancer Res Clin Oncol, 2009. **135**(10): p. 1369-76.

14. Nakanishi, H., et al., *Impact of P-glycoprotein and breast cancer resistance protein on the brain distribution of antiepileptic drugs in knockout mouse models.* Eur J Pharmacol, 2013. **710**(1-3): p. 20-8.

15. Mousavi, S.F., et al., *ABCG2, SCN1A and CYP3A5 genes polymorphism and drug-resistant epilepsy in children: A case-control study.* Seizure, 2022. **97**: p. 58-62.

16. Kim, D.W., et al., *Lack of association between ABCB1, ABCG2, and ABCC2 genetic polymorphisms and multidrug resistance in partial epilepsy.* Epilepsy Res, 2009. **84**(1): p. 86-90.

17. Chen, J., et al., *Correlation of MCT1 and ABCC2 gene polymorphisms with valproic acid resistance in patients with epilepsy on valproic acid monotherapy.* Drug Metab Pharmacokinet, 2019. **34**(3): p. 165-171.

18. Kondo, C., et al., *Functional analysis of SNPs variants of BCRP/ABCG2.* Pharm Res, 2004. **21**(10): p. 1895-903.

19. Furukawa, T., et al., *Major SNP (Q141K) variant of human ABC transporter ABCG2 undergoes lysosomal and proteasomal degradations.* Pharm Res, 2009. **26**(2): p. 469-79.

20. Brackman, D.J., et al., *Genome-Wide Association and Functional Studies Reveal Novel Pharmacological Mechanisms for Allopurinol.* Clin Pharmacol Ther, 2019. **106**(3): p. 623-631.

21. Song, Y., et al., *The Association between ABCG2 421C>A (rs2231142) Polymorphism and Rosuvastatin Pharmacokinetics: A Systematic Review and Meta-Analysis.* Pharmaceutics, 2022. **14**(3).

22. Cusatis, G., et al., *Pharmacogenetics of ABCG2 and adverse reactions to gefitinib.* J Natl Cancer Inst, 2006. **98**(23): p. 1739-42.

23. Robey, R.W., et al., *Mutations at amino-acid 482 in the ABCG2 gene affect substrate and antagonist specificity.* Br J Cancer, 2003. **89**(10): p. 1971-8.

24. Fowler, D.M. and S. Fields, *Deep mutational scanning: a new style of protein science.* Nat Methods, 2014. **11**(8): p. 801-7.

25. Macdonald, C.B., et al., *DIMPLE: deep insertion, deletion, and missense mutation libraries for exploring protein variation in evolution, disease, and biology.* Genome Biol, 2023. **24**(1): p. 36.

26. Coyote-Maestas, W., et al., *Probing ion channel functional architecture and domain recombination compatibility by massively parallel domain insertion profiling.* Nat Commun, 2021. **12**(1): p. 7114.

27. Matreyek, K.A., et al., *An improved platform for functional assessment of large protein libraries in mammalian cells.* Nucleic Acids Res, 2020. **48**(1): p. e1.

28. Coyote-Maestas, W., et al., *Determinants of trafficking, conduction, and disease within a K(+) channel revealed through multiparametric deep mutational scanning.* Elife, 2022. **11**.

29. Yee, S.W., et al., *The full spectrum of OCT1 (SLC22A1) mutations bridges transporter biophysics to drug pharmacogenomics.* bioRxiv, 2023.

30. Van der Auwera, G.A., O'Connor, B.D. , *Genomics in the Cloud: Using Docker, GATK, and WDL in Terra. 'O'Reilly Media, Inc.'.* 2020.

31. Rubin, A.F., et al., *A statistical framework for analyzing deep mutational scanning data.* Genome Biol, 2017. **18**(1): p. 150.

32. Wen, C.C., et al., *Genome-wide association study identifies ABCG2 (BCRP) as an allopurinol transporter and a determinant of drug response.* Clin Pharmacol Ther, 2015. **97**(5): p. 518-25.

33. Polgar, O., R.W. Robey, and S.E. Bates, *ABCG2: structure, function and role in drug response.* Expert Opin Drug Metab Toxicol, 2008. **4**(1): p. 1-15.

34. Eckenstaler, R. and R.A. Benndorf, *3D structure of the transporter ABCG2-What's new?* Br J Pharmacol, 2020. **177**(7): p. 1485-1496.

35. Yu, Q., et al., *Structures of ABCG2 under turnover conditions reveal a key step in the drug transport mechanism.* Nat Commun, 2021. **12**(1): p. 4376.

36. Manolaridis, I., et al., *Cryo-EM structures of a human ABCG2 mutant trapped in ATP-bound and substrate-bound states.* Nature, 2018. **563**(7731): p. 426-430.

37. Nakagawa, H., et al., *Disruption of N-linked glycosylation enhances ubiquitin-mediated proteasomal degradation of the human ATP-binding cassette transporter ABCG2.* FEBS J, 2009. **276**(24): p. 7237-52.

Chapter 4. Conclusions and Perspectives

The Blood-Brain Barrier (BBB) acts as a selective barrier for the brain, allowing in necessary nutrients while keeping out harmful toxins. This dissertation aims to shed light on the mechanisms underlying changes in BBB function, with a particular focus on its development and aging, as well as the impact of mutations in the ATP-binding cassette sub-family G member 2 (ABCG2) transporter, which is highly expressed in the BBB and crucial for CNS drug disposition.

The first chapter provided fundamental information about the various factors that influence BBB functionality, with a special focus on transporters. It begins with the introduction of the structural components of the BBB, emphasizing their integral role in preserving the integrity of the barrier. The narrative then shifts to explore the diverse transport mechanisms employed by the BBB, such as active efflux transport, carrier-mediated transport, and transcytosis. These mechanisms are critical for the delivery of nutrients and pharmaceuticals to the brain. The discussion broadens to include the impact of development, aging, and diseases on the BBB, illustrating how these factors contribute to the barrier's dynamic nature over the lifespan and their implications for pharmaceutical development. Furthermore, this chapter addresses the challenges that the BBB poses to the development of central nervous system (CNS) drugs and explores genetic factors that influence BBB functionality and drug disposition. Particular attention is given to the highly expressed ATP-binding cassette transporters, ABCB1 and ABCG2, at the BBB. The concluding section calls for further research to enhance our comprehension of the BBB's physiological functions and underscores the necessity of developing targeted strategies to improve drug delivery to the brain.

Chapter 2 explored the dynamic of the Blood-Brain Barrier (BBB), highlighting the adaptation of its transport mechanisms across various growth stages, and the alterations it undergoes due to aging and neurodegenerative conditions. Despite the critical importance of these changes, fully understanding the mechanisms behind them in the human BBB remain challenging. To address

this gap, the chapter presents a comprehensive proteomics analysis focused on the development (ontogeny) and aging of proteins within BMVs. The study analyzed BMVs from the largest cohort of healthy individuals, ranging from neonates to the elderly. This analysis identified approximately seven thousand proteins in the BMV proteome and unveiled potential changes in BBB permeability across the lifespan. It also pinpointed transporters critical for nutrient delivery and drug penetration that exhibit age-dependent expression patterns. In conclusion, this chapter sheds light on the dynamic regulation of BBB proteins, emphasizing the variability of transporter expression with age and its consequential effects on drug permeability. The findings from this study are crucial for enhancing physiologically based pharmacokinetic modeling and developing therapeutic strategies that are tailored to different stages of life, offering a deeper understanding of the BBB's adaptability and its implications for drug delivery and neuroprotection.

Chapter 3 utilizes deep mutational scanning to explore the functional nuances of ABCG2 variants and shed light on the impact of transporter mutations on CNS drug delivery and cancer drug resistance mechanisms. Utilizing DMS, this research assesses 12,724 ABCG2 gene variants, including the full spectrum of single missense, synonymous, and deletion variants. Our methodical assay quantifies ABCG2 abundance, evaluates its membrane expression, and determines the functional consequences of each variant when challenged with the anticancer drugs: mitoxantrone. By producing a thorough functional atlas that dovetails with the structural information of the transporter, this integrative approach was able to identify essential amino acid residues fundamental to ABCG2's functionality. This study not only enriches our understanding of ABCG2 but also lays the groundwork for future exploration into other ABC transporters, showcasing the crucial role of DMS in revealing the complicated nature of pharmacogenes and the mechanisms underpinning drug resistance.

In summary, this dissertation provides a detailed exploration of the transporters on BBB, highlighting its critical functions cross lifetime, the impact of genetic variations on transporter efficacy, and the potential for targeted therapeutic strategies. By integrating proteomics and deep mutational scanning techniques, we provide a detailed insight into the physiological and pharmacological roles of transporters on the BBB. Our work lays the foundation for future breakthroughs in personalized medicine, enabling the development of tailored therapeutic strategies that account for individual variations in BBB transporter function.

Part B

Development of *cis*-regulation therapy for

Non-alcoholic fatty liver disease/ steatohepatitis

Chapter 5. Introduction

5.1 Introduction to Non-alcoholic fatty liver disease/steatohepatitis

Nonalcoholic fatty liver disease (NAFLD) is a common liver disorder worldwide [1]. NAFLD encompasses a spectrum of conditions with varying clinical outcomes, but it becomes particularly concerning in its advanced form known as non-alcoholic steatohepatitis (NASH). NASH is characterized by liver damage, inflammation, and fibrosis, building upon the initial fatty buildup in the liver [2]. The inflammatory processes that drive the onset and progression of NASH not only exacerbate the condition but also pave the way for severe complications, including cirrhosis and hepatocellular carcinoma (HCC)[3]. These advanced stages often necessitate a liver transplant or can be fatal, highlighting the critical need for early intervention and effective treatment strategies [4]. While the progression to cirrhosis occurs in approximately 4% of patients with simple steatosis, the number rises above 20% for those with NASH. The period from 2004 to 2016 saw a significant increase in liver transplant waitlist registrations due to NASH—114% for men and 80% for women. Consequently, NASH is anticipated to become the top reason for liver transplants in the next few years. In 2017, direct medical costs for NASH patients in the U.S. were about $222 billion. By 2039, the number of NASH cases in the U.S. is expected to rise by 82.6%, achieving approximately 19.53 million and there will be 18.71 million deaths overall, with 6.72 million heart-related and 1.71 million liver-related. The total direct healthcare costs by this time are projected at $1662.76 billion, with the cost per NASH patient rising from $3636 to $6968 [5].

NASH is a complex liver condition intertwined with various metabolic issues, complicating its management [6]. The optimal treatment would not only reverse liver damage and fibrosis but also positively impact, or at least not worsen, metabolic or cardiovascular issues. Despite significant advances in understanding NASH's underlying mechanisms over the past decade, no specific approved treatment exists yet. The primary management strategy currently

recommended is lifestyle changes, focusing on dietary adjustments and physical activity to achieve weight loss. While the type of diet can influence liver fat levels, no particular diet has been proven superior for NASH patients. The main dietary advice is to reduce overall calorie intake. It's also advised to minimize fructose intake, as it's linked to the onset of NASH in NAFLD patients and the progression of fibrosis [7]. Additionally, it's important for NASH patients to avoid or greatly reduce alcohol intake to prevent further liver damage and support the resolution of NASH during treatment [8]. Physical activity can lessen liver fat, improve insulin sensitivity, and alter fatty acid synthesis, which may benefit NASH patients [9]. While the evidence is scarce, rigorous physical activity seems to prevent NAFLD from advancing to NASH.

The most significant correlation with histological recovery in NASH is weight loss. A reduction of at least 5% is needed to decrease hepatic steatosis. Studies show that losing over 7% of body weight can markedly enhance liver conditions, and patients shedding more than 10% can see substantial reductions in their disease activity. This level of weight loss might also lead to fibrosis regression in nearly half of the patients. Nonetheless, a smaller weight reduction of 5% may still help to halt fibrosis progression. The initial therapeutic objective for NASH patients should be a 7-10% body weight reduction ([10], [11], [12]). However, achieving and maintaining this weight loss is challenging, with less than half of patients reaching this target, even with closely supervised lifestyle interventions in clinical trials. For significant and lasting weight loss, bariatric surgery is the most effective option and can also alleviate related conditions [13]. However, the surgery is typically offered to NASH patients only if they meet criteria based on other obesity-related health issues, since the safety of bariatric surgery specifically for NASH patients, and especially for those with cirrhosis due to NASH, remains uncertain [14].

While no drugs have been officially approved by the FDA specifically for NASH, certain medications have demonstrated potential benefits in clinical trials. Vitamin E, an antioxidant, and pioglitazone, a thiazolidinedione class drug that sensitizes the body to insulin via PPAR-γ activation, have shown promise [15]. The PIVENS trial, which involved 247 non-diabetic NASH patients, compared the effects of pioglitazone, vitamin E, and a placebo over 96 weeks. Vitamin E led to a significant improvement in the liver's health status compared to the placebo, as measured by the NAFLD activity score, but pioglitazone did not meet the statistical threshold set for significance in this study. Discrepancies in the assessment of liver cell damage may have influenced these outcomes. Neither treatment improved liver fibrosis. Despite this, a substantial portion of patients receiving either pioglitazone or vitamin E experienced a resolution of their liver inflammation. However, concerns regarding the safety of long-term vitamin E use have surfaced, citing increased risks of hemorrhagic stroke, prostate cancer, and possibly higher overall mortality rates [16].

Additionally, a phase 2 clinical trial examining Cenicriviroc (CVC), a dual antagonist for C-C chemokine receptors type 2 and 5, indicated that CVC might improve liver fibrosis without significantly affecting the accompanying steatohepatitis. Additionally, the improvements in fibrosis appeared to be more sustainable when compared to the placebo group. Despite these promising phase 2 results, the subsequent AURORA study—a larger phase 3 clinical trial including 1778 patients with NASH and stage 2/3 liver fibrosis—did not validate the effectiveness of CVC in treating liver fibrosis as measured by histological analysis in adults with NASH. The discrepancy between the phase 2 trial outcomes and the phase 3 AURORA study highlights the complexities involved in developing successful treatments for NASH-related fibrosis. Currently, six drugs have progressed from phase 2 to phase 3 clinical trials, with numerous other treatments still in phase 2. Despite this advancement, the landscape of Phase 3 trials in 2020 has seen limited success. Obeticholic acid (OCA) is the only treatment that

completed a Phase 3 trial in 2020. In contrast, trials for three other drugs—cenicriviroc, elafibranor, and selonsertib—were discontinued due to their inability to meet the predetermined endpoints in mid-term evaluations [17]. Although OCA managed to complete the entire Phase 3 trial process, the FDA has not yet granted approval, underscoring the critical and ongoing need for effective treatments for NASH.

5.2 Introduction to Animal Model for Non-alcoholic fatty liver disease/steatohepatitis

Researchers have utilized animal models to explore the underlying mechanisms of NASH pathogenesis for decades. The limited human data for examining disease progression at the cellular and molecular levels is largely due to the challenges in obtaining liver tissue samples. Employing mouse models for disease study facilitates experimental manipulations, and also takes account of the complex physiological environment within the organism such as the neuroendocrine, metabolic, adipose, and immune systems. Mice models enable genetic modifications, as well as adjustments in diet and exercise routines, and allow for the collection of tissue samples at specific intervals. Additionally, mouse models offer several benefits, including the relatively brief duration of studies (ranging from 3 to 6 months) and lower costs in comparison to studies involving larger animals. In contrast to human studies, which are often limited to single-time-point sampling, mouse models permit extensive tissue collection without the risk of sampling errors and facilitate the observation of changes in physiology, as well as molecular and cellular dynamics throughout the course of the disease or its regression. An ideal mouse model of NAFLD/NASH would be capable of replicating the entire disease spectrum, from simple steatosis to more advanced stages like steatohepatitis (NASH) with fibrosis, and potentially the progression to HCC. [18]

Diet-induced obesity is a significant factor contributing to the development of NAFLD and NASH in humans, even when other variables like age, gender, and hypertension are considered. NASH involves a complex interplay between various metabolic organs including the pancreas, adipose tissue, and skeletal muscle, along with the immune system and gut microbiota. Consequently, dietary-based preclinical models for NASH are viewed as the most appropriate to accurately reflect and replicate the human condition and its progression over time. These models also enable researchers to explore the disease mechanism both globally and locally. Over time, a wide array of dietary-based models for NAFLD/NASH has been established, including the Amylin liver NASH model, Gubra Amylin NASH model, choline-deficient high-fat diet model, and the methionine-choline-deficient diet model [19].

While diet and lifestyle are crucial in the onset of NASH, it's essential to acknowledge the significant role of genetic factors in its development and the progression of related conditions like type 2 diabetes. This is underscored by the observation that not all obese individuals develop type 2 diabetes, metabolic syndrome, or NASH. Specifically for NASH, factors like a family history of type 2 diabetes and metabolic syndrome, in addition to genetic mutations such as the rs738409 polymorphism in the *PNPLA3* gene, are known to expedite the disease progression [20], [21]. Furthermore, the high incidence and early onset of NAFLD stands as a pathological hallmark of Alström syndrome, which caused by the mutations in the *ALMS1* gene [22]. The genetic background of mice has also been pinpointed as a crucial determinant in the development of NASH. Mouse models that incorporate both diet and genetic predispositions have been successful in mimicking various aspects of NASH including metabolic, inflammatory, fibrogenic, and hepatocarcinogenic pathways observed in human.

5.2.1 Diet-induced animal model of non-alcoholic fatty liver disease (DIAMOND)

The DIAMOND (Diet-Induced Animal Model of Non-Alcoholic Fatty Liver Disease) model utilizes an isogenic strain created from a crossbreed of the standard WT C57BL/6J strain with the 129S1/SvImJ strain, the latter of which is frequently employed to generate mice with specific genetic alterations. This hybrid strain inherits approximately 60% of its genetic makeup from the C57BL/6 lineage. The uniform genetic background of these mice and the consistent replication of the disease phenotype across numerous generations have been meticulously documented. These mice were subjected to a Western-style diet, rich in fats and carbohydrates (42% kcal from fat and 0.1% cholesterol), alongside unlimited access to water sweetened with high levels of fructose and glucose (23.1 g/L D-fructose and 18.9 g/L D-glucose). DIAMOND mice quickly exhibit signs of obesity, insulin resistance, hypertriglyceridemia, and elevated levels of total and LDL cholesterol, as well as AST and ALT enzymes. When maintained on this diet for extended periods, the mice sequentially develop fatty liver (steatosis) within 4–8 weeks, steatohepatitis by 16–24 weeks, advancing fibrosis starting at 16 weeks, with severe bridging fibrosis evident by week 52, and spontaneous hepatocellular carcinoma (HCC) occurring in 89% of the population between weeks 32 and 52. Notably, at the transcriptomic level, DIAMOND mice exhibit a pattern of pathway activation closely mirroring that observed in humans with NASH, with the activation of lipogenic, inflammatory, and apoptotic signaling pathways [23].

5.2.2 Foz/Foz transgenic mice

Genetic obesity models like *ob/ob* or *db/db* mice, which lack leptin or its receptor, respectively, do not accurately replicate the full spectrum of NASH, as they primarily induce hepatic steatosis without leading to necro-inflammation and fibrosis. *Foz/Foz* mice, which have a mutation in the *Alms1* gene, exhibit an overeating behavior similar to *ob/ob* and *db/db* mice. The human equivalent of this mutation, although exceedingly rare, causes Alström syndrome, characterized

by early-onset obesity, metabolic syndrome, diabetes, and infertility [24]. *Foz/Foz* mice fed with an HFD with 0.2% cholesterol for 24 weeks, displayed the comprehensive range of NASH pathology including steatosis, cell ballooning, significant inflammation, and fibrosis [25]. With modulated Western diet (containing 45% fat, 20% protein, 35% carbohydrates), *Foz/Foz* mice develop NASH within 4-8 weeks, coupled with cardiovascular and renal complications, and advanced to grade-3 hepatic fibrosis by 12 weeks. The liver transcriptomic profile of these *Foz/Foz* mice is closely resembling that of human NASH. By 24 weeks, about 75% of these mice developed visible HCC tumors within a cirrhotic liver [26]. Although the *Foz/Foz* model closely mimics human NASH, which often results from a mix of genetic, environmental, and dietary factors, the rarity of *ALMS1* mutations in humans means it represents only a fraction of the NASH population. Furthermore, the full function of *ALMS1* remains unclear in both humans and mice. Given its widespread expression, with the highest levels in the testes, mutations in *ALMS1* can lead to infertility, a symptom not directly related to NASH, illustrating the complexity of correlating specific genetic models to human diseases.

5.2.3 MS-NASH mice (FATZO mice)

The FATZO mouse model was created by interbreeding C57BL/6J and AKR/J mice, both of which naturally tend to become obese on a high-fat diet without any genetic modifications [27]. Through selective breeding of their offspring, a line was established that exhibits a high susceptibility to developing features of metabolic syndrome early in life. As a result, FATZO mice inherently tend towards obesity and manifest insulin resistance, and dyslipidemia even without any special diet treatment. When fed the FATZO mice with a Western diet and 5 % fructose water (WDF), it only takes 20 weeks for these mice to develop NAFLD and NASH, characterized by progressive steatosis, ballooning, inflammation, and mild fibrosis. Elevated plasma levels of liver enzymes (ALT/AST) and cholesterol in FATZO mice on a WDF were

noted as early as 4 weeks, with liver triglycerides rising from the 12-week mark in comparison to a chow diet (CD). The livers of mice fed with WDF were lighter in color and exhibited a significantly higher liver-to-body weight ratio than those on CD. Histological analysis showed early signs of steatosis, which evolved into steatohepatitis marked by ballooned cells, lobular inflammation, and fibrosis. By 20 weeks on the diet, the FATZO mice reached a composite NAFLD Activity Score (NAS) of ~5, indicative of definitive NASH. Notably, mild fibrosis was observed in 50% of these mice by 16 weeks, escalating to moderate fibrosis in all animals by week 20 [28].

Unlike other rodent models of NASH that rely on genetic mutations or chemical induction, FATZO mice offer greater physiological relevance to human metabolic syndrome, incorporating common risk factors like fructose to induce NASH while preserving essential biochemical and histopathological traits. This led us to select FATZO mice for evaluating the efficacy of our newly developed NASH therapy.

5.3 Introduction to *Cis* Regulation Therapy

Variations in gene expression levels, whether increased or decreased beyond specific thresholds, can significantly contribute to various human diseases [29]. Mutations within a gene's coding region may lead to altered gene expression, causing a reduction or enhancement in protein function. Additionally, mutations in gene-regulatory elements, known as *cis*-regulatory elements (CREs), can impact the intensity, timing, or spatial distribution of gene expression across different cell or tissue types. CREs include promoters situated adjacent to the gene's transcription start site, initiating expression at precise timing, locations, and levels. Promoters are influenced by other distal CREs, such as enhancers and silencers, which control gene expression in a manner that is both tissue-specific and time-sensitive [30]. In addition to

mutations, epigenetic mechanisms like DNA methylation, histone modifications, chromatin remodeling, and the action of noncoding RNAs (ncRNAs) play significant roles in modulating gene expression [31]. These epigenetic changes are instrumental in the onset and progression of numerous diseases, including diabetes, obesity, non-alcoholic fatty liver disease (NAFLD), osteoporosis, gout, and thyroid disorders [32].

Although various gene expression modulation technologies show promise, they have limitations, particularly for diseases sensitive to gene dosage, highlighting the need for new therapeutic methods. Gene replacement therapy, which delivers a functional gene copy, is effective for certain recessive conditions but is constrained by the size limit of the adeno-associated virus (AAV) delivery system [33]. This 4,700-bp size restriction prevents the use of AAV for genes longer than a certain length, affecting a significant number of disease-causing genes. While oligonucleotide-based therapies, including antisense oligonucleotides (ASOs), encouraging outcomes in treating conditions like spinal muscular atrophy and Huntington's disease, they require sufficient target transcript presence, necessitating alternatives for complete loss-of-function mutations ([34], [35]). Additionally, gene editing tools like CRISPR-Cas9 offer mutation correction possibilities but carry risks of off-target effects and require customization for each mutation.

cis-Regulatory Therapy (CRT) offers a precise and alternative method of treatment that specifically addresses CREs within the genome, adjusting the expression of associated genes to correct disease-related anomalies. This technique leverages the capabilities of gene-editing platforms devoid of nuclease activity, such as zinc finger proteins, transcription activator-like effector (TALE) systems, or the CRISPR-associated protein 9 (Cas9) in its inactive form, known as dead-Cas9 (dCas9). These systems are engineered to bind to proteins or functional domains—like transcriptional activators or repressors, epigenetic modifiers, chromatin

remodelers, or DNA looping factors—that can influence gene activity upon being directed to CREs. One of the primary benefits of CRT is its ability to fine-tune gene expression through the native gene-regulation mechanisms to levels that are both physiologically appropriate and beneficial [36].

Presently, three gene-editing frameworks are at the forefront for application in CRT: zinc finger nucleases, TALENs, and the CRISPR-Cas9 system. These systems are engineered to precisely target and bind to the DNA sequences of CREs. Each platform brings a unique set of strengths and constraints that must be weighed when determining the most fitting technology for a given experimental objective. Zinc finger nucleases, which represent the first generation of gene-editing tools, and TALENs, the second generation, are both modular in design, with a distinct DNA-binding component that can be attached to the Fok1 nuclease to induce DNA cleavage ([37], [38]). These two systems offer the versatility to merge with a spectrum of effector domains, enabling targeted DNA site modifications without the need for DNA breaks. CRISPR-Cas systems, known as the third generation of gene editors, function as a ribonucleoprotein complex, utilizing a guide RNA to direct the Cas nuclease to the target DNA. Alterations to the Cas nuclease, resulting in a 'dead' Cas9 (dCas9) form, circumvent DNA cutting, thus permitting the attachment of effector domains for precise gene regulation without disrupting the DNA integrity [39]. These DNA targeting modules can be fused with one of four primary types of effector domains: those that directly influence the transcription of the target gene, those that alter DNA CpG methylation patterns, those that add or remove specific histone modifications, and those that induce chromatin looping interactions.

The initial demonstration of a CRISPR-based gene activation approach for treating diseases linked to reduced gene expression was marked by reversing obesity in mice due to *Sim1* haploinsufficiency [40]. This condition, caused by heterozygous loss-of-function mutations in the

single-minded family of basic helix-loop-helix transcription factors *SIM1* gene, contributes to obesity in humans. Matharu et al. utilized CRISPR activation (CRISPRa) with dCas9 linked to the transcription activator domain -- VP64 (consisting of four repeats of the viral protein 16) to specifically enhance *Sim1* expression, effectively improving the obesity phenotype in affected mice. This highlights the potential of precise gene regulation strategies in treating diseases stemming from gene expression imbalances.

5.4 *Nurr1* as a Novel Target for NASH Treatment

Chronic liver inflammation plays an important role in the onset of conditions like NASH and hepatitis C. NASH, a subset of non-alcoholic fatty liver disease (NAFLD), has yet to have a specific drug treatment officially approved. While lifestyle modifications remain the cornerstone of treatment, the urgent demand for more therapeutic options for NASH is evident.

The CCL2-CCR2 pathway is especially activated in patients with NASH [41]. Elevated levels of CCL2, the primary CCR2 ligand, are evident in the livers of NASH patients and in experimental models of fatty liver disease and fibrosis [42]. This pathway is crucial for the recruitment of monocytes/macrophages to the liver, contributing to ongoing inflammation and fibrosis. mNOX-E36, which selectively binds and inhibits CCL2, has demonstrated efficacy in preventing monocyte/macrophage infiltration in liver injury models, indicating its potential as a therapeutic agent for hepatic inflammation [43]. Meanwhile, Cenicriviroc, a dual CCR2/CCR5 antagonist, has shown promise in early-phase trials for treating liver fibrosis in NASH but failed to prove effective in a subsequent phase III trial ([44], [45]). Beyond the activation of CCL2-CCR2 pathway, significant correlations have been found between NAFLD/NASH and increase levels of inflammatory indicators such as C-reactive protein (CRP), interleukin-1β (IL-1β), interleukin-6 (IL-6), tumor necrosis factor-α (TNF-α), and intercellular adhesion molecule-1 (ICAM-1) [46].

Nuclear receptor-related 1, also known as *Nurr1* or *Nr4a2*, is a transcription factor that plays a crucial role in developing and maintaining dopaminergic neurons, with significant implications for Parkinson's disease pathology [47]. Moreover, *Nurr1* is recognized for its anti-inflammatory properties outside of neuronal functions [48]. According to Saijo et al., *Nurr1* protects neurons from inflammation-induced damage by suppressing pro-inflammatory mediator production such as interleukin-1β (IL-1β) and tumor necrosis factor-α (TNF-α), in microglia and astrocytes [49]. Furthermore, Liu et al. discovered that heightened *Nurr1* levels offer neuroprotection and mitigate inflammation by reducing *CCL2 in vitro* and *in vivo* Parkinson's disease models [50]. *Nurr1*'s influence extends beyond the brain. For instance, inflammatory triggers like LPS enhance *Nurr1* mRNA in macrophages, where it acts to suppress inflammatory gene activation, crucial in atherosclerosis development [51]. In Multiple Sclerosis*, Nurr1* levels are notably lower in certain immune cells compared to healthy individuals [52]. Additionally, *Nurr1* is expressed in the monocytes and T cells in the liver, and activating *Nurr1* has been proven to enhance metabolism and reduce liver fat accumulation in a diet-induced NAFLD model and ob/ob mice[53].

Given the critical role of inflammation in the progression of NASH and the insights gained from Cenicriviroc—a dual *CCR2/CCR5* antagonist that showed initial promise but ultimately failed in a phase III trial due to lack of efficacy—it becomes clear that targeting a single inflammatory pathway may not adequately address the disease. Activating *Nurr1*, a transcription factor that controls several anti-inflammatory pathways simultaneously, offers a promising strategy for NASH management. This study aims to leverage a CRISPR-based method to target Nuclear receptor-related 1, *Nurr1*, with the goal of developing a potential therapeutic for NASH.

5.5 References

1. Teng, M.L., et al., *Global incidence and prevalence of nonalcoholic fatty liver disease.* Clin Mol Hepatol, 2023. **29**(Suppl): p. S32-S42.
2. Hwang, S., et al., *Role of Neutrophils in the Pathogenesis of Nonalcoholic Steatohepatitis.* Front Endocrinol (Lausanne), 2021. **12**: p. 751802.
3. Huby, T. and E.L. Gautier, *Immune cell-mediated features of non-alcoholic steatohepatitis.* Nat Rev Immunol, 2022. **22**(7): p. 429-443.
4. Burra, P., C. Becchetti, and G. Germani, *NAFLD and liver transplantation: Disease burden, current management and future challenges.* JHEP Rep, 2020. **2**(6): p. 100192.
5. Younossi, Z.M., et al., *The Growing Economic and Clinical Burden of Nonalcoholic Steatohepatitis (NASH) in the United States.* J Clin Exp Hepatol, 2023. **13**(3): p. 454-467.
6. Diehl, A.M. and C. Day, *Cause, Pathogenesis, and Treatment of Nonalcoholic Steatohepatitis.* N Engl J Med, 2017. **377**(21): p. 2063-2072.
7. Chalasani, N., et al., *The diagnosis and management of nonalcoholic fatty liver disease: Practice guidance from the American Association for the Study of Liver Diseases.* Hepatology, 2018. **67**(1): p. 328-357.
8. Ajmera, V., et al., *Among Patients With Nonalcoholic Fatty Liver Disease, Modest Alcohol Use Is Associated With Less Improvement in Histologic Steatosis and Steatohepatitis.* Clin Gastroenterol Hepatol, 2018. **16**(9): p. 1511-1520 e5.
9. van der Windt, D.J., et al., *The Effects of Physical Exercise on Fatty Liver Disease.* Gene Expr, 2018. **18**(2): p. 89-101.
10. Patel, N.S., et al., *Effect of weight loss on magnetic resonance imaging estimation of liver fat and volume in patients with nonalcoholic steatohepatitis.* Clin Gastroenterol Hepatol, 2015. **13**(3): p. 561-568 e1.

11. Musso, G., et al., *Impact of current treatments on liver disease, glucose metabolism and cardiovascular risk in non-alcoholic fatty liver disease (NAFLD): a systematic review and meta-analysis of randomised trials.* Diabetologia, 2012. **55**(4): p. 885-904.
12. Vilar-Gomez, E., et al., *Weight Loss Through Lifestyle Modification Significantly Reduces Features of Nonalcoholic Steatohepatitis.* Gastroenterology, 2015. **149**(2): p. 367-78 e5; quiz e14-5.
13. Lassailly, G., et al., *Bariatric Surgery Reduces Features of Nonalcoholic Steatohepatitis in Morbidly Obese Patients.* Gastroenterology, 2015. **149**(2): p. 379-88; quiz e15-6.
14. Jan, A., M. Narwaria, and K.K. Mahawar, *A Systematic Review of Bariatric Surgery in Patients with Liver Cirrhosis.* Obes Surg, 2015. **25**(8): p. 1518-26.
15. Sanyal, A.J., et al., *Pioglitazone, vitamin E, or placebo for nonalcoholic steatohepatitis.* N Engl J Med, 2010. **362**(18): p. 1675-85.
16. Abner, E.L., et al., *Vitamin E and all-cause mortality: a meta-analysis.* Curr Aging Sci, 2011. **4**(2): p. 158-70.
17. Yang, Y.Y., et al., *Updates on novel pharmacotherapeutics for the treatment of nonalcoholic steatohepatitis.* Acta Pharmacol Sin, 2022. **43**(5): p. 1180-1190.
18. Farrell, G., et al., *Mouse Models of Nonalcoholic Steatohepatitis: Toward Optimization of Their Relevance to Human Nonalcoholic Steatohepatitis.* Hepatology, 2019. **69**(5): p. 2241-2257.
19. Gallage, S., et al., *A researcher's guide to preclinical mouse NASH models.* Nat Metab, 2022. **4**(12): p. 1632-1649.
20. De Pergola, G., et al., *A family history of type 2 diabetes as a predictor of fatty liver disease in diabetes-free individuals with excessive body weight.* Sci Rep, 2021. **11**(1): p. 24084.

21. Manchiero, C., et al., *The rs738409 polymorphism of the PNPLA3 gene is associated with hepatic steatosis and fibrosis in Brazilian patients with chronic hepatitis C.* BMC Infect Dis, 2017. **17**(1): p. 780.

22. Bettini, S., et al., *Liver Fibrosis and Steatosis in Alstrom Syndrome: A Genetic Model for Metabolic Syndrome.* Diagnostics (Basel), 2021. **11**(5).

23. Asgharpour, A., et al., *A diet-induced animal model of non-alcoholic fatty liver disease and hepatocellular cancer.* J Hepatol, 2016. **65**(3): p. 579-88.

24. Arsov, T., et al., *Fat aussie--a new Alstrom syndrome mouse showing a critical role for ALMS1 in obesity, diabetes, and spermatogenesis.* Mol Endocrinol, 2006. **20**(7): p. 1610-22.

25. Van Rooyen, D.M., et al., *Hepatic free cholesterol accumulates in obese, diabetic mice and causes nonalcoholic steatohepatitis.* Gastroenterology, 2011. **141**(4): p. 1393-403, 1403 e1-5.

26. Ganguly, S., et al., *Nonalcoholic Steatohepatitis and HCC in a Hyperphagic Mouse Accelerated by Western Diet.* Cell Mol Gastroenterol Hepatol, 2021. **12**(3): p. 891-920.

27. Droz, B.A., et al., *Correlation of disease severity with body weight and high fat diet in the FATZO/Pco mouse.* PLoS One, 2017. **12**(6): p. e0179808.

28. Sun, G., et al., *The FATZO mouse, a next generation model of type 2 diabetes, develops NAFLD and NASH when fed a Western diet supplemented with fructose.* BMC Gastroenterol, 2019. **19**(1): p. 41.

29. Wolf, S., et al., *Characterizing the landscape of gene expression variance in humans.* PLoS Genet, 2023. **19**(7): p. e1010833.

30. Wittkopp, P.J. and G. Kalay, *Cis-regulatory elements: molecular mechanisms and evolutionary processes underlying divergence.* Nat Rev Genet, 2011. **13**(1): p. 59-69.

31. Gibney, E.R. and C.M. Nolan, *Epigenetics and gene expression.* Heredity (Edinb), 2010. **105**(1): p. 4-13.

32. Wu, Y.L., et al., *Epigenetic regulation in metabolic diseases: mechanisms and advances in clinical study.* Signal Transduct Target Ther, 2023. **8**(1): p. 98.

33. Wang, D., P.W.L. Tai, and G. Gao, *Adeno-associated virus vector as a platform for gene therapy delivery.* Nat Rev Drug Discov, 2019. **18**(5): p. 358-378.

34. Mercuri, E., et al., *Nusinersen versus Sham Control in Later-Onset Spinal Muscular Atrophy.* N Engl J Med, 2018. **378**(7): p. 625-635.

35. Kaemmerer, W.F. and R.C. Grondin, *The effects of huntingtin-lowering: what do we know so far?* Degener Neurol Neuromuscul Dis, 2019. **9**: p. 3-17.

36. Matharu, N. and N. Ahituv, *Modulating gene regulation to treat genetic disorders.* Nat Rev Drug Discov, 2020. **19**(11): p. 757-775.

37. Urnov, F.D., et al., *Genome editing with engineered zinc finger nucleases.* Nat Rev Genet, 2010. **11**(9): p. 636-46.

38. Wright, D.A., et al., *TALEN-mediated genome editing: prospects and perspectives.* Biochem J, 2014. **462**(1): p. 15-24.

39. Adli, M., *The CRISPR tool kit for genome editing and beyond.* Nat Commun, 2018. **9**(1): p. 1911.

40. Matharu, N., et al., *CRISPR-mediated activation of a promoter or enhancer rescues obesity caused by haploinsufficiency.* Science, 2019. **363**(6424).

41. Marra, F. and F. Tacke, *Roles for chemokines in liver disease.* Gastroenterology, 2014. **147**(3): p. 577-594 e1.

42. Kang, J., et al., *Notch-mediated hepatocyte MCP-1 secretion causes liver fibrosis.* JCI Insight, 2023. **8**(3).

43. Baeck, C., et al., *Pharmacological inhibition of the chemokine CCL2 (MCP-1) diminishes liver macrophage infiltration and steatohepatitis in chronic hepatic injury.* Gut, 2012. **61**(3): p. 416-26.

44. Ratziu, V., et al., *Cenicriviroc Treatment for Adults With Nonalcoholic Steatohepatitis and Fibrosis: Final Analysis of the Phase 2b CENTAUR Study.* Hepatology, 2020. **72**(3): p. 892-905.

45. Anstee, Q.M., et al., *Cenicriviroc Lacked Efficacy to Treat Liver Fibrosis in Nonalcoholic Steatohepatitis: AURORA Phase III Randomized Study.* Clin Gastroenterol Hepatol, 2024. **22**(1): p. 124-134 e1.

46. Duan, Y., et al., *Association of Inflammatory Cytokines With Non-Alcoholic Fatty Liver Disease.* Front Immunol, 2022. **13**: p. 880298.

47. Decressac, M., et al., *NURR1 in Parkinson disease--from pathogenesis to therapeutic potential.* Nat Rev Neurol, 2013. **9**(11): p. 629-36.

48. Al-Nusaif, M., et al., *Advances in NURR1-Regulated Neuroinflammation Associated with Parkinson's Disease.* Int J Mol Sci, 2022. **23**(24).

49. Saijo, K., et al., *A Nurr1/CoREST pathway in microglia and astrocytes protects dopaminergic neurons from inflammation-induced death.* Cell, 2009. **137**(1): p. 47-59.

50. Liu, W., Y. Gao, and N. Chang, *Nurr1 overexpression exerts neuroprotective and anti-inflammatory roles via down-regulating CCL2 expression in both in vivo and in vitro Parkinson's disease models.* Biochem Biophys Res Commun, 2017. **482**(4): p. 1312-1319.

51. Bonta, P.I., et al., *Nuclear receptors Nur77, Nurr1, and NOR-1 expressed in atherosclerotic lesion macrophages reduce lipid loading and inflammatory responses.* Arterioscler Thromb Vasc Biol, 2006. **26**(10): p. 2288-94.

52. Pansieri, J., et al., *A potential protective role of the nuclear receptor-related factor 1 (Nurr1) in multiple sclerosis motor cortex: a neuropathological study.* Brain Commun, 2023. **5**(2): p. fcad072.

53. Amoasii, L., et al., *NURR1 activation in skeletal muscle controls systemic energy homeostasis.* Proc Natl Acad Sci U S A, 2019. **116**(23): p. 11299-11308.

Chapter 6. CRISPR activation rescues metabolic abnormalities in a non-alcoholic fatty liver disease/steatohepatitis mouse model

6.1 Methods

6.1.1 CRISPRa in vitro optimization

Ten sgRNAs targeting mouse *Nurr1* were developed using the GPP sgRNA Design Tool from the Broad Institute's Genetic Perturbation Platform. These sgRNAs were individually inserted into the pAAV-U6-sasgRNA-CMV-mCherry-WPREpA vector at the BstXI and XhoI sites utilizing the In-Fusion HD Cloning Kit by Clontech. For AAV vector construction, the pcDNA-dCas9-VP64 (Addgene #47107) and U6-sgRNA-CMV-mCherry-WPREpA were recombined by replacing the Ef1a-FAS-hChR2(H134R)-mCherry-WPRE-pA segment with U6-sgRNA-CMV-mCherry-WPREpA in the pAAV-Ef1a-FAS-hChR2(H134R)-mCherry-WPRE-pA backbone (Addgene #37090). These mouse sgRNAs were evaluated in Neuro-2A neuroblastoma cell line (ATCC CCL-131), which was cultured according to ATCC's recommended practices. For transient transfections, Neuro-2A cells were co-transfected with the sgRNA-containing pAAV-U6-sasgRNA-CMV-mCherry-WPREpA and pCMV-sadCas9-VP64 using Opti-MEM Reduced Serum Medium (Thermo Fisher 31985088) and X-tremeGENE HP transfection reagent (Sigma-Aldrich). Forty-eight hours post-transfection, cells were harvested and processed with Trizol for RNA extraction, followed by cDNA synthesis and qRT-PCR analysis as detailed in the RNA Isolation and qRT-PCR methods section.

6.1.2 RNA Isolation and qRT-PCR

Total RNA was extracted utilizing the RNeasy Kit (Qiagen 74104), adhering to the protocol provided by the manufacturer. cDNA generation was carried out with the SuperScript III First-Strand Synthesis System (Invitrogen 18080051), followed by qPCR analysis using SsoFast EvaGreen Supermix (Bio-Rad). The ΔΔCT method was employed for statistical analysis, with Gapdh or β-actin primers serving as the reference (refer to Table S2 for primer sequences). The gene expression data were derived from averaging over n=3 biological replicates for the *in vitro* studies and n=5-8 biological replicates for the in vivo studies.

6.1.3 Mouse husbandry and Special Diet Treatment

All animal experiments were conducted following the guidelines set by the University of California San Francisco Institutional Animal Care and Use Committee. Mice were maintained on a 12:12 hour light-dark cycle, with free access to chow diet (Envigo, 2018S) and water. The mice were given either a standard chow diet or a Western diet (Research Diet, D12079B) supplemented with 5% Fructose Water (WDF).

6.1.4 CRISPRa in vitro optimization

The two gRNAs that showed the most significant increase in *Nurr1* expression were encapsulated into the AAV-9 serotype virus. To produce the AAV-9 serotype virus, AAVpro 293T cells (Takara; 6322723) were transfected with pCMV-sadCas9-VP64 (Addgene; 115790) or pAAV-U6-sasgRNA-CMV-mCherry-WPREpA, alongside packaging vectors PAAV2/9n (Addgene; 112865) and pHelper vectors, using TransIT293 reagent (Mirus; 2700). After 72 hours, the AAV particles were harvested, purified using the AAVpro Cell & Sup. Purification Kit Maxi (Takara; 6676), and their concentrations determined with the AAVpro Titration Kit (Takara; 6233). Four-week-old C57BL/6J mice were anesthetized with isoflurane at a concentration of 1.0%-2.0%. They received a one-time intravenous injection via the tail vein of AAV9-dCas9-VP64 and AAV9-gRNA at a 1:1 ratio, with dosages of either 1 x 10^10 or 5 x 10^10 vg per mouse. Six weeks after the injection, the livers of the mice were excised, and RNA was extracted for cDNA synthesis and qRT-PCR analysis, as detailed in the RNA Isolation and qRT-PCR section.

6.1.5 In vivo CRISPRa administration

MSNASH/PcoJ mice at 4week old for the preventative study or 8 week old for the imprvomental study were kept under live anesthetic isoflurane at 1.0%-2.0%. A single dose of AAV9-dCas9-

VP64 and AAV9-gRNA (5×10^{10}vg/mouse) at 1:1 ratio were injected intravenously via tail-vein. Body weight was recorded weekly.

6.1.6 Glucose tolerance test (GTT)

Mice underwent overnight fasting before their blood glucose levels were assessed to establish a baseline (0 time point). The glucose concentration was measured from tail vein blood using the Contour Next Blood Glucose Meter (Contour, 7277), with blood obtained through tail snipping. Following this, glucose (1g/kg of body weight) (Sigma-Aldrich, G8270) was administered intraperitoneally. Subsequent blood glucose measurements were taken at intervals of 30, 60, and 120 minutes post-injection.

6.1.7 Insulin tolerance test (ITT)

Mice underwent a 4-hour fasting period before their baseline blood glucose levels (0 time point) were recorded. These levels were measured using the Contour Next Blood Glucose Meter (Contour, 7277) from blood drawn from the tail vein. Subsequently, recombinant human insulin (ranging from 7.5 to 10 IU/kg body weight) (Sigma-Aldrich, I9278) was administered intraperitoneally. Blood glucose levels were then assessed at intervals of 30, 60, 120, and 180 minutes following the insulin injection.

6.1.8 Special Diet Study Design

In the prevention study, 4-week-old male *MSNASH/PcoJ* mice (FATZO mice) received injections of either CRISPR activation components (AAV9-dCas9-VP64 combined with AAV9-gRNA) or a Negative Control (AAV9-dCas9-VP64 alone). Four weeks after the injection, the mice were placed on WDF for 20 weeks. Glucose Tolerance Tests (GTT) and Insulin Tolerance Tests (ITT) were conducted 6 weeks and 18 weeks, respectively, after the start of the diet regimen.

In the intervention study, 4-week-old male *MSNASH/PcoJ* mice were first subjected to WDF for 4 weeks. After this period, they received injections of either CRISPR activation components (including AAV9-dCas9-VP64 and AAV9-gRNA) or a Negative Control (only AAV9-dCas9-VP64). To evaluate the metabolic effects of the treatments, GTT and ITT were conducted 8 weeks after the injections.

6.1.9 Liver histology and pathological assessment

Liver tissue specimens were immersed in 10% neutral buffered formalin (NBF) for 24 hours, followed by preservation in 70% ethanol. While stored in 70% ethanol, the samples were forwarded to the UCSF Liver Core for further processing. There, after embedding in paraffin and cooling, the sections were cut and subjected to standard staining techniques, including Haematoxylin and Eosin (H&E) and Sirius Red Staining. A skilled liver pathologist, unaware of the study group allocations, reviewed the liver samples according to the NASH liver scoring system. This detailed analysis covered the assessment of steatosis, lobular inflammation, hepatocyte ballooning, fibrosis, and the characterization of NASH based on pattern recognition.

6.2 Result

6.2.1 Extended exposure to a WDF heightened inflammation in FATZO mice.

Prolonged WDF consumption (21 weeks) led to a gradual exacerbation of NAFLD symptoms in FATZO mice, though fibrosis was not detected. The livers of these mice appeared notably pale at necropsy(Supplementary Figure 1B). The expression of CCR2 mRNA, known for its role in promoting liver fibrosis by facilitating the migration of circulating monocytes to the damaged liver and activating hepatic stellate cells, was significantly elevated following extended WDF treatment (Supplementary Figure 1C).

6.2.2 Nurr1-CRISPRa optimization in vitro and in vivo

To optimize mouse Nurr1-CRISPRa constructs, we tested the ability of ten different sgRNAs targeting the *Nurr1* promoter along with a Staphylococcus aureus (sa) dCas9 fused to the transcriptional activator VP64 to upregulate *Nurr1* in mouse neuroblastoma cells (Neuro-2a). The VP64 transcriptional activator was selected due to its small size, allowing it to fit into an AAV vector, and due to its modest upregulation potential, which has been shown to provide close to physiological wild-type levels in mice heterozygous for other forms of haploinsufficiency [1]. Forty- eight hours post-transfection, *Nurr1* mRNA expression was measured by quantitative polymerase chain reaction (qPCR), finding three sgRNAs that significantly increase *Nurr1* mRNA expression compared to a no sgRNA transfection condition (Fig. 1A). We packaged two of these three sgRNAs and the transcriptional activator plasmid into the AAV-9 serotype, as it provides strong liver expression([2]). AAV- sgRNA viruses were then co-administrated with the AAV-sadCas9-VP64 activator to 4-week-old mice by tail vein injection. After a 5-week period following adeno-associated virus (AAV) administration, the expression of *Nurr1* mRNA in the liver was quantitatively analyzed. Among the two AAV-single guide RNA (AAV-sgRNA) constructs tested, one was identified to notably enhance *Nurr1* mRNA levels in a dose-responsive fashion. This specific construct was subsequently chosen for further investigation in mouse model (Figure 1B).Due to the importance of *Nurr1* in dopaminergic neuron development and maintenance, we tested if our AAVs would cross BBB for off-target effects; we measured *mCherry* mRNA expression changes following plasmid CRISPRa injection in the brain and confirmed that the mRNA expression level of *mCherry* is comparable to mice without the sgRNA injection (Figure 1C).

6.2.3 Administration of CRISPRa prevent glucose resistance and inflammation in FATZO mice

To explore the potential of Nurr1-AAV-CRISPRa (AAV-sadCas9-VP64 + AAV-Nurr1-sgRNA) in preventing the onset of NAFLD/NASH, we administered this combination to 4-week-old FATZO mice via tail vein injection, bypassing the WDF treatment. As a control, FATZO mice received only AAV-sadCas9-VP64 without sgRNA under the same conditions. Three weeks post-injection, the mice were fed a WDF for 21 weeks, then the tissues including liver, kidney, quadriceps muscle, interscapular brown adipose tissue (iBAT), inguinal white adipose tissue (iWAT), and epididymal white adipose tissue (eWAT) were collected for weighing and qPCR analysis. Nurr1-CRISPRa showed an upregulation of *Nurr1* mRNA of 2.1 fold compared to the control group (Figure. 2C). FATZO mice treated with Nurr1-CRISPRa for 11 weeks (with 8 weeks on WDF), showed a trend towards improved glucose tolerance, which became significantly better after 21 weeks of CRISPRa treatment (with 18 weeks on WDF) (Figure. 2A-B, Supplementary Figure 1A-B). However, there was no observed improvement in insulin tolerance. Additionally, there was no significant difference in body weight between the treated group and the NC, aligning with the lack of change in adipocyte size within the white and brown adipose tissues of WDF-fed FATZO mice treated with Nurr1-CRISPRa compared to control mice (Supplementary Figure 3, Supplementary Figure 4).

To evaluate the effectiveness of Nurr1-CRISPRa in preventing the onset of NAFLD/NASH, we analyzed the presence of steatosis, lobular inflammation, hepatocyte ballooning, and fibrosis in the livers of FATZO mice fed with WDF. Consistent with expectations, after 21 weeks on a WDF, FATZO mice developed hepatic steatosis, lobular inflammation, and hepatocyte ballooning, mirroring the characteristics of NAFLD/NASH observed in humans, yet without the fibrosis typically seen in human NASH. Between the group treated with Nurr1-CRISPRa and the NC, there was no notable histological difference observed (Supplementary Figure 2D).

Furthermore, the expression of genes associated with lipid accumulation, such as *CD36/FAT* (a free fatty acid transporter), fat-specific protein 27 (*Fsp27*), *SREBP1c*, and *Pcsk9*, remained unchanged in FATZO mice on a WDF when compared to the treated group (Supplementary Figure 2C). This observation aligns with the lack of improvement in steatosis seen in the histological analysis.

Although we did not observe a reduction in inflammation through histological analysis, we noted a delayed progression of glucose intolerance in FATZO mice fed WDF, suggesting a potential improvement in the Nurr1-CRISPRa treated group compared to the control. Suppressing inflammation has been shown to effectively improve glucose tolerance *in vivo* [3]. To delve deeper into the mechanisms by which CRISPRa treatment may mitigate glucose resistance, we investigated the expression of specific inflammatory genes in the liver. Notably, *CCL2*, which is known to be negatively regulated by *Nurr1* both *in vitro* and *in vivo*, along with its receptor *CCR2*, were found to be downregulated in the livers of mice treated with Nurr1-CRISPRa on WDF (Figure. 2D). These findings indicate that Nurr1-CRISPRa treatment can slow inflammation in WDF-fed FATZO mice, thereby facilitating an improvement in glucose metabolism.

6.2.4 CRISPRa Administration as a Potential Therapeutic Intervention for NAFLD/NASH

In a subsequent experiment, we aimed to determine the therapeutic potential of Nurr1-AAV-CRISPRa in FATZO mice that had been on a WDF for 4 weeks. The treated group received Nurr1-CRISPRa via tail vein injection, while the control group received only AAV-sadCas9-VP64. After 8 weeks post-injection (with 12 weeks on WDF), we collected liver, kidney, quadriceps muscle, iBAT, iWAT, and eWAT for analysis. Similar to our prevention study, Nurr1-CRISPRa treatment resulted in a 2.3-fold increase in *Nurr1* mRNA expression and significantly

improved glucose tolerance after 6 weeks of treatment (with 10 weeks on WDF), without improving insulin tolerance or body weight (Figure 3A-C, Supplementary Figure 5). Glucose tolerance was also improved in the Nurr1-CRISPRa treated group. The downregulation of *CCL2* in the livers of treated mice further supports the potential of *Nurr1* upregulation to suppress liver inflammation and improve glucose metabolism in FATZO mice on a WDF (Figure. 3C).

6.3 Figures

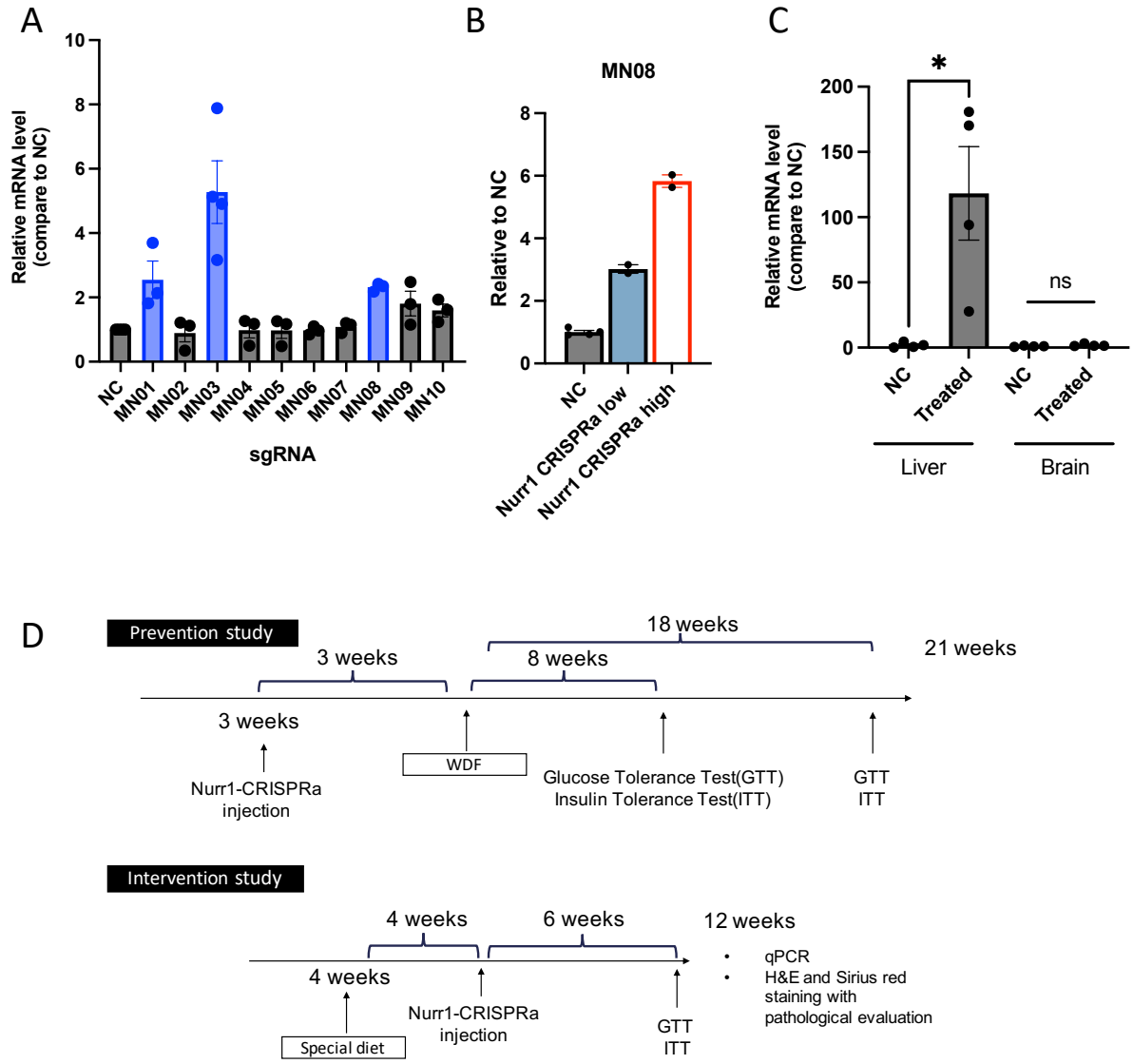

Figure 6.1. *In vitro* and *in vivo* optimization of CRISPRa constructs in mouse Neuroblastoma- 2A (N2A) cells and Wild-type (WT) mice.
(A) Fold change in *Nurr1* expression in N2A cells transfected with plasmids expressing sgRNAs targeting the promoter of mouse *Nurr1* compared to a no sgRNA VP64 only treated control. (B) Fold change in *Nurr1* expression in the livers of wild-type (WT) mice treated with AAV9-packaged sgRNAs targeting the promoter of mouse *Nurr1* and dCas9-VP64 (Nurr1-CRISPRa), compared to control mice treated only with dCas9-VP64 (NC) at various concentrations.(C) Analysis of off-target effect arising from possible AAV9 delivery to the brain. (D) Schematic representation of the experimental timeline for a prevention study (upper) and intervention (lower) conducted with FATZO mice.

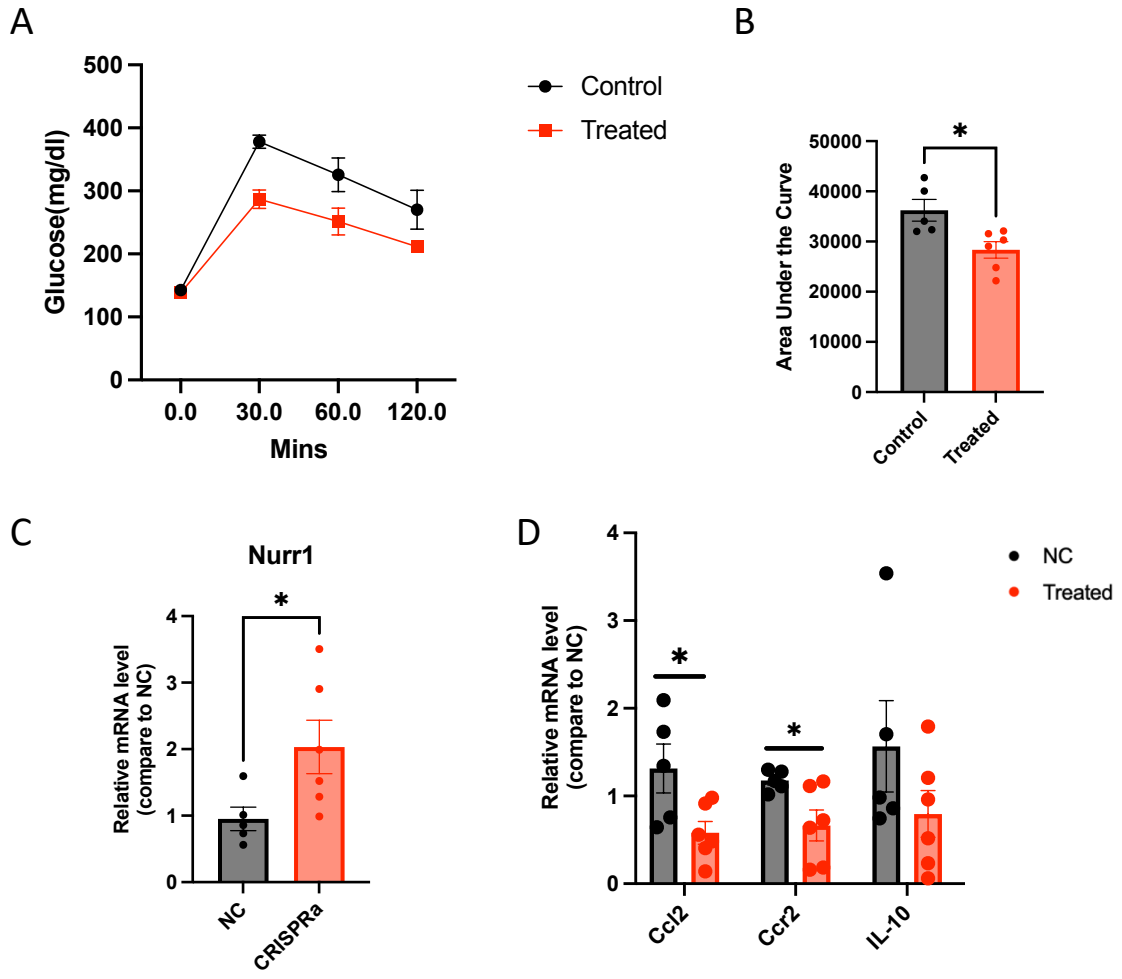

Figure 6.2. *Nurr1* CRISPR activation enhances resistance to glucose metabolism impairment and suppresses inflammation mediated by the *Ccl2-Ccr2* pathway (Prevention Study).
(A) Glucose tolerance of FATZO mice on WFD with Nurr1-CRISPRa, or only dCas9-VP64 as a negative control(NC). Values were measured after 18 weeks after WFD started (21 weeks after tail vein injection). (B) Area under the curve (AUC) analysis of glucose responses in FATZO mice following an 24-week administration of Nurr1-CRISPRa or NC. (C, D) *In vivo* fold change in *Nurr1* expression(C), Ccl2, Ccr2, and IL-10 expression(D) in the FATZO mice liver after 21 weeks on WDF (24 weeks post tail vein injection with Nurr1-CRISPRa, compared to mice treated with NC.

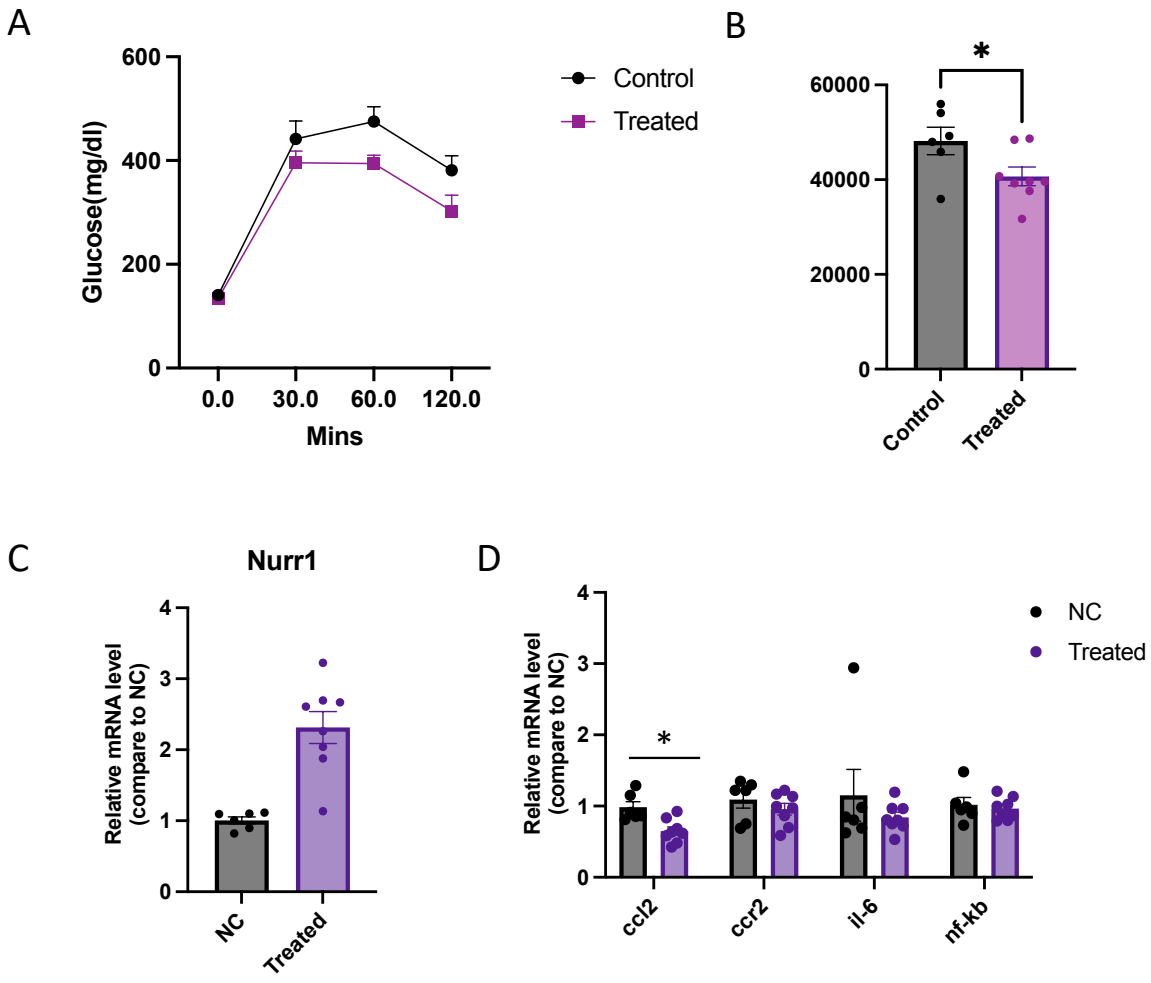

Figure 6.3. *Nurr1* CRISPR activation reverts glucose metabolism impairment and reduces inflammation mediated by the Ccl2-Ccr2 pathway (Intervention Study).
(A) Assessment of glucose tolerance in FATZO mice fed WFD and treated with Nurr1-CRISPRa versus those administered only dCas9-VP64 as a negative control (NC). Glucose tolerance was measured 10 weeks after the initiation of WFD, corresponding to 6 weeks post-tail vein injection. (B) Area Under the Curve (AUC) analysis of glucose responses in FATZO mice following 6 weeks of treatment with either Nurr1-CRISPRa or NC.
(C, D) Analysis of *in vivo* fold changes in gene expression within the liver of FATZO mice after 12 weeks on WFD (8 weeks post-tail vein injection): (C) *Nurr1* expression levels; (D) expression levels of inflammatory markers Ccl2, Ccr2, IL-6, and Nf-kb, comparing Nurr1-CRISPRa treated mice to NC-treated controls.

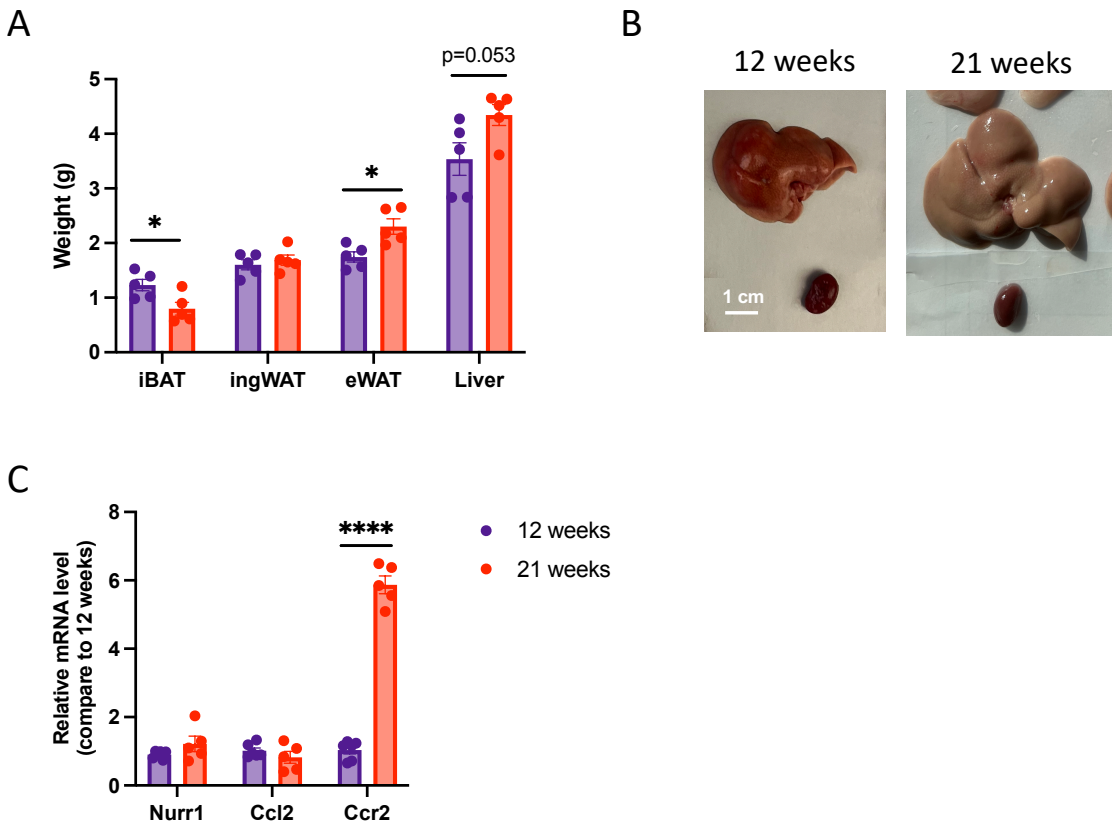

Supplementary Figure 6.1. WDF exacerbated metabolic disorders and liver inflammation caused in FATZO mice

(A) Weight changes in iBAT, ingWAT, eWAT and liver of FATZO mice 12 weeks or 21 weeks on WDF. (B) Gross images of liver tissue from the FATZO mice after 12 weeks or 21 weeks on WDF. (C) *In vivo* fold change in *Nurr1 Ccl2, Ccr2* expression in the FATZO mice liver after 12 weeks or 21 weeks on WDF.

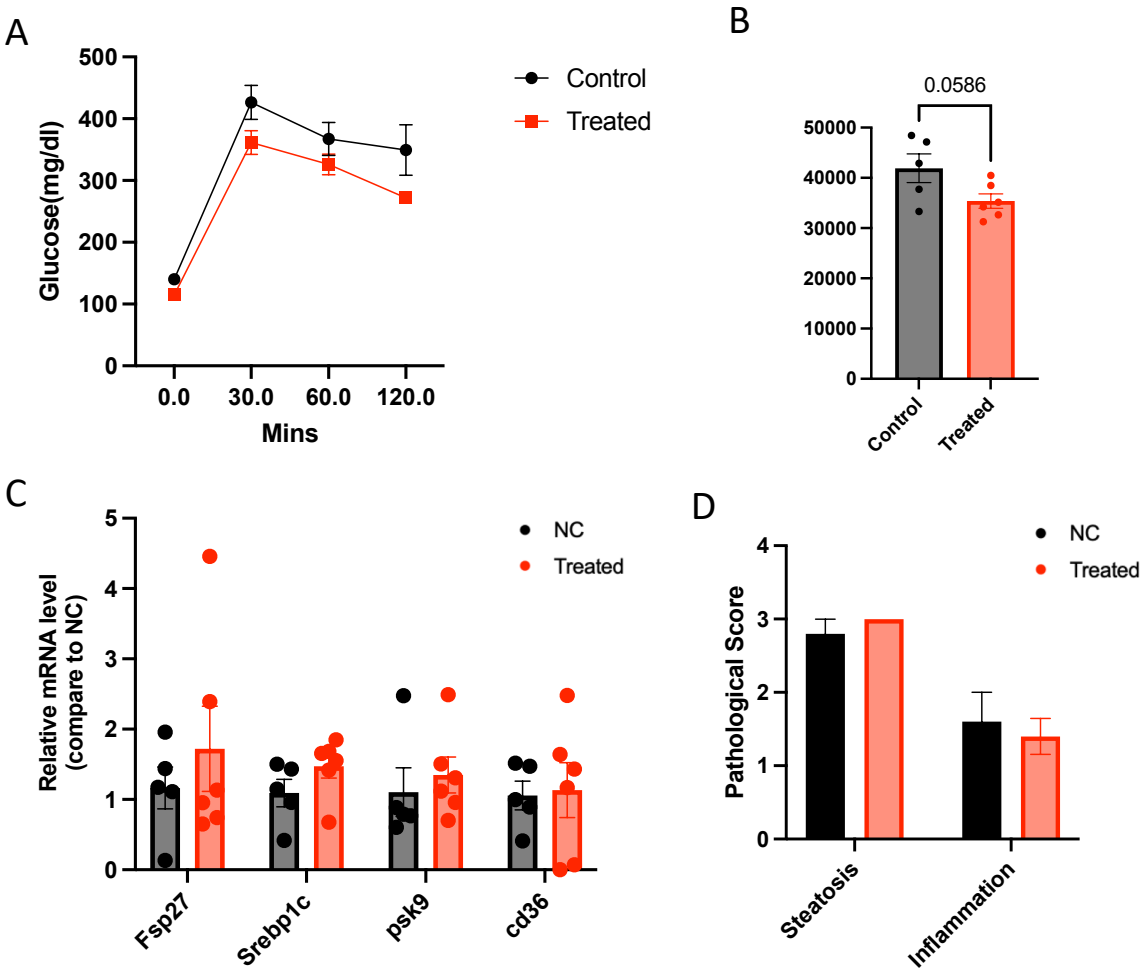

Supplementary Figure 6.2. *Nurr1* CRISPR has no effects on steatosis and histopathological assessment of inflammation (Intervention Study).
(A) Glucose tolerance in FATZO mice fed with a Western Diet Fat (WFD) and treated with Nurr1-CRISPRa or dCas9-VP64 as a negative control (NC). The tolerance was quantified 8 weeks following the commencement of WFD, which corresponds to 11 weeks post-tail vein injection. (B) Area Under the Curve (AUC) analysis of the glucose response in FATZO mice after an 11-week regimen of either Nurr1-CRISPRa or NC treatment.(C) Comparative *in vivo* analysis of the fold change in the expression of Fsp27, Serbp1c, Psk9, and Cd36 in the livers of FATZO mice, assessed 21 weeks after starting WFD, or 24 weeks following tail vein injection with Nurr1-CRISPRa versus NC treatment. (D) Evaluation of steatosis and inflammation in the livers of WFD-fed FATZO mice treated with Nurr1-CRISPRa or NC, highlighting the impact of Nurr1-CRISPRa on liver health.

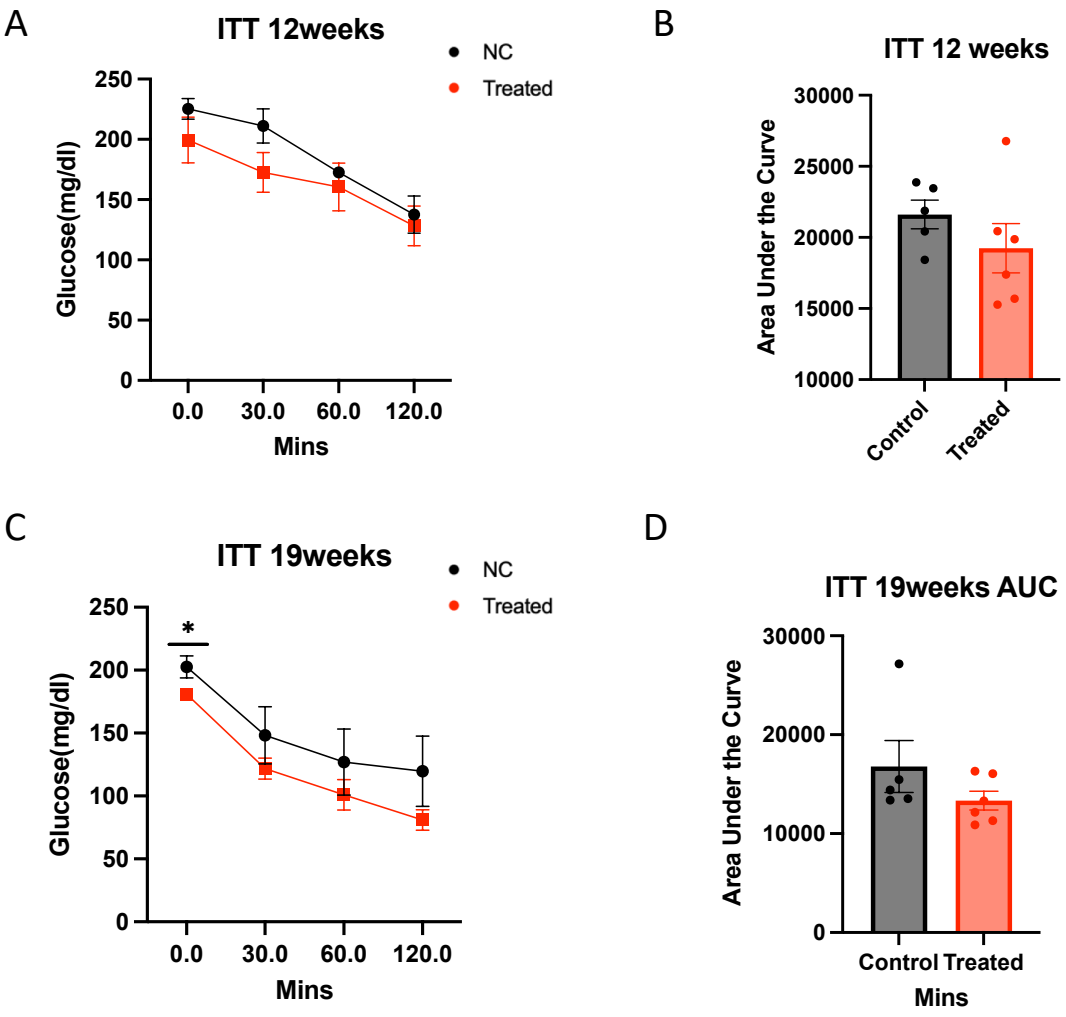

Supplementary Figure 6.3. *Nurr1* CRISPR has no effects on insulin resistance in FATZO mice (Prevention Study).
(A,C) Insulin tolerance of FATZO mice on WFD with Nurr1-CRISPRa, or only dCas9-VP64 as a negative control(NC). Values were measured after 12 weeks after WFD started (A) and after 19 weeks after WFD started(C). (B,D) Area under the curve (AUC) analysis of insulin responses in FATZO mice after 15-week(B) or 22weeks(D) of Nurr1-CRISPRa or NC.

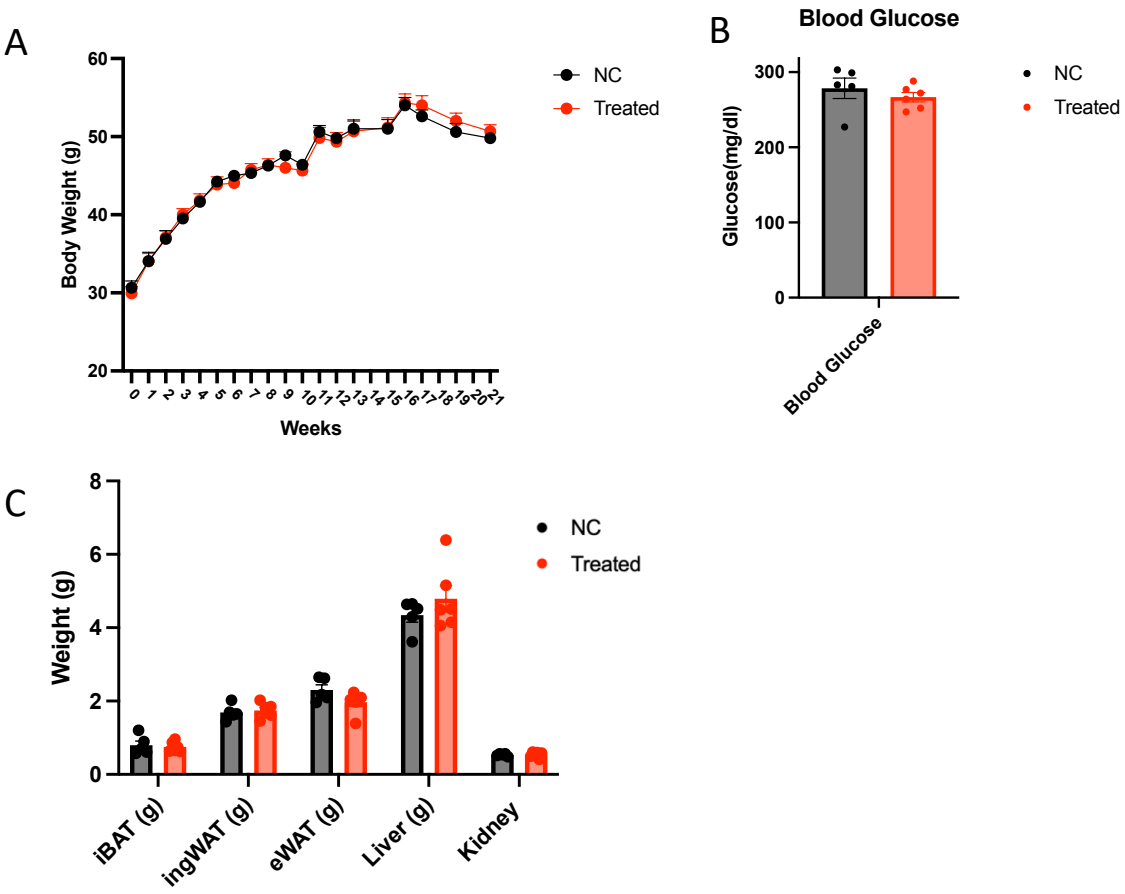

Supplementary Figure 6.4. *Nurr1* CRISPR activation lead to no changes in body or tissue weights (Prevention Study).
(A) Body weight changes of FATZO mice on WFD with Nurr1-CRISPRa, or only dCas9-VP64 as a negative control(NC). (B) Fasting blood glucose of FATZO mice with Nurr1-CRISPRa, or only dCas9-VP64 as a negative control(NC) after 21 weeks on WDF (24 weeks post tail vein injection with Nurr1-CRISPRa, compared to mice treated with NC. (C) Weight of iBAT, ingWAT, eWAT and liver of WDF fed FATZO mice with Nurr1-CRISPRa or NC.

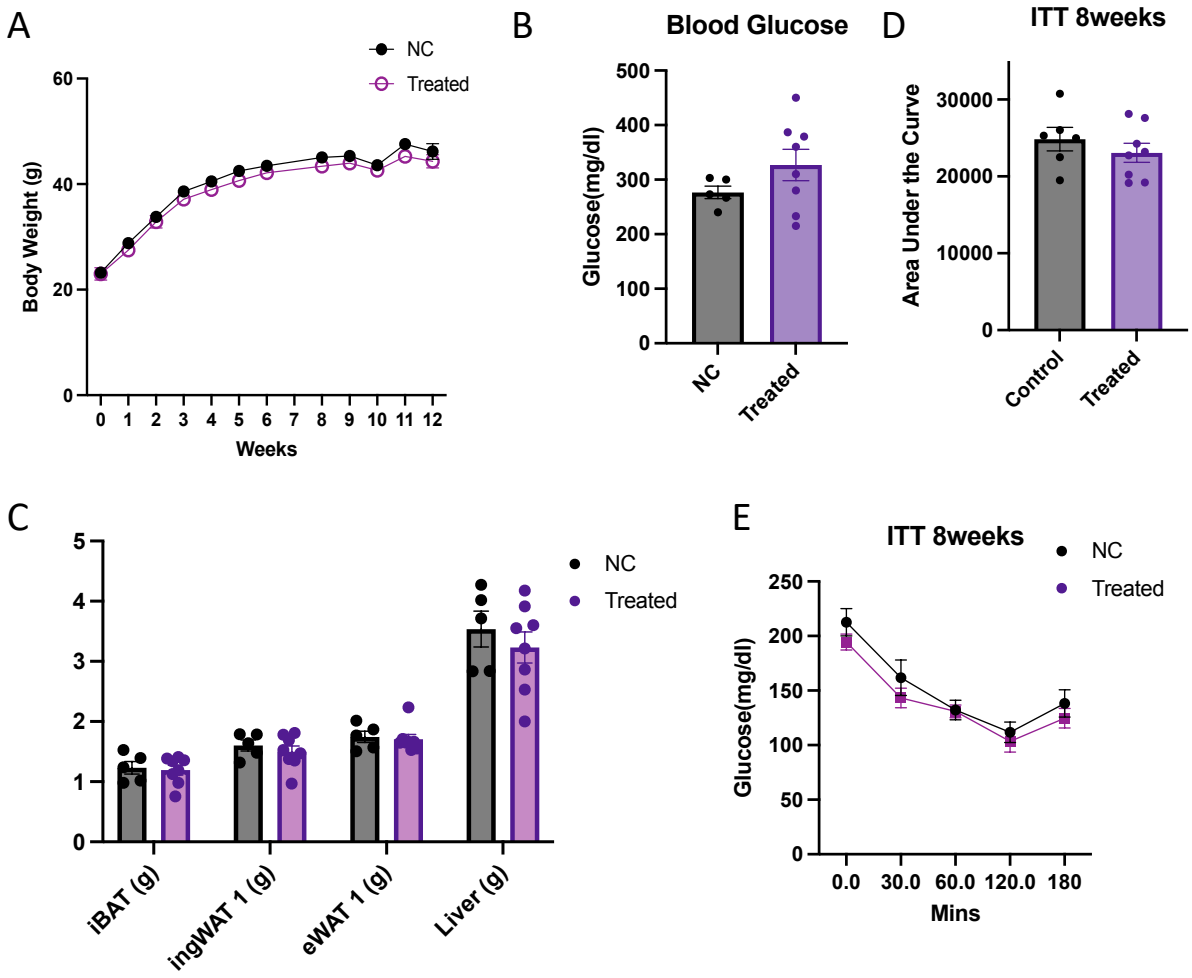

Supplementary Figure 6.5. *Nurr1* CRISPR activation has no effects on weights and insulin resistence (Prevention Study).
(A) Body weight alterations in FATZO mice following a Western Diet Fat (WFD), treated with Nurr1-CRISPRa or dCas9-VP64 as a negative control (NC). (B) Fasting blood glucose levels in FATZO mice subjected to Nurr1-CRISPRa or dCas9-VP64 (NC) following 21 weeks on WFD, assessed 24 weeks after tail vein injection with Nurr1-CRISPRa versus NC treatment. (C) Tissue weights, including interscapular brown adipose tissue (iBAT), inguinal white adipose tissue (ingWAT), epididymal white adipose tissue (eWAT), and liver, from WFD-fed FATZO mice treated with Nurr1-CRISPRa or NC. (D) Insulin tolerance in FATZO mice on WFD treated with Nurr1-CRISPRa or NC, measured 12 weeks after the start of the diet. (E) Area Under the Curve (AUC) analysis for insulin responses in FATZO mice after 8 weeks of treatment with either Nurr1-CRISPRa or NC.

6.4 References

1. Matharu, N., et al., *CRISPR-mediated activation of a promoter or enhancer rescues obesity caused by haploinsufficiency.* Science, 2019. **363**(6424).
2. Van Alstyne, M., et al., *Gain of toxic function by long-term AAV9-mediated SMN overexpression in the sensorimotor circuit.* Nat Neurosci, 2021. **24**(7): p. 930-940.
3. Parker, R., et al., *CC chemokine receptor 2 promotes recruitment of myeloid cells associated with insulin resistance in nonalcoholic fatty liver disease.* Am J Physiol Gastrointest Liver Physiol, 2018. **314**(4): p. G483-G493.

Chapter 7. Conclusion and Perspectives

7.1: Overview

Non-Alcoholic Fatty Liver Disease (NAFLD) represents a growing health concern, affecting up to 30% of the global population. Among these individuals, approximately 25% may advance to Non-Alcoholic Steatohepatitis (NASH), a more serious condition characterized by inflammation that can lead to liver cirrhosis. Despite its widespread prevalence, the market lacks FDA-approved pharmacological treatments specifically for NASH. Recent efforts have increasingly centered on anti-inflammatory approaches as essential strategies for preventing and managing liver fibrosis. Promising treatments are advancing rapidly from Phase II to Phase III clinical trials, driven by the critical need for effective therapies. The interaction of C-C chemokine receptors types 2 (*CCR2*) and 5 (*CCR5*) with their ligands (*CCL2* and *CCL5*) exacerbates liver fibrosis by triggering inflammatory signals and promoting immune cell infiltration. Cenicriviroc (CVC), a dual antagonist of *CCR2* and *CCR5*, was explored as a treatment option for liver fibrosis in NASH patients. Although Phase II trials showed promising fibrosis improvement, the subsequent Phase III AURORA trial (NCT03028740) was prematurely stopped due to insufficient efficacy.

Recent meta-analyses and single-cell RNA sequencing (scRNA-seq) studies have revealed distinct gene expression patterns between healthy and NAFLD/NASH livers, offering insights into the complex mechanisms behind this disease and also the potential of gene therapy a promising anti-fibrosis method ([1], [2]). While NAFLD and NASH are fundamentally metabolic disorders, the transition to NASH involves significant contributions from immune cell-mediated inflammatory pathways. Inflammation plays a crucial role in driving the disease's progression at this stage. The liver's immune cell composition, which varies in health, undergoes further changes during NASH, impacting the severity of the disease [3]. This aligns with findings that

link transcriptome alterations in NASH patients to activated pro-inflammatory pathways, underscoring the inflammatory aspect of the disease's progression.

Currently, liver transplantation is considered to be the only effective treatment for end-stage liver fibrosis. However, this approach has significant limitations, including the scarcity of liver donors, risk of immune rejection, and often unsatisfactory long-term outcomes [4]. In an effort to address these challenges, recent advancements have focused on gene therapy modalities like antisense oligonucleotides, RNA interference, and decoy oligonucleotides. Given the crucial role of inflammation in NASH progression and the experience learned from Cenicriviroc, it is clear that targeting single genes or inflammatory pathways might be insufficient. Instead, activating *Nurr1*, a transcription factor that modulates multiple anti-inflammatory pathways, presents a compelling approach for NASH therapy. This study seeks to apply a CRISPR-based technique to activate *Nurr1*, aiming to forge a new path in NASH treatment.

In this study, we explored the potential of Cis-Regulation Therapy (CRT), an innovative treatment strategy employing nuclease-deficient gene-editing tools such as dead Cas9 (dCas9) fused with transcriptional modulators. This method aims to alter the activity of gene regulatory elements for therapeutic outcomes. Our objective was to assess whether CRT could effectively target multiple anti-inflammatory pathways through upregulating *Nurr1*, thereby preventing or decelerating the progression of NAFLD/NASH. We selected FATZO mice for our research because they closely mimic human metabolic syndrome more accurately than other rodent models of NASH that rely on genetic modifications or chemical treatments. Additionally, FATZO mice rapidly develop characteristics of the NASH phenotype, such as steatosis, ballooning, and inflammation, making them an ideal model for studying the disease's progression and potential treatments. Our application of CRISPR-based CRT in FATZO mice, both prior to and following the onset of the NAFLD phenotype, demonstrated an improvement in glucose metabolism and

suppression of the *CCL2-CCR2* signaling axis. Collectively, our findings suggest a promising new therapeutic avenue for tackling NAFLD/NASH.

7.2 Towards a Therapy and Future Directions

Our successful improvement of glucose tolerance in FATZO mice underscores the promise of our approach. However, several aspects of this approach require further optimization, including the safety evaluation of AAV components, minimization of off-target effects, and the employment of a humanized rodent model and non-human primates for assessing delivery efficiency, upregulation levels, cytotoxicity, and immunogenicity. The following sections detail each of these challenges and possible strategies for their improvement.

7.2.1 Challenges and innovations in the CRT delivery

In this study, we employed AAVs as the delivery mechanism for our CRT constructs. AAVs have been a preferred choice for gene therapy, widely utilized in numerous clinical trials because of their relatively low pathogenicity and ability to sustain long-term episomal expression of transgenes [5]. Nevertheless, AAVs face several challenges that limit their effectiveness in gene therapy. A primary constraint is their vector capacity. While CRT strategies reduce the necessity to package the complete transgene into the AAV, thereby broadening the scope of genes that can be targeted for therapeutic purposes, our current system still struggles to incorporate both sgRNA and dCas9-VP64 within a single AAV vector without exceeding its capacity [6]. This limitation is crucial for translating CRT to human applications, as using two AAVs can significantly vary transduction efficiency. Even though we can achieve tissue-specific upregulation with CRT, we cannot ensure that all cells receive both AAVs, which is essential for effective CRISPR activation. This issue is particularly critical for conditions like NAFLD/NASH, where the pathology is complex and targeting multiple genes with various sgRNAs could yield improved outcomes. An approach to enhance vector capacity involves leveraging smaller,

nuclease-free Cas variants from the CRISPR toolkit, such as Cas12a or Cas14. These alternatives are much smaller than Cas9, yet they can still effectively target and modify human cells, offering a promising direction for overcoming current limitations [7].

Another challenge with viral delivery systems like AAV concerns their potential for pathogenicity, especially with higher dose and repeated doses [8]. Prior studies employing the CRISPRa method, particularly targeting the brain, have shown sustained upregulation of the targeted gene and phenotypic improvements over a nine-month period post-injection. Unlike the brain, the liver possesses a notable capacity for regenerating functional tissue after injury, attributed to the proliferative abilities of its cells. However, this regenerative potential might also cause a reduction in the effectiveness of liver-targeted therapies over time. Research has demonstrated that while AAV9-mediated GFP expression remained stable in the motor and proprioceptive neurons of wild-type mice from day 11 to day 300, liver GFP expression, though initially high at P11, became nearly undetectable by P300 [9]. In our studies, both the preventive approach with 24-week Nurr1-CRISPRa administration and the interventional approach with Nurr1-CRISPRa injections given 8 weeks before euthanasia showed around a twofold increase in Nurr1 expression relative to controls. However, the variability in expression was significantly higher, and the mRNA expression of dCas9-VP64 was substantially lower in samples with prolonged AAV exposure, highlighting the transient nature of the AAV9-packaged Nurr1-CRISPRa effect. Moreover, our study did not reveal any histological improvement or significant changes in body weight and insulin resistance. These results suggest that a twofold upregulation of Nurr1 may not be adequate to achieve a therapeutic effect significant enough to decelerate disease progression. Future research should explore higher or repeated dosages to ensure the durability of the Nurr1-CRISPRa effect as the disease progresses. To circumvent the limitations posed by AAV-induced immunogenicity, alternative delivery mechanisms are being considered. Non-viral carriers, such as synthetic nanoparticles, offer a promising solution. These particles,

constructed from materials such as lipids, gold, and polymers, are being evaluated in numerous clinical trials [10]. They have the capacity to carry larger genetic payloads and enable repeated dosing without encountering neutralizing antibody interference. For instance, MC-3-Lipid nanoparticles (LNPs), which are FDA-approved for liver cell RNA therapy, exemplify a successful non-viral vector [11]. Additionally, a novel lipid nanoparticle designed for precise CRISPR-Cas9 mRNA delivery to the liver has shown promise, significantly reducing serum *ANGPTL3* protein, low-density lipoprotein cholesterol, and triglyceride levels, highlighting its potential for liver disease treatment [12].

7.2.2 Overcoming the non-target effects

Amodiaquine and chloroquine are established anti-malarial drugs known to act as *Nurr1* agonists, demonstrating beneficial outcomes for NAFLD and Parkinson's disease in rodent models. However, their use in treating these diseases in humans is complicated due to associated adverse effects. In 2023, the phase 1 clinical trial for HL192, a small molecule sharing structural similarities with amodiaquine and chloroquine for Parkinson's disease treatment, initiated its first human dosing [13]. Nevertheless, the widespread expression of *Nurr1* across various tissues, including the brain, liver, mammary glands, and heart, poses a challenge. In our research, we opted for AAV9 due to its notable liver transduction efficiency. Our qPCR findings indicated a restricted penetration of AAV9 into the brain following tail vein injection. However, like many other serotypes, AAV9 accumulates in the heart, which could result in severe side effects ([14], [15]). To date, only three capsid serotypes (AAV1, AAV2, and AAV9) have been approved for clinical use, with no liver-directed AAV therapies yet receiving market approval. Since the capsid is crucial in determining vector tropism, extensive efforts are underway to engineer AAV capsids to enhance tissue-specific targeting. These efforts include rational design, directed evolution, and in silico approaches. The creation of novel AAV-SYDs vectors ('SYD' denoting Sydney, Australia), which show increased tropism for human liver cells

in liver xenograft mouse models with primary human hepatocytes, represents a promising avenue to mitigate off-target effects [16]. Another strategy to reduce off-target impact is the targeting of tissue-specific enhancers. Previous research has validated the efficacy of targeting a tissue-specific enhancer employing CRISPRa, successfully reversing disease phenotypes. Further investigation is required to pinpoint liver-specific *Nurr1* enhancers as one of the approaches to overcome the off-target effect.

7.2.3 Innovative preclinical model for NAFLD/NASH

Although FATZO mice closely mimic human metabolic syndrome more accurately than other rodent models of NASH that rely on genetic modifications or chemical treatments, there are obvious differences in metabolic pathways, pathologic progression and therapeutic efficacy between animals and humans. ([17], [18]). Such disparities emphasize the limitation that findings from animal models might not reliably translate to humans. Humanized mice and human liver organoids have become increasingly utilized to better comprehend the pathogenesis of NASH and facilitate the discovery of new therapeutics. Utilizing human fetal liver organoids, researchers have been able to recreate steatosis by introducing specific dietary and genetic triggers. These models have been proven to identify new therapeutic targets and mechanisms for NAFLD. Additionally, liver organoids derived from the damaged livers of NASH patients have displayed upregulation of pro-inflammatory and cytochrome p450 pathways, as well as markers linked to liver fibrosis and cancer, which recapitulate human NASH [19]. Furthermore, the development of a "humanized" mouse model of NASH through the transplantation of human hepatocytes into fumarylacetoacetate hydrolase-deficient mice has led to a model that faithfully recapitulates human NASH when subjected to a high-fat diet [20]. This is reflected across various levels, including histological, cellular, biochemical, and molecular aspects. The transcriptome landscape of these models has identified profound dysregulation in critical signaling pathways integral to liver homeostasis, mirroring the disruptions observed in

human NASH. These advanced humanized models offer a more predictive and patient-relevant platform for studying NASH. These humanized models provide a platform that is more aligned with human clinical outcomes for the study of NASH. Subsequent research should utilize these models to confirm the effectiveness of CRISPRa in targeting the human *NURR1* gene, potentially paving the way for more translatable therapeutic interventions.

7.3 Conclusion

Our success in improving glucose tolerance in FATZO mice through the upregulation of *Nurr1* highlights the clinical translation potential of our approach. Yet, transitioning from laboratory research to clinical application remains with challenges that demand thorough investigation and refinement. Essential aspects requiring optimization include detailed safety assessments of AAV components, minimization of off-target effects, and extensive validation in humanized models and non-human primates, as outlined in this chapter.

In summary, this research showcases the potential effectiveness of CRT utilizing CRISPRa to target and upregulate *Nurr1* specifically. This key transcription factor plays an important role in mitigating the pro-inflammatory pathways associated with NAFLD/NASH. CRT stands out as an adaptable platform technology capable of correcting gene mutations without the need for direct genomic editing, proving its efficacy in treating haploinsufficiency disorders. This therapeutic approach expands our knowledge of the biological mechanisms underlying NAFLD/NASH, identifying biologically pertinent targets to address the multifaceted pathology characteristic of metabolic syndrome.

7.4 References

1. Wen, W., et al., *Comprehensive Analysis of NAFLD and the Therapeutic Target Identified.* Front Cell Dev Biol, 2021. **9**: p. 704704.
2. Hasin-Brumshtein, Y., et al., *A robust gene expression signature for NASH in liver expression data.* Sci Rep, 2022. **12**(1): p. 2571.
3. Huby, T. and E.L. Gautier, *Immune cell-mediated features of non-alcoholic steatohepatitis.* Nat Rev Immunol, 2022. **22**(7): p. 429-443.
4. Tan, Z., et al., *Liver Fibrosis: Therapeutic Targets and Advances in Drug Therapy.* Front Cell Dev Biol, 2021. **9**: p. 730176.
5. Wang, D., P.W.L. Tai, and G. Gao, *Adeno-associated virus vector as a platform for gene therapy delivery.* Nat Rev Drug Discov, 2019. **18**(5): p. 358-378.
6. Matharu, N., et al., *CRISPR-mediated activation of a promoter or enhancer rescues obesity caused by haploinsufficiency.* Science, 2019. **363**(6424).
7. Hillary, V.E. and S.A. Ceasar, *A Review on the Mechanism and Applications of CRISPR/Cas9/Cas12/Cas13/Cas14 Proteins Utilized for Genome Engineering.* Mol Biotechnol, 2023. **65**(3): p. 311-325.
8. Ertl, H.C.J., *Immunogenicity and toxicity of AAV gene therapy.* Front Immunol, 2022. **13**: p. 975803.
9. Van Alstyne, M., et al., *Gain of toxic function by long-term AAV9-mediated SMN overexpression in the sensorimotor circuit.* Nat Neurosci, 2021. **24**(7): p. 930-940.
10. Anselmo, A.C. and S. Mitragotri, *Nanoparticles in the clinic: An update post COVID-19 vaccines.* Bioeng Transl Med, 2021. **6**(3): p. e10246.
11. Han, X., et al., *Ligand-tethered lipid nanoparticles for targeted RNA delivery to treat liver fibrosis.* Nat Commun, 2023. **14**(1): p. 75.

12. Qiu, M., et al., *Lipid nanoparticle-mediated codelivery of Cas9 mRNA and single-guide RNA achieves liver-specific in vivo genome editing of Angptl3.* Proc Natl Acad Sci U S A, 2021. **118**(10).

13. Kim, C.H., et al., *Nuclear receptor Nurr1 agonists enhance its dual functions and improve behavioral deficits in an animal model of Parkinson's disease.* Proc Natl Acad Sci U S A, 2015. **112**(28): p. 8756-61.

14. Rode, L., et al., *AAV capsid engineering identified two novel variants with improved in vivo tropism for cardiomyocytes.* Mol Ther, 2022. **30**(12): p. 3601-3618.

15. Issa, S.S., et al., *Various AAV Serotypes and Their Applications in Gene Therapy: An Overview.* Cells, 2023. **12**(5).

16. Cabanes-Creus, M., et al., *Novel human liver-tropic AAV variants define transferable domains that markedly enhance the human tropism of AAV7 and AAV8.* Mol Ther Methods Clin Dev, 2022. **24**: p. 88-101.

17. Teufel, A., et al., *Comparison of Gene Expression Patterns Between Mouse Models of Nonalcoholic Fatty Liver Disease and Liver Tissues From Patients.* Gastroenterology, 2016. **151**(3): p. 513-525 e0.

18. McLaren, D.G., et al., *DGAT2 Inhibition Alters Aspects of Triglyceride Metabolism in Rodents but Not in Non-human Primates.* Cell Metab, 2018. **27**(6): p. 1236-1248 e6.

19. McCarron, S., et al., *Functional Characterization of Organoids Derived From Irreversibly Damaged Liver of Patients With NASH.* Hepatology, 2021. **74**(4): p. 1825-1844.

20. Ma, J., et al., *A Novel Humanized Model of NASH and Its Treatment With META4, A Potent Agonist of MET.* Cell Mol Gastroenterol Hepatol, 2022. **13**(2): p. 565-582.

Publishing Agreement

It is the policy of the University to encourage open access and broad distribution of all theses, dissertations, and manuscripts. The Graduate Division will facilitate the distribution of UCSF theses, dissertations, and manuscripts to the UCSF Library for open access and distribution. UCSF will make such theses, dissertations, and manuscripts accessible to the public and will take reasonable steps to preserve these works in perpetuity.

I hereby grant the non-exclusive, perpetual right to The Regents of the University of California to reproduce, publicly display, distribute, preserve, and publish copies of my thesis, dissertation, or manuscript in any form or media, now existing or later derived, including access online for teaching, research, and public service purposes.

DocuSigned by:
Xuyia Zhou
87A42BE239944E9...
Author Signature

3/18/2024
Date